POLITECNICO DI TORINO

Master's program in Biomedical Engineering

Master's thesis

Optimization of transfection process to obtain fluorescent Influenza Virus-like particles for drug delivery

Supervisors

Gianni Ciofani

Danilo Demarchi

Co-supervisor

Sílvia Pujals

Candidate

Eleonora Giro

Academic year 2019/2020

The present work has been developed in collaboration with the Istitute for Bioengineering of Catalonia, Spain, in the group “Nanoscopy for Nanomedicine”.

Index

List of abbreviations

Ag	Antigens
AHA	Azidohomoalanine
BCA assay	Bicinchoninic acid assay
BFP	Blue fluorescent protein
BSA	Bovine serum albumin
C1q	Complement component 1q
CCMV	Cowpea chlorotic mottle virus
CFP	Cyan fluorescent protein
CHO	Chinese hamster ovary
cLIA	Competitive Luminex immunoassay
CPMV	Cowpea Mosaic Virus
CTLs	Cytotoxic T lymphocytes
DCs	Dendritic cells
DLS	Dynamic light scattering
DMEM	Dulbecco's modified Eagle's medium
DMSO	Dimethyl sulfoxide
DNA	Deoxyribonucleic acid
dsDNA	Double stranded deoxyribonucleic acid
DSP	Downstream process
eGFP	Enhanced green fluorescent protein
ELISA	Enzyme-linked immunosorbent assay
EMA	European Medicines Agency
EPR	Enhanced permeability and retention
EV71	Enterovirus 71
EYFP	Enhanced yellow fluorescent protein
FDA	Food and Drug Administration
GAP-43	Growth Associated Protein 43
GFP	Green fluorescent protein
HA	Hemagglutinin
HBcAg	Core antigen of Hepatitis B Virus
HBsAg	Surface antigen of Hepatitis B Virus
HBV	Hepatitis B Virus

HCC Human hepatocellular carcinoma

HIV Human immunodeficiency viruses

HPLC High performance liquid chromatography

HPV Human Papilloma Virus

IgG Immunoglobulin G

IgM Immunoglobulin M

M1 Matrix protein 1

M2 Matrix protein 2

MALS Multi-angle light scattering

mGFP Membrane green fluorescent protein

MHC Major histocompatibility complex

NA Neuraminidase

NEP Nuclear export protein

NP Nucleocapsid protein

NPs Nanoparticles

NTA Nanoparticle tracking analysis

PA Polymerase acidic protein

pAF P-amino-phenylalanine

PB1 Polymerase basic protein 1

PB2 Polymerase basic protein 2

PBS Phosphate-buffered saline buffer

PDI Polidispersity Index

PEG Polyethylene glycol

PFA Paraformaldehyde

PRRs Pattern recognition receptors

PTMs Post-translational modifications

RGD Arginylglycylaspartic acid

RNA Ribonucleic acid

RNP Ribonucleotide core of the particle

ROI Region of interest

SDS-PAGE Sodium Dodecyl Sulphate - PolyAcrylamide Gel Electrophoresis

SEAP Secreted alkaline phosphatase

siRNA Short interfering ribonucleic acid

TEM Transmission electron microscopy

TIRF Total internal reflection fluorescence

TLRs Toll-like receptors

USP Upstream process

VLP Virus-like particle

VP2 Viral protein 2

WHO World Health Organization

1. Introduction

1.1 Objectives

This thesis is the result of the internship I carried at IBEC, the Institute for Bioengineering of Catalonia in Barcelona, Spain. Inside IBEC I worked in the Nanoscopy for Nanomedicine group, led by Prof. Lorenzo Albertazzi.

The aim of my work was to produce and characterize Influenza Virus-like particles (VLPs) that can be designed to express different types of proteins, both on the inside and on the surface of the nanoparticle. In particular, my final VLPs were modified to express either the GFP protein, used as a reference for the internal part of the particle, or a modified version of it, mGFP, which is bound on the lipid bilayer of the particle. The two types of GFP were used as markers for the particle, allowing the study of the samples with fluorescence microscopy techniques.

Therefore, the purpose was to obtain VLPs that express proteins that are not present in the original virus, both on the membrane of the particle and on the inside. The modification of bare nanoparticles is used in the context of drug delivery systems, where VLPs could play a role as novel carriers for nanomedicine purposes.

These new drug carriers would benefit from their virus-like behavior in two ways: they would follow a simple self-assembly process, obtained with a previous cell transfection step, and they would interact easily with cells, without being rejected from the physiological environment.

My experimental work can be divided in three steps temporally successive one to the other:

- Optimization of cell transfection with GFP and mGFP: the expression of the two types of GFP has been obtained through a transfection process. One cell population has been transfected with GFP and another one with mGFP. This step involved the optimization of the transfection process, analyzed both from the point of view of the percentage of transfected cells and of the fluorescence intensity.
- Optimization of cell transfection with Influenza proteins and the two types of GFP. Cells have been transfected with four types of plasmids simultaneously to obtain the expression of influenza proteins together with the fluorescent agent (either GFP or mGFP). Immunostaining and fluorescence microscopy have been used to check the presence of all types of proteins on transfected cells.

- Production and characterization of modified VLPs with each type of GFP. The aim here was to obtain, starting from the transfected cells, influenza Virus-like particles, to verify and characterize them and to check the presence of GFP and mGFP.

1.2 Influenza Virus

1.2.1 General features

Influenza viruses are a group of enveloped viruses with a negative-sense, single stranded RNA genome belonging to *Orthomyxoviridae* family. Basing on the differences that viruses have in the nucleoproteins and the matrix protein four different genera can be found: A, B, C and D, of which only the first three can affect humans, with A and B being the most common[1].

Influenza A virus affects mainly the respiratory system, infecting the nose, throat and sometimes lungs, where the most common signs of influenza's infection are fever, cough, headache, muscle and joint pain, sore throat and runny nose. Most people recover from all the symptoms within a week without requiring medical attention, while in other cases the infection could lead to a more severe condition.

The World Health Organization indeed calculates that every year 1 billion people are affected by Influenza, of which 3 to 5 million cases lead to severe illnesses. It is estimated that up to 650 000 deaths annually are associated with respiratory diseases from seasonal influenza [1], [2].

In industrialized countries, the most affected people are aged 65 or older, while other people at risk are pregnant women, children under 59 months of age, individuals with chronical medical conditions and the ones with immunosuppressive conditions.

The effects of seasonal influenza in developing countries are not fully known, but it is estimated that 99% of deaths in children under 5 years of age are due to lower respiratory tract infections related with influenza [1].

Mutations in the genetic material of Influenza constantly happen, leading to a great variability that allows the spread and adaptation of the virus on living organisms [3]. The modification in the gene's expression indeed changes the appearance of influenza antigens, which may interfere with the ability of the immune system to recognize and block the sickness. This is why this type of virus is still causing a very high rate of infection all around the world, and every year we need a new anti Influenza vaccine.

1.2.2 Virus' morphology

Influenza virus can appear with different morphologies depending on the strain [4]. Between the possible shapes, one can be assimilated to a sphere, with a diameter in the range of 80-100 nm [5]. Two different filamentous shapes can also be found, longer in one case, with lengths up to 20 µm [5], and shorter in the other case, with a short-capsule shape with lengths up to 250 nm [4]. Sometimes, filamentous virions can appear with bulbous heads at their leading ends, either empty or containing genome segments [4].

In particular, this work will be focused on Influenza A virus, which shows the greatest variability in protein expression. The virion particles contain 8 genome segments coding for 11 proteins, of which 8 are present on the inside and 3 on the lipid surface of the particle[5] (figure 1 [6]).

The external envelope consists of a lipid bilayer containing glycoproteins hemagglutinin (HA) and neuraminidase (NA) and ion channel M2 [7].

Inside the envelope, protein M1 is present, which binds the lipid surface to the ribonucleotide core of the particle (RNP); here polymerase complex proteins are found (PB1, PB2 and PA) and nucleocapsid protein (NP) is also present, which mediates binding and packaging of the viral genome. On the inside of the virion another protein, nuclear export protein (NEP), is present [5]. The particle does not include a capsid, which means that all the genome is not protected by an additional protein capsule inside the envelope.

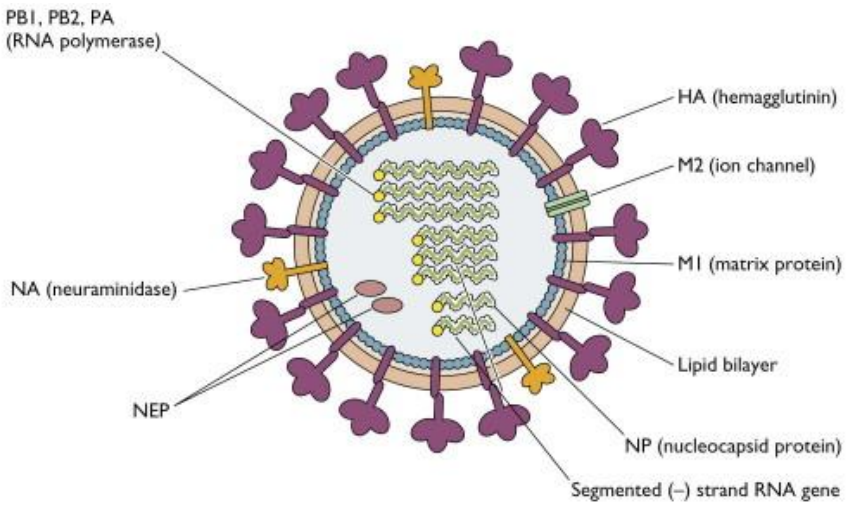

Figure 1: structure of influenza virus. Obtained from ref. [6]

On the surface of the virus it is shown that HA is the most abundant protein, with an usual observed HA:NA ratio of 4:1, while M2 is the less abundant, with an observed HA:M2 ratio that varies from 100:1 to 10:1 [8].

In Influenza A viruses, different major genomic mutations brought to the modification of HA and NA, in a phenomenon known as antigenic shift, so it is possible to classify the virus into different subtypes. 18

different types of HA and 11 types of NA have been found so far [9]. Usually, to identify a virus strand, the type of HA and NA are indicated with numbers: HxNy.

The complete nomenclature for all the types of Influenza nomenclature also includes:

- The antigenic type (A, B, C, D)
- The host of origin (specified only when it's not human)
- Geographical origin, which is where the virus was first isolated
- Strain number
- Year of collection

Ex. A/Sydney/05/97(H3N2)[10]

1.2.3 Viral cell infection

The transmission of the virus occurs when infected droplets reach conjuctival, nasopharingeal or other respiratory mucosal epithelium [11]. First the virus enters the cell, where it can use its machinery to replicate its genome and synthesize new viral proteins. Then the budding process can start, which is the process of recruitment of viral proteins and expulsion of the new viral particles from the cell (figure 2).

Viral entry and replication

When virions reach epithelial cells, HA complexes present on the surface of the virion interact with sialic acid residues of cell glycoproteins, allowing the attachment with the membrane and, subsequently, a receptor-mediated endocytosis of the viral particle [12]. Inside the cell, the phagosome undergoes a progressive decrease of pH which causes the liberation of the RNPs in the cytoplasm of the cell and the disconnection of the different viral proteins [12].

The RNPs are transported to the nucleus where transcription and replication occur. At this point, new mRNA reaches ribosomes in the cytoplasm, where new viral proteins can be produced. Some of them need to be processed in the endoplasmic reticulum and in Golgi apparatus to be glycosylated. These modified proteins are transported to the cell membrane, where they are incorporated in the lipid bilayer [12]. More specifically, HA and NA are present on the lipid raft domains of the membrane, which are parts of the membrane enriched in cholesterol, sphingolipids and proteins, thus serving as functional domains [5]. M2, instead, is excluded from these domains [5].

Budding process

When these proteins reach a high enough concentration in the membrane, M1 protein and RNPs condensate in that site and budding can start, which is the process where these new viral particles are released from the cell (figure 3 [5]) [7]. So, thanks to the presence of its own proteins, new viral particles are able to undergo a self-assembly process that starts on the cell membrane and results in the production of new virions, present in the intercellular environment and therefore capable to infect other cells [7].

Budding is a complex process that requires functional steps and biological components both from the virus and the host cell. It is between the least understood processes in viral biology because it's a very uncommon phenomenon exhibited by living cells [7].

As mentioned before, at the end of the infection and budding process, new viral particles will be released, which will be able to infect other cells. In the new virions it is usually shown that the expression of M2 is visibly decreased in comparison with the expression of the same protein on the cell membrane: this would be due to the fact that M2 is not present on the lipid raft domains of the membrane, where the budding process occurs, which would turn out in a decrease of M2 expression on the new virions [13].

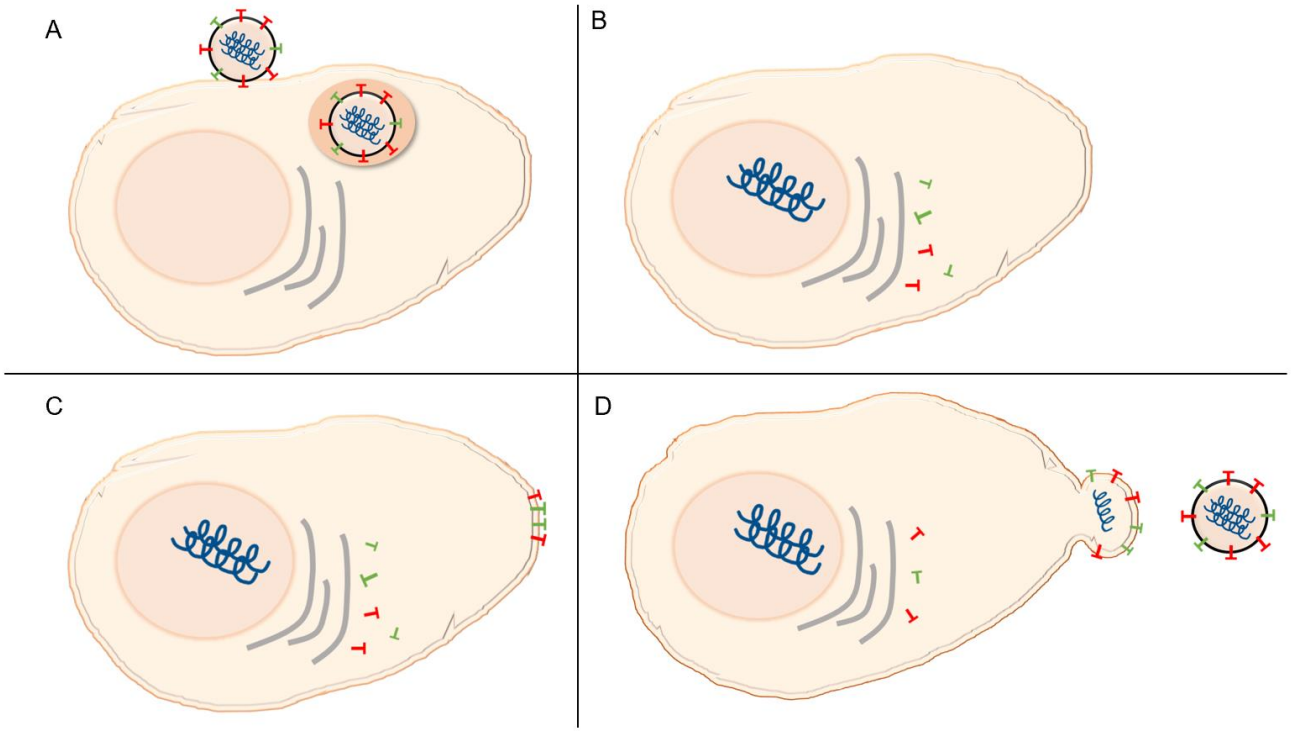

Figure 2: Cell infection. A) The virion interacts with the cell membrane and enters through endocytosis. B) the RNPs enter the nucleus allowing the synthesis of new viral proteins. C) the viral proteins are concentrated on the lipid raft domains of the cell membrane, where the budding process will occur. D) the budding process can evolve, and new virions are released

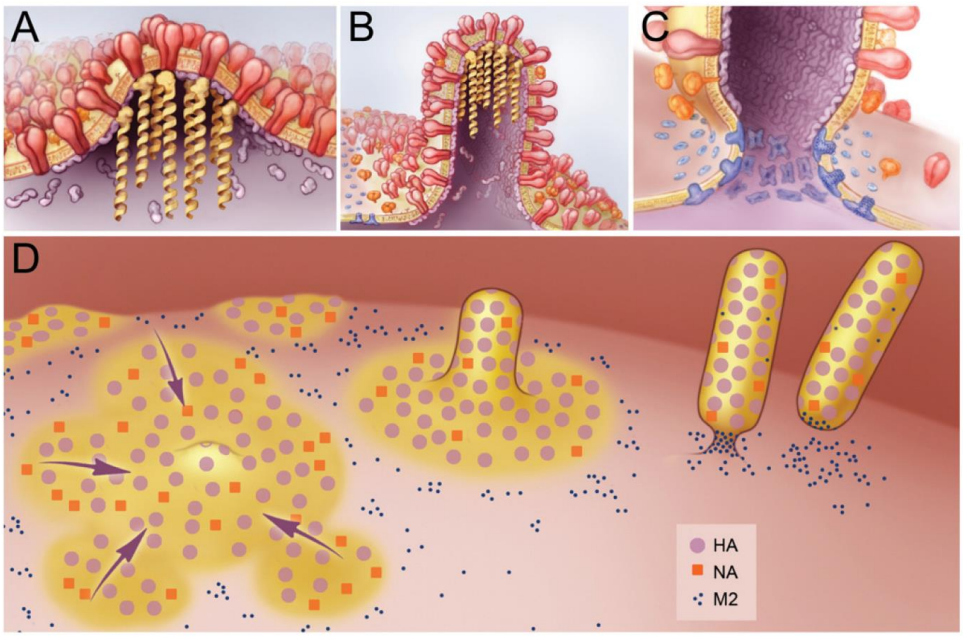

Figure 3: model of influenza budding. A) clustering of HA (red) and NA (orange) on the lipid raft domains of the cell membrane. M1 (purple) binds HA and NA cytoplasmatic tails with RNP chains (yellow). B) polymerization of M1 and elongation of the budding virion. C) recruitment of M2 protein at the neck of the budding site that allows the scission of the membrane and the release of the viral bud. D) overview of the process leading to the formation of rod-shaped virions. Lipid raft domains on the cell membrane are shown in yellow. Obtained from ref. [5]

Both viral entry and budding processes are possible thanks to the action of the different viral proteins. In figure 4 ([14]–[17]) we see the four main proteins involved in these processes. HA is essential in the viral entry because it interacts with sialic acid residues on the cell membrane. It is also important in the first steps of viral budding [5].

NA has a role during viral entry in the cell binding polysaccharide chains on the cell surface [15]. It is involved in budding process cleaving sialic acid residues to release the virus from the surface of the infected cell [5], [18].

M1 has a regulatory function in viral structures: it binds both the membrane and the RNA complexes (RNP) providing structure and support to the ensemble. During the budding process M1 interacts with HA and NA cytoplasmic tails, mediating their incorporation in the new virions [5].

M2 mediates the alteration of pH across the viral membrane during cell entry, allowing the detachment of RNPs from M1 and releasing it in the cytoplasm [8]. During the budding process, it has a crucial role in generating membrane curvature[19].

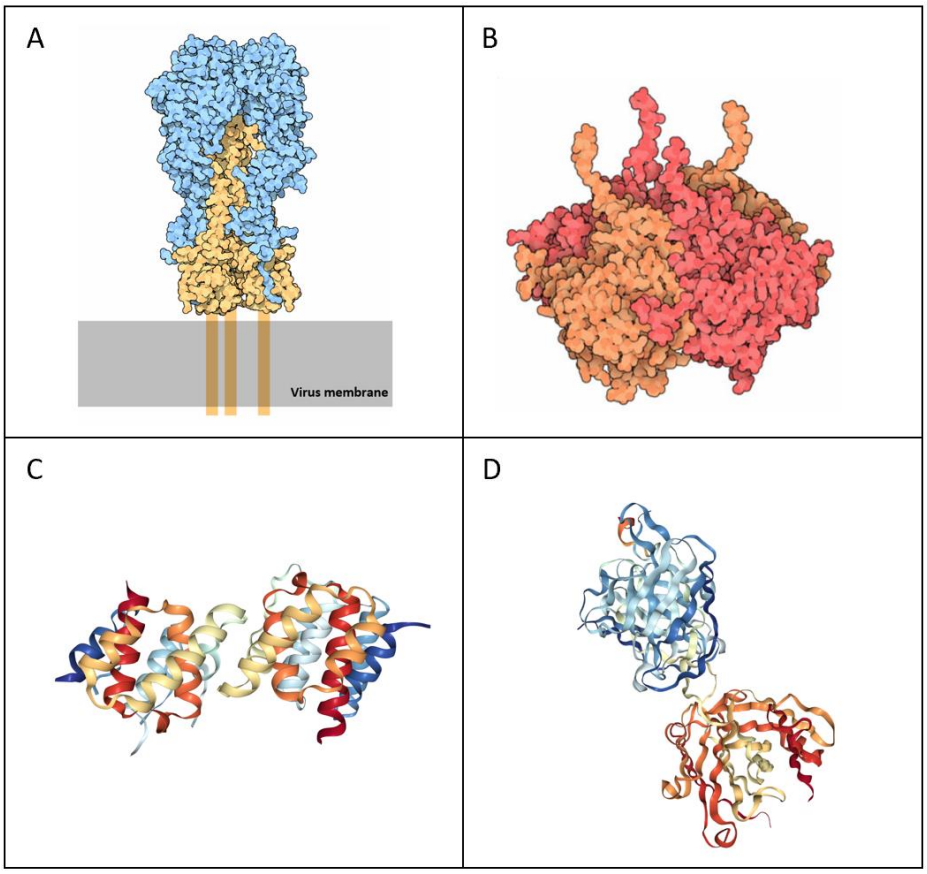

Figure 4: structure of Influenza HA (A), NA (B), M1 (C) and M2 (D). Obtained from ref. [14]-[17]

1.2.4 Influenza vaccines

Current influenza vaccines are synthetically produced every year basing on the strains that are predicted to be prevalent in the upcoming flu season. They are called trivalent vaccines because they consist of three inactivated or attenuated influenza viruses, two from type A (H1N1 and H3N2 subtypes) and one from type B. It is also possible to add a second type B virus, obtaining a quadrivalent alternative[20], [21].

The goals of influenza vaccinations are to protect people from infection and disease and to induce herd immunity in order to restrict transmission between individuals [22]. Indeed, after the vaccination, our organism recognizes the presence of new external agents, activates the immune system and produces specific antibodies against the present strains. In this way, if we will be exposed to any of these strains, there will be the response of the antibodies blocking viral antigens and the spread of the virus will be stopped.

However, a complication of this system could occur when minor changes in the virus' genome, known as antigenic drifts, modify the viral expression, which means that the final conformation of the viral antigens present on the surface of the virus would be different. In this case the antibodies produced against the vaccine's strain could not match the new viral antigens, so the virus could evade immune recognition, and

the efficacy of the vaccine would decrease [23]. In figure 5 [12] this mechanism is shown: in steps 1-3 it is shown how antibodies produced during vaccination attack viral particles, blocking the infection. If a genetic drift occurs (step 4) new antigens are produced (step 5) that cannot match the antibodies produced in the vaccinated organism (step 6) thus resulting in a new infectious virus.

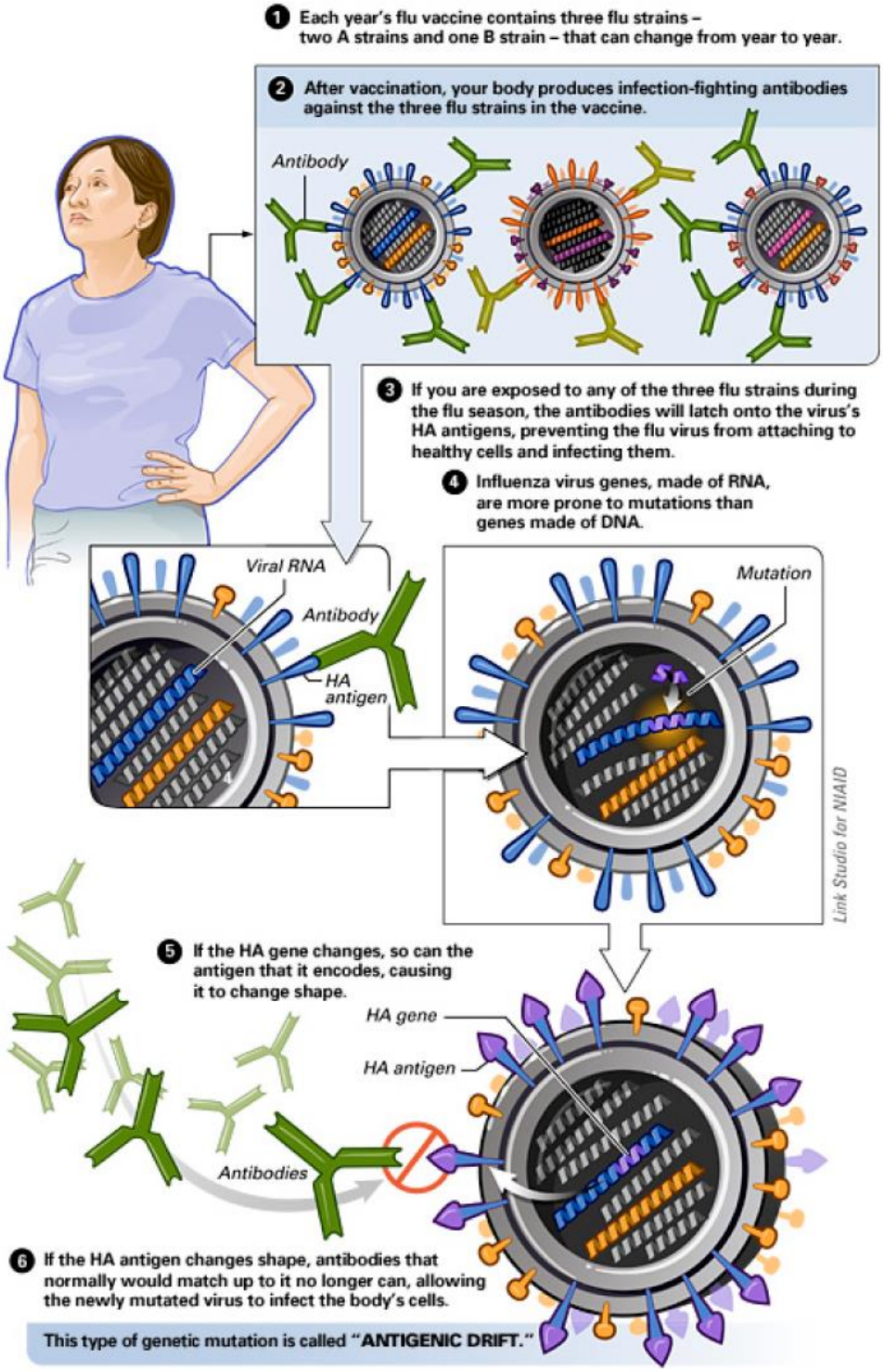

Figure 5: antigenic drift. Obtained from ref [12]

From a classification point of view, there are three types of trivalent inactivated vaccines, which are whole virus vaccines, split virus vaccines and subunit vaccines, with the last two being the most commonly used nowadays.

In split virus vaccines the virus' lipid envelope is disrupted by a detergent to expose the viral antigens, while in subunit vaccines HA and NA antigens are purified by removal of other viral components [23].

Live attenuated vaccines were created to better mimic the natural infection process; they are reassorted viruses that are sensitive to temperature, meaning that they replicate in the cold environment of nasopharynx, but behave poorly at body temperature in the lower respiratory tract, where therefore they become harmless [23].

All of these types of vaccines are considered safe and proven to be efficacious, thus recommended for groups at risk by the World Health Organization. Nevertheless, Influenza remains a big threat worldwide, causing considerable morbidity that leads to significant socioeconomic implications.

The main problems associated with current available vaccines include their limited immunogenicity, antigenic drifts, manufacturing limitations and limited availability in resources-limited countries [22].

It is therefore important to keep track of the evolving situation and continue the study of the subject to better understand the infectious process and find new ways of prevention and treatments.

In this context, novel vaccines based on Virus-like particles could be relevant thanks to their safety and easier manipulation. The research of VLPs indeed started in the vaccinology field, and subsequently became more and more relevant also for future drug delivery applications. The possibility to modify the main particle structure leads to new studies types of functionalized nanoparticles, designed with specific agents of interest for nanomedicine purposes.

1.3 Virus-like particles

1.3.1 Main characteristics

Virus-like particles (VLPs) are self-assembly structures that resemble the morphology of a virus. They are composed of one or more structural proteins of a virus but lack their genetic material. Their dimension ranges between 10 and 2000 nm and depends on the size of the original virus [24], [25].

As previously reported, when the genetic material of the virus enters the nucleus of the infected cell, it is able to express all the characteristic proteins of the virus, that go on the surface of the cell and can be expelled forming a new virus particle. Although this process, budding, is not completely understood yet, we know that all these surface proteins play an important role in the formation of the new virus particle[5], [7], [18], [26].

Instead of going through the viral infection process, to obtain the viral proteins on a cell it is possible to perform a transfection, which means that genomic sequences coding for the proteins of interest are directly

inserted in the cell, modifying its final expression and allowing the synthesis of these proteins. In this way we obtain the viral proteins without having the viral genome, because the genomic material only encodes for the proteins we wanted.

With these viral proteins it will be possible to obtain again a budding process, that will lead to the creation of new particles which are exactly the same as the virus particle in shape and protein formulation, but they do not bring the virus genome inside them. This special aspect allows these new virus-like particles to be harmless to the organism, and this makes them perfect candidates for nanomedicine purposes.

To obtain VLPs two different types of transfection can be performed: in stable transfection the genetic material introduced integrates with the cell's genome hence surviving cell division, while in transient gene expression the new genetic sequences do not interact with the cell's genome and are eventually lost with cell division[18].

Stable transfection allows a long-term study of the transfected cells because the new genetic material will be permanently present in the system, but it needs higher production times because it is required to only select cells that incorporated the new genome [18]. To do so, additional genetic sequences are incorporated in the plasmids, in order to give a resistance to a drug that will be administered to the cell culture [27]. Transient gene expression only requires the incorporation of plasmids encoding for the proteins of interest, but the study of transfected cells and the VLPs production will not be possible in a long-term period.

The study of VLPs has included a wide variety of structures coming from viruses of microbial, plant, insect and mammalian origin. In total, more than 100 types of VLPs have been studied, with spherical or filamentous shapes, enveloped or non-enveloped depending on the type of virus they mimic [28].

1.3.2 VLPs in nanomedicine

The study of VLPs had in the past different goals, starting from the study of a virus of interest, its structure and assembly. Nowadays, the two main fields of study include vaccinology, where VLPs could play an important role as new alternatives to traditional vaccines [24] and drug delivery, where the aim would be to use the advantages of VLPs to transport other additional agents inside the organism [28].

VLPs for vaccines production

As a first application VLPs could be used as vaccines because they lack genetic material, so they are harmless and do not need any modification, while the most used vaccines nowadays require seasonal administration resulting in a meticulous and long manufacturing process [18]. On the other hand, they already express viral

antigens, which are the fundamental agents that ensure an immune response and production of antiviral antibodies.
Two types of VLPs are already approved by FDA and currently used as vaccines, one against Hepatitis B and the other against Human Papilloma Virus [28].

Since traditional vaccines are produced against the specific virus' strain that is predicted to circulate in the coming season, their efficacy is compromised in case of inaccurate epidemiological predictions [29] and if they do not match with the antigenic formulation of the circulating virus, which also means that they could not be effective in case of a new pandemic strain [30].

In this kind of situation another possible use of VLPs would be the creation of new universal VLP-based vaccine, which would be specifically prepared to express highly conserved epitopes of the surface's proteins thus resulting efficacious against multiple epidemic strains[30].

VLPs for drug delivery

As a second important field of study, VLPs could be designed to be drug carriers: they interact very easily with cells, they are recognized by the immune system and considered safe. They also have no toxicity nor biodegradability problems and they avoid lysosomal degradation that instead could be very problematic with synthetic nanoparticles [18], [28]. VLPs have moreover the possibility to attach or encapsulate proteins or other small molecules, that would be then released in order to obtain a targeting effect [28].
It was reported that they are also capable of packaging foreign DNA plasmids, thus representing good candidates for gene therapy [31].

The strategies to obtain VLP based drug carriers are different and can be divided in three main groups: physical modifications, genetic modifications and chemical modifications.

The physical modification (figure 6A) results in a non-covalent interaction between the structural proteins of the VLPs and the new agent [32], so it requires the knowledge of the main physical characteristics of the particle, possible ionic interactions and the nature of the bonds keeping VLPs together [32]. For example, to entrap molecules inside the VLP it is possible to induce pH variations that lead to a swollen state of the particle and thus permit the cargo molecules to enter [28]. Another example would be the incorporation of lipophilic dyes, that for their nature could interact with the lipid bilayer of the particle and used as markers [32].

The genetic modifications (figure 6B) are performed before the transfection step and allow the expression of heterologous peptides or proteins. The vectors used during transfection, indeed, contain different sequences that are needed to have the expression of structural viral proteins, but they can also be modified to insert

other genetic sequences to produce other agents of interest, that will be expressed and incorporated in the budding site [28]. This type of modification guarantees the exact placement of the added compound, in the interior or exterior part of the VLP and can be used to mark the particle or to give a targeting effect [33].

Finally, to functionalize VLPs it is also possible to proceed with a chemical modification of the structural proteins found on the surface of the particle (figure 6C), in order to have new specificity and/or new physical properties [28]. A covalent attachment is in this case performed, making advance of reactive residues present on the proteins displayed on the particle. For example, several cancer cell targeting ligands were attached to different types of VLPs, including small molecules, antibodies, peptides and DNA aptamers [34].

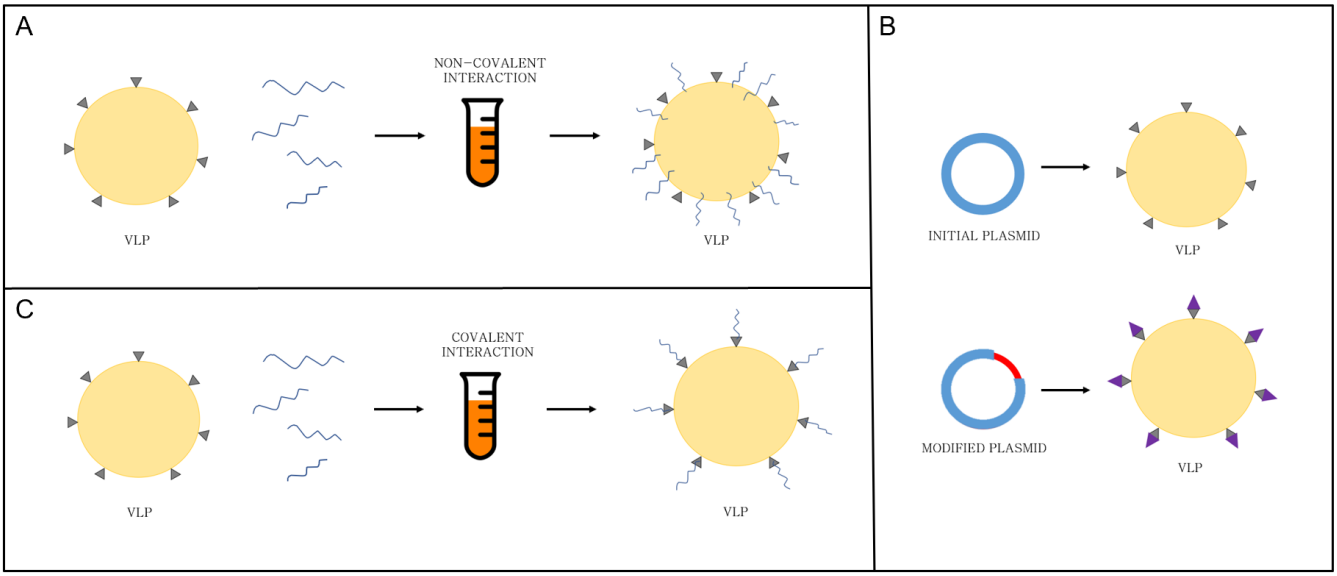

Figure 6: Different types of VLP modification for drug delivery applications. A) physical modification B) genetic modification C) chemical modification

Despite the promising approaches of using VLPs, one of the main problem in using VLPs as drug carriers would be the quantification and the control of the encapsulated dose, but no data is available so far indicating whether it is possible to obtain that [28].

Another problem of VLPs lays in their large variability, because during the budding process they carry with them host proteins from the transfected cells as well as genomic RNA or DNA. In addition, during the budding process the cell also produces other types of particles, similar to VLPs in size, derived from residues of cell membrane and called extracellular vesicles. This turns out in a challenging purification process and in a delicate choice on what type of cell line to use for the transfection [35].

1.3.3 Influenza VLPs

In this work nanoparticles that resemble Influenza A virus were considered. These Influenza VLPs were obtained with the transfection of the three influenza surface proteins (HA, NA and M2) and protein M1. Influenza virus causes a very common infection worldwide, and the study of its morphology, infection process and possible vaccines existed and developed throughout decades. For this reason, the study of Influenza VLPs became one of the most present in this field, as it is possible to observe from the works published about Influenza VLPs in the last years [36]. The availability of more and more studies considerably increased the relevance of this research area and made possible further tests even at clinical levels [37], also increasing the promising applications of this technology in future years.

The literature shows how to obtain different types of Influenza VLPs using different combinations of HA, NA, M1 and M2 [18] (figure 7 [18]). Although the budding process resulting in VLPs release is not fully understood, it seems that to produce new particles it is necessary to have at least HA or NA, because M1 and M2 are not able to initiate the budding process [5]. However, the greatest VLP release occurred with the presence of all four proteins, suggesting that the interaction between them is able to increase the efficiency of the process [5].

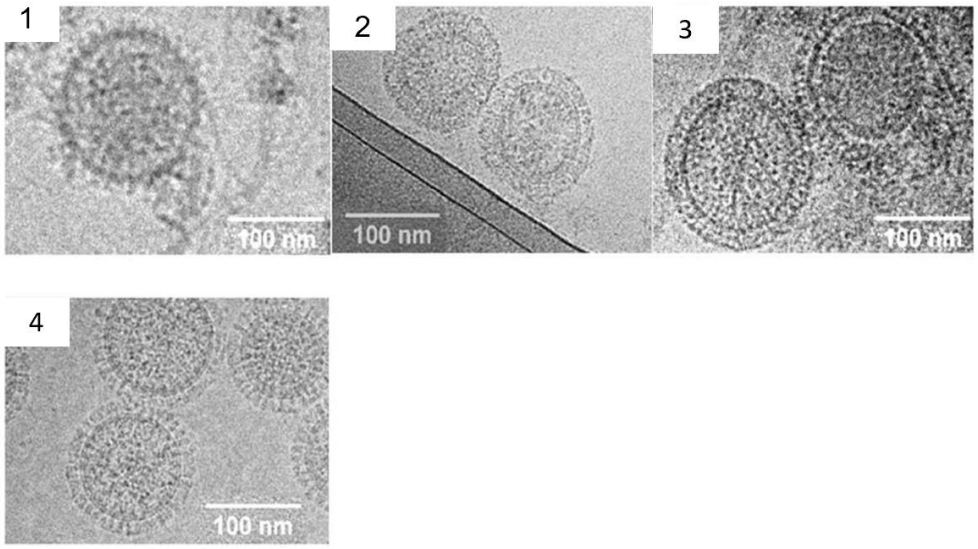

Figure 7 :examples of Influenza A VLPs produced with different cell lines (1-3) and a Influenza A particle (4) used as a positive control. Obtained from ref. [18]

Another issue to comment is that the VLP budding is different from the budding process that occurs when the cell is infected by the virus and even in this case the reasons why this happens are not clear. In VLPs a virus-regulation of protein synthesis is missing, resulting in an aberrant protein levels that may affect the budding process. Finally, in the VLP systems HA is able to initiate a budding process and form new particles

alone, while in the case of the viral infection it is dependent on additional proteins to complete the budding event [5].

Qualitatively, Influenza VLPs can be assimilated to spheres with a diameter of approximately 80 to 100 nm. They show on the lipid surface the three proteins in the same proportion as the virus particles: HA is the most abundant, then there is NA and the less present is M2 [13].

The principal technique used so far to characterize the appearance of the particles has been electron microscopy. It is indeed necessary to have a final visual proof of the particles because other indirect techniques, such as Western Blot and ELISA, could also detect other types of protein aggregates [24].

Influenza VLPs have already been tested as vaccines [29], [38] to prevent different types of infections that in the past resulted in pandemics, such as avian influenza, 2009 swine-origin virus and 1918 pandemic strain. It seems that HA is the most relevant antigen inducing protective response [29], [38], and that in general Influenza VLPs decrease morbidity and mortality in vaccinated animals, inducing protection against different types of strains [32].

1.3.4 Fluorescent VLPs

As previously reported, modification of VLPs includes many different techniques experimented in the last years. This interesting property leads to the possibility to produce fluorescent VLPs and other viral or not viral particles, using different techniques and different types of dyes (figure 8 [32]). In this way, it will be possible to check the presence of the particles and study their characteristics using fluorescence microscopy techniques. Fluorophores are therefore used as markers, but at the same time they also act as foreign agents, so they can be used as models for other types of molecules of interest that in future applications could be attached, encapsulated or expressed to obtain the drug carrier of interest; for example, fluorescent molecules could become the model of and encapsulated drug, or of a chain molecule attached to the surface of the particle to give it a functionalization.

Chemical compounds can be attached either covalently or not covalently to the particles, or in alternative it is possible to perform a genetic modification that will lead to the expression of the fluorescent compound [32].

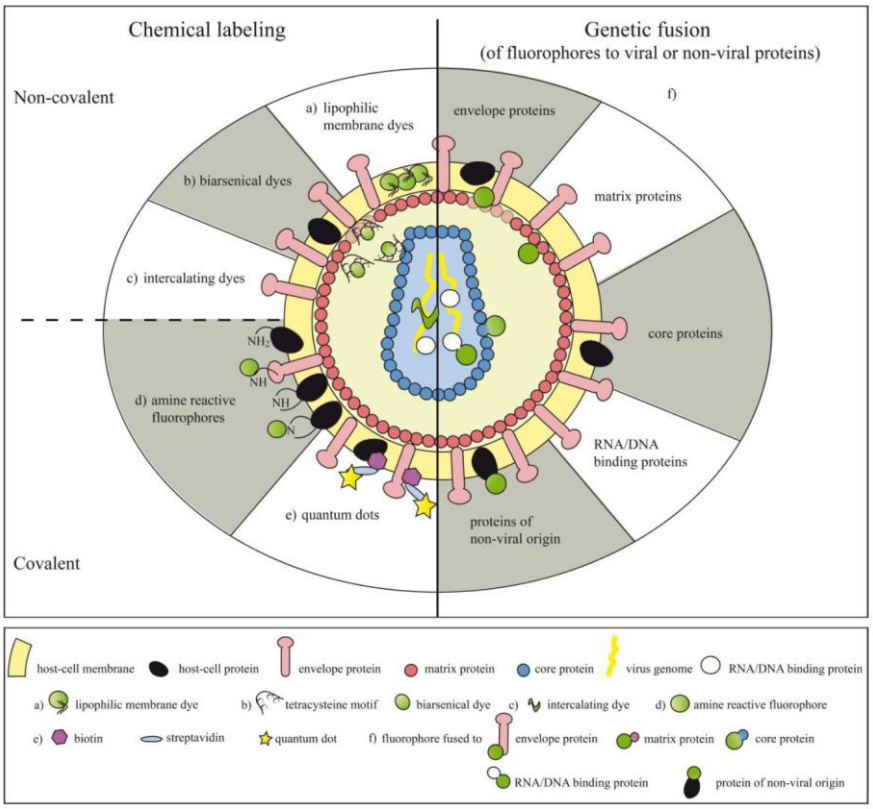

Figure 8: possible modification of viral and non-viral particles with fluorescent molecules. Obtained from ref. [32]

1.3.5 GFP modification to visualize viral structures

GFP (green fluorescent protein) is a protein found in jellyfish *Aequorea Victoria* that has natural fluorescent properties. It was discovered and isolated by Shimomura, Chalfie and Tsien, which consequently received the Nobel Prize for Chemistry in 2008 [39]–[41].

The two main excitation peaks are found at 395 nm and 475 nm, while the emission peak is influenced by environmental factors but it is in the range of 507-510 nm [42]. Its natural role is to transduce the chemiluminescence of the protein aequorin (blue light) into green fluorescent light by energy transfer (figure 9 [43]) [44].

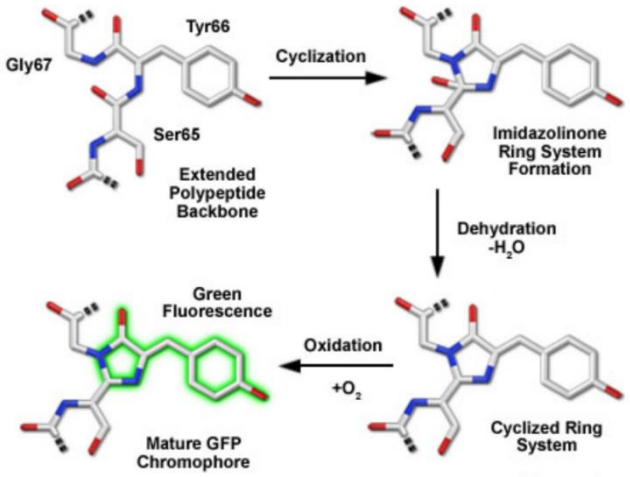

Figure 9:autocatalytic fluorescent protein chromophore formation. Obtained from ref. [43]

The structure of the protein (figure 10 [43]) consists of a 11-stranded β-barrel 42 Å long and with a 24 Å diameter, with an α-helix on the inside which is attached to the chromophore. A total of 238 amino acid residues are found, with a molecular weight of 26,9 kDa [41], [42].

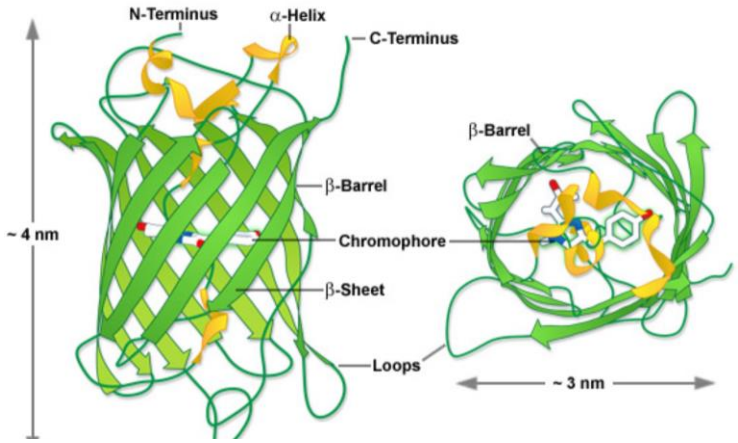

Figure 10: architecture of GFP. Obtained from ref. [43]

GFP is largely used in fluorescence microscopy to mark cells, also in live conditions, and to monitor the expression of proteins attached with the fluorescent agent. It is also possible to incorporate the GFP genome into a new genetic sequence to study the expression of different structures of interest.

So in the past few decades GFP has become one of the most famous marker used in molecular biology, due to its small size and relatively easy manipulation; many genetic modifications have been performed so far to obtain different variants of the protein (figure 11 [43]), leading to better fluorescence and photostability or to different peaks shifts in the emission spectra [45].

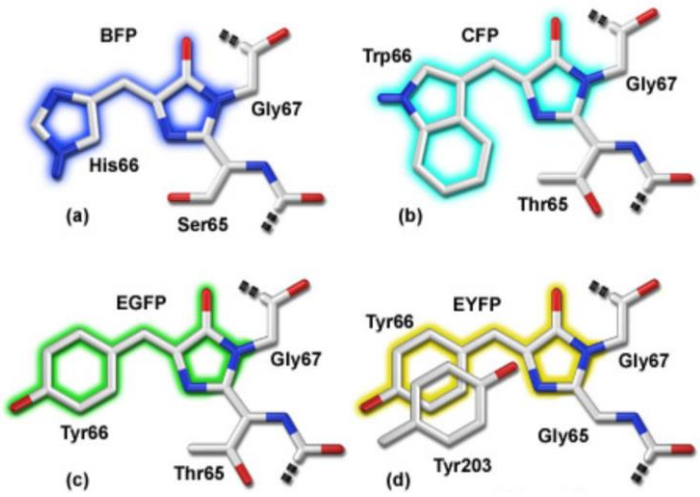

Figure 11: chromophore structure of GFP mutations: a) BFP, b) CFP, c) eGFP and d) EYFP. Obtained from ref. [43]

In this work GFP and one of its variants, mGFP, were used. mGFP is modified with a palmitoylation sequence of GAP43 protein at its N-terminus, that covalently interacts with lipid raft domains of the cell [46].

GFP and mGFP have been chosen over other types of dyes, such as organic dyes, because the modification of the VLPs was in this case performed through a genetic method: plasmids encoding for the two types of GFP have been expanded and transfected into cells to obtain fluorescent cells and, subsequently, fluorescent VLPs. So, the modification occurred during the assembly of the particle itself, without requiring any further external modification. GFP is a soluble molecule found in the cytoplasm of the cell and therefore was ideal to imitate an encapsulated agent and to label the interior part of the particle; mGFP attached the lipid raft domains of the cells, where the budding process occurs, thus it was used to label the surface of the particle, modelling an agent present on this part of the particle.

Among the ways to obtain fluorescent VLPs through genetic modification, the production of fluorescent VLPs using GFP is by far the most famous and studied so far. Between the firsts to try this approach, Charpilienne et al. modified the plasmid encoding for protein VP2 of Rotavirus to express GFP together with it and obtaining fluorescent Rotavirus-like particles [47]. In a similar way, Kratz et al. obtained fluorescent Hepatitis B VLPs inserting a genetic sequence coding for GFP in the plasmid of the nucleocapsid of the particle, HBcAg [48].

Influenza VLPs expressing eGFP were produced by Young et al. operating genetic manipulations to obtain an HA-GFP fusion construct. HA in this case was the only viral protein used to obtain the VLPs and it was derived from H5N1 strain [49].

In all cases it was possible to obtain new fluorescent VLPs, indicating that the size of GFP is small enough to permit the budding process and the creation of those new particles.

2. Review on the state of the art of VLPs

In the last years VLPs became an attractive topic in the field of vaccinology and drug delivery, as it is possible to see in the increasing number of scientific publications on them (figure 12). In this review chapter I will briefly analyze the state of the art of the research on them, focusing on their production and characterization process, their effect on the organism and the path towards the availability on the market.

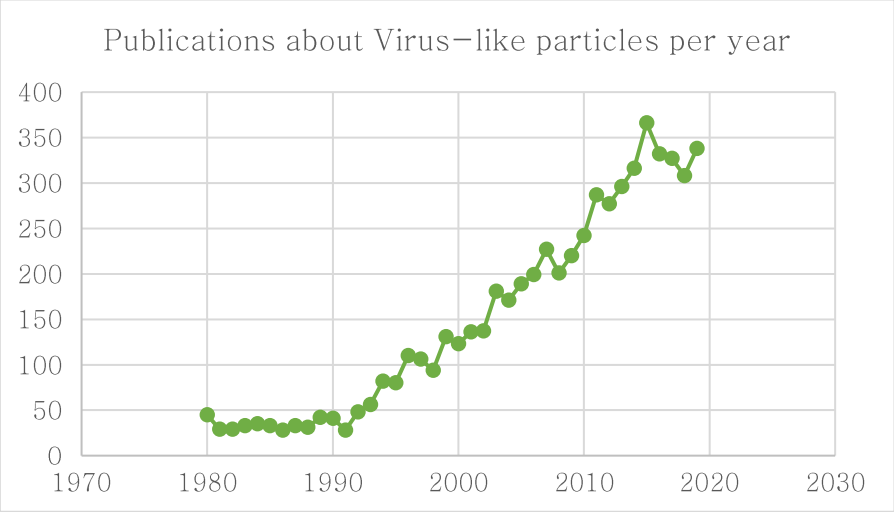

Figure 12: publications about Virus-like particles from 1980 to 2019. Data from PubMed search engine

2.1 Expression host system

To produce VLPs it is essential to select a system in which viral particles are expressed and the budding process can occur. Generally we can find 5 different expression systems, depending on the cell type that expresses the VLP. In his review about VLPs, Zeltins [24] shows how often the different systems are used, basing his results on 174 successful studies (figure 13). The two most used systems are bacteria and insect systems, followed by yeast, mammalian systems and, at last, plant systems.

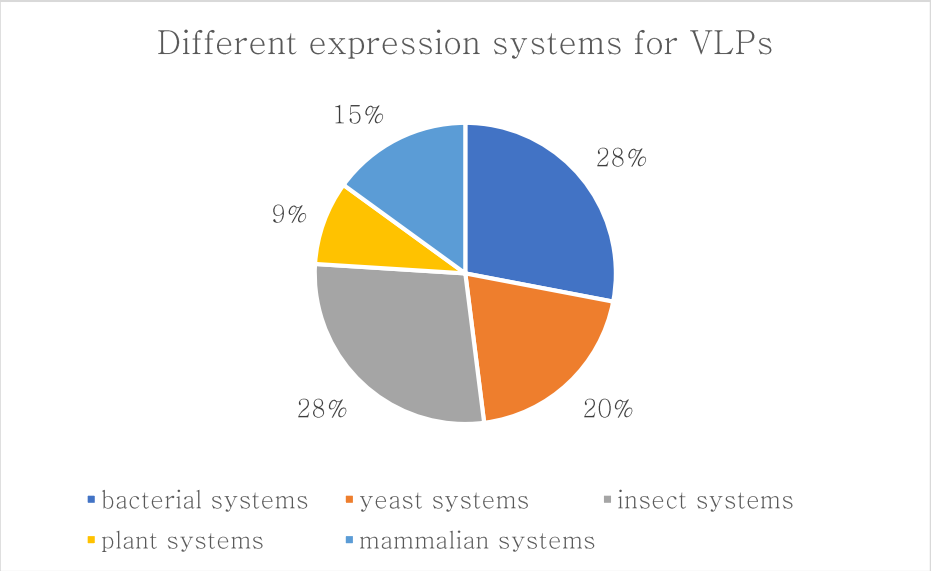

Figure 13: distribution of expression systems used to produce VLPs

Each expression system has its pros and cons, since they are based on different cell types:

-Bacterial systems mostly rely on well-characterized *E. Coli* strands and are mainly used to produce bacterial and plant VLPs. They are better suited to produce VLPs from a singular viral protein of non-enveloped viruses, since they do not have a lipid membrane as mammalian cells [25]. The main advantage of using this system is a very high yield of the proteins of interest, while between the disadvantages there are, first, the inability to produce recombinant proteins with post-translational modifications (PTMs): this is a chemical modification of the proteins occurring after their synthesis, and could be important for the immunogenicity properties of the particles. As a second disadvantage, endotoxins could be present during the protein biosynthesis, with the production of possible toxic compounds.
Bacterial systems *Lactobacillus casei* and *Lactobacillus lactis* have already been used to test a VLP-based vaccine against Human Papilloma Virus to treat cervical cancer, with the second currently undergoing clinical trials [34], [50], [51].

-Yeast systems represent a step forward in the production of VLPs, since their ability to produce post-translational modifications. These systems are more complicated than E. Coli ones because first they require the proteins' genetic sequences to be obtained in bacteria, and then inoculated into the yeast cells with the transfection process. It is also possible to obtain multigene expression systems with an ease of expression. The yield of the process, though, is significantly lower compared to the results in bacteria systems [24], [25]. Yeast systems are currently between the most promising ones in clinical applications. Several licensed Hepatitis B vaccines include yeast system *Saccharomyces cerevisiae* (Engerix-B, Euvax-B, Recombivax HB),

while others use Pichia Pastoris systems (Enivac HB, Heberbiovac HB) [34]. The first licensed VLP-based vaccine against Human Papilloma Virus, Gardasil, also uses *Saccharomyces cerevisiae* as expression system [52].

-Insect cell-based expression systems are widely used for VLP production on the laboratory or industrial scale thanks to their versatility [53]. They show fast growth rates in animal product-free media, a capacity for large-scale cultivations, and the ability of post-translationally modifying the recombinant proteins. The main disadvantage is that enveloped baculoviruses are also produced at the same time as VLPs, making purification a difficult and expensive step. The most used insect cell-lines are Sf9 and High five cells. Cervarix, the second licensed VLP-vaccine against Human Papilloma Virus, uses an insect cell line (*Trichoplusia ni*) [54]. Insect systems are studied in clinical trials to study also other possible vaccines against Influenza A, Human Immunodeficiency Virus, Human Parvovirus and Norovirus [34].

-The use of plant systems to produce VLPs has been widely discussed. Some types of bacteria such as *Agrobacterium tumefaciens* have already been used to introduce new genetic material in the plant host genome and some examples of VLPs have been obtained [25]. Plants are able to express both enveloped and non-enveloped VLPs, with discrete rates of expression [34]. These systems are more difficult to compare to the others from the point of view of the yield of the process, since their production is generally calculated per mg of vegetal tissue, with the others using µg of protein per mL of culture. The plant systems have been studied in clinical trials to express Influenza A VLPs [55], [56] and other studies include VLPs resembling HPV virus, Hepatitis B virus and Norovirus [25], [34], [57]. The plant systems can be various, such as *Nicotiana tabacum*, *Arabidopsis thaliana*, potato, tomato, tobacco and lettuce [25], [58].

-Mammalian systems have more accurate and complex PTMs, although the yield of the process is often lower compared with the other systems. Mammalian cell cultures have been used in both lab practices and at an industrial level with the aim to produce efficient vaccines candidates[18], [24], [25]. They are mainly used to produce complex enveloped VLPs, that express different types of structural proteins. Many different mammalian cell lines have been used to study VLPs, such as CHO cells, VERO cells and HEK 293 cells [18]. CHO cells are currently used as expression systems in two licensed VLP-based vaccines against Hepatitis B, GenHevac B and Scigen [59].

Expression system	Yield (μg of protein/mL of culture)
Bacterial systems	0.75−700 μg/mL
Yeast systems	0.75−700 μg/mL
Insect systems	0.2−18 μg/mL

Plant systems	4–2380 pg of protein per mg of leaf
Mammalian systems	0.018–2 μg/mL

Table 1: Yields for the different expression systems [25]

Expression system	Cell lines
Bacterial systems	E. coli, Lactobacillus casei
Yeast systems	P. pastoris, Hansenula strains
Insect systems	Spodoptera frugiperda (Sf9), Trichoplusia ni (High five cells)
Plant systems	Nicotiana tabacum, Arabidopsis thaliana
Mammalian systems	Chinese Hamster Ovary (CHO) cell line, HEK293, Vero cells

Table 2: Examples of cell lines used for different expression systems [18], [24], [25]

Expression system	Advantages	Disadvantages
Bacteria	• Ease of expression • Ability to scale–up • Low production cost	• Does not allow for glycosylation • Endotoxins
Yeast	• Ease of expression • Ability to scale up • Low production cost	• Non–appropriate protein glycosylation • Risk of incorrect folding and assembly
Insects	• Can produce large amounts of correctly folded VLP in high density cell culture conditions • Ability to scale–up • The risk of culturing opportunistic pathogens is minimized compared with mammalian cell cultures • Host–derived insect cell/baculovirus components may act as vaccine adjuvants, help trigger a more effective immune response	• Baculovirus contaminants may be difficult to remove • Host–derived insect cell/baculovirus components may also mask the immune response against the desired epitope
Plants	• Ease of expression • Ability to scale–up • No human–derived virus contamination	• Cannot undergo PTMs and VLP assembly • Low expression level • Stability: antigen degradation

Mammalian	• Producer cells more closely related to the natural host • Appropriate PTMs and authentic assembly of VLPs	• Higher production cost • Lower productivities

Table 3: Advantages and disadvantages of VLPs expression systems [25]

Bacteria remain between the most used systems due to the high levels of production of VLPs (table 1), the easy scale-up process and a cost-effective solution, which makes possible a well spread use in laboratories. Insect and yeast systems are also a valid alternative since they balance the possibility to produce more complex VLPs with some of the advantages of bacteria, such as high growth rates and large-scale cultivation [24]. These aspects are crucial to ensure a high productivity needed for commercial viability, which is why current approved vaccines based on VLPs mostly rely on either insect or yeast systems [59].
Mammalian systems are used less often, typically to study more specific properties of VLPs that require a higher level of complexity [24]. They show the ideal environment to provide PTMs and authentic VLP assembly, but they remain the less used after the plant systems due to their higher production costs (table 3).

2.2 Production process

As for all the products that can be considered for clinical applications, VLPs require a scalable, cost-effective and reproducible manufacturing process [53]. It is indeed convenient to differentiate the manufacturing process that leads to the production of VLPs in two steps: the upstream processing (USP) includes all the first basic steps of an experiment involving cells, such as the choice of expression system, optimization of the yield, possible use of bioreactors, choice and optimization of medium's parameters. Biological processes are complex and very sensitive to environmental factors, meaning that all these steps could interfere with the cell growth and metabolic activity. For example, protein stability in VLPs production systems was shown to be highly dependent on pH, ionic strength and temperature [53].
The second step, downstream processes (DSP), includes all the procedures to purify the VLPs and the quality control checks to permit a consistent and scalable final product [53].

The downstream processes (figure 14[53]) start with the cell lysis or other extraction systems that allow VLPs to be expelled from the cell membrane. For insect and mammalian cell lines, though, this step is not required as the budding process already leads to an efficient expulsion of the new particles [24], [53]. Then, the actual clarification process can occur, which is needed to ensure the removal of the cell debris and other aggregates and it is performed through a centrifugation or ultrafiltration step. The following step will be to further

concentrate and purify the product: in laboratories this step is normally performed by an ultracentrifugation in cesium chloride or in sucrose gradients. This process normally ensures to have suitable results for the following experiments, however these types of procedures are non-scalable, long and dependent on the operator's ability. To avoid that, in industrial processes this step is mainly performed though a chromatography step, that could be different basing on the type of VLP produced, for example it could include size-exclusion, ion exchange, and other affinity columns. Chromatography or ultracentrifugation steps are also used as a polishing step, that is essential to discard residual host-cell proteins and DNA. There are some threshold levels to respect to guarantee the purity of the particles, which typically are 100 µg/dose for proteins and 10 ng/dose for DNA.

Further steps of centrifugation may be performed in the end to concentrate the sample [24], [53].

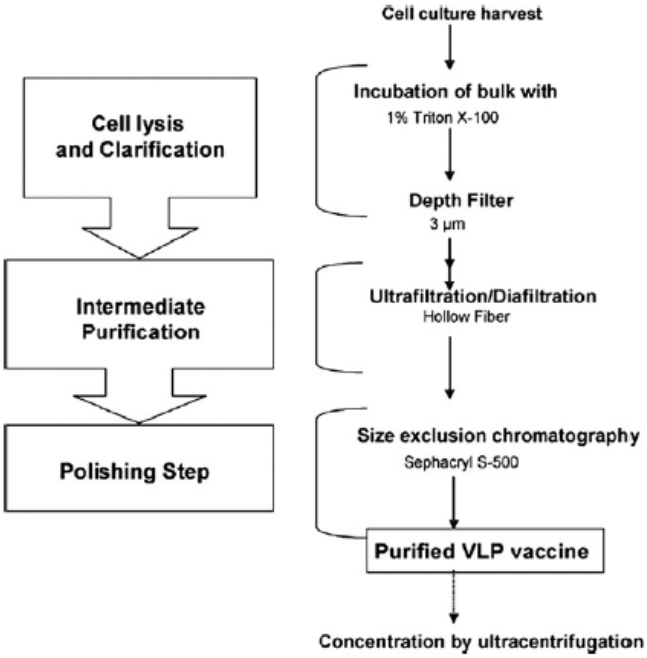

Figure 14: Downstream process in VLPs production. Obtained from ref. [53]

In figure 14 Peixoto and alia [60] describe their downstream process to produce Rotavirus like particles in a scalable and high-yield technique. Previously, they grew an insect cell line from *Spodoptera frugiperda* in spinner flasks, then moved it to 2 liters bioreactors and performed the incubation with DNA plasmids encoding for rotaviral particles vp2, vp6 and vp7. The downstream process begins with the harvesting of the cells from the bioreactor suspension, performed 120 hours post-infection. Then, the bulk is incubated with Triton X-100 and, to ensure that all the cells were lysed and cell debris "dissolved", samples are collected during this incubation period and visualized by microscopy. The clarification is performed using a depth filter with pores through a peristaltic pump. The samples are further purified and concentrated with an

ultrafiltration step using hollow fiber cartridge, and polished using a size exclusion chromatography. A final step of ultracentrifugation is performed to collect the VLPs.

This is an example of a scalable procedure, applicable in future industrial production. Instead of using a traditional two-dimensional static culture, cells are kept in suspension, simplifying their handling and allowing an easier and faster scale-up. In the purification step an ultracentrifugation in sucrose gradient is avoided, to ensure a better reproducibility.

2.3 *In vitro* characterization

2.3.1 Semi-quantitative techniques

Given the great variability of the production process, it is fundamental to characterize VLPs both in a qualitative and quantitative way.

Usually, the first tests to be performed are semi-quantitative assays to check the presence of the viral proteins expressed by the particles: the most common are SDS-PAGE, ELISA and Western blot [53].

SDS-PAGE and Western Blot are often performed in combination (figure 15 [18]). The different proteins present in the sample are divided by their molecular weight using gel electrophoresis. This step consists in the application of an electric field to the sample that allows the proteins to move. They have in fact a negative charge that is proportional to the length of their chains, which means that they will try to migrate towards the positive electrode. The smallest chains will move easily through the gel due to their dimension, while longest chains will remain close to the starting point. The final step will be an immunostaining step where a primary and a secondary antibody selectively bind the proteins of interest. Secondary antibodies are linked to luminescent substrates for the detection of the protein and a semi-quantitative result which indicates which protein is the most expressed.

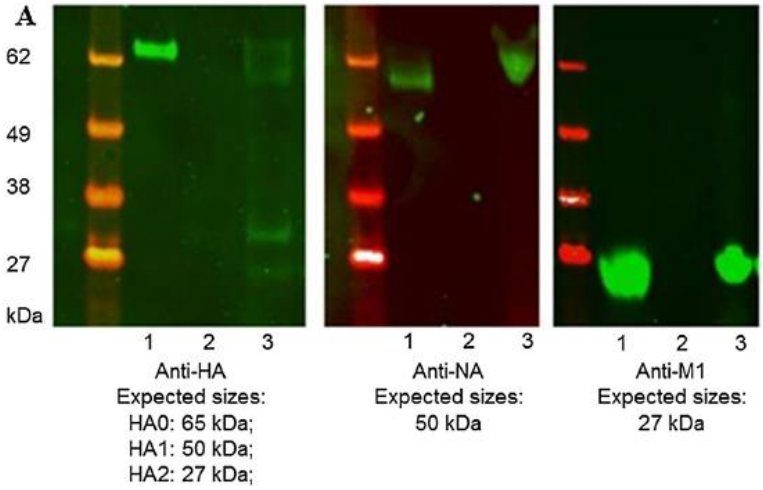

Figure 15: Example of Western Blot results on Influenza VLPs. For each of the studied protein (HA, NA, M1), the results are compared with the reference column on the left. Obtained from ref. [18]

ELISA (enzyme-linked immunosorbent assay) is also used to detect a specific protein of interest. The detection occurs thanks to the binding of the protein with a primary antibody and the binding of this primary antibody with a secondary antibody. The secondary antibody is linked to an enzyme that allows a substrate present in the solution to emit fluorescence. This technique will allow detecting if VLPs contain viral proteins and if they have the same structure and immunology activity than the original virus, since a defective synthesis of the proteins of VLPs would lead to a lack of interaction with the primary antibody.

Other types of analysis typically present in studies about VLPs are DNA and RNA assays. It is important to consider this aspect since genetic material coming from host cell systems is usually found in the new particles. With these tests it is possible to check the purity of the sample, which is fundamental for future clinical applications.

Different types of commercial assays are available, which mainly rely on two types of techniques, spectrophotometry and fluorometry [61]. Spectrophotometry is based on Lambert-Beer law, that links the absorbance of a compound at a specific wavelength with the concentration of that compound in the sample which is what we want to obtain in the end.

Nucleic acids have their absorbance peak at 260 nm, so it is possible to calculate the absorbance there with a spectrophotometer and therefore calculate the DNA or RNA concentration expressed in a weight/volume ratio. The main disadvantage of this technique is the lack of specificity of the measurements, since

measuring the presence of total protein will not inform us about the type of protein or if they are part of the VLPs.

Fluoroscopy (figure 16 [61]) uses fluorescent dyes that specifically bind DNA or RNA sequences. The sample is first excited at the excitation wavelength of the dye and, as a respond to that, light at emission wavelength is detected. A calibration curve can be built to have the relation between the quantum yield of fluorescence and the concentration of the nucleic acid, thus quantifying the nucleic acid as a weight/volume ratio.

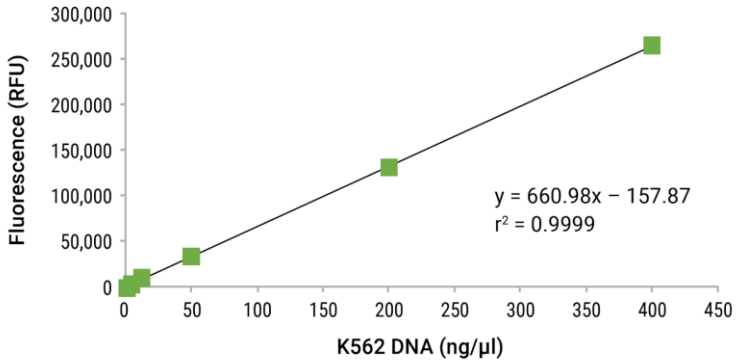

Figure16: example of fluoroscopy calibration curve. From the calculated fluorescence intensity it is possible to obtain the DNA concentration of the sample. Obtained from ref. [61]

2.3.2 Quantification techniques

Another important step in the evaluation of the sample is the quantification of total VLPs. It is not an easy process because, since they are not infective, traditional virus quantification techniques cannot be used, and previously described techniques such as Western Blot identify the proteins but do not differentiate between embedded proteins and proteins found in solution [62]. The easier way to have an idea of the particles' concentration is to quantify the total amount of proteins, which can be obtained using again spectrophotometric and fluorometric techniques. Two famous examples are UV absorbance assays, in which you measure the amino acid absorbance at 280 nm, and Bradford assay, which uses dyes to bind and quantify proteins [63]. A similar alternative is the BCA assay, where proteins, in alkaline environment, allow the reduction of Cu2+ to Cu+. At this point, Cu+ reacts with BCA reagent, forming a complex which exhibits a strong linear absorbance at 562 nm with increasing protein concentration [64].

Three more complex techniques are used to quantify the number of VLPs in a fixed volume of sample, thus providing new analytical tools for a more specific study of these particles [62], [65]. These methods are nanoparticle tracking analysis (NTA), size-exclusion high performance liquid chromatography (size-exclusion HPLC) coupled with detection with multi-angle light scattering (MALS) and flow virometry [62], [66]:

-NTA is a non-invasive method where the sample is subjected to a laser beam that alters the brownian movement of the particles. A video is analyzed to obtain a particle-by-particle tracking, allowing the quantification of the total number of particles. Knowing the volume of the sample, the concentration can be obtained [62].

-Size-exclusion HPLC is a common technique used for the purification and concentration of nanoparticles. The sample goes through a column of a stationary phase, and the compounds are separated by their size being eluted with different times. To have a quantification of VLPs, the purified sample is analyzed by the MALS detector, which calculating the scattering intensity of the sample is able to obtain the total number of the particles [62], [67].

-Flow virometry has developed from flow cytometry techniques to track small viral particles. Two separate dyes are used to stain proteins and nucleic acids, so only events with both positive detections are considered, eliminating non-specific targeting [66].

In table 4, the main advantages and drawbacks of these techniques are indicated [66]. All of them are relatively new techniques used in this field, and they are still not widespread in laboratories. The prize itself of each device could vary significantly.

Technique	Advantages	Disadvantages
NTA	Additional fluorescence measure enhancing specificity	Narrow concentration range
MALS	Separation step included, size measurement	Elaborate set-up, little testing on virus
Flow virometry	Easy handling, quick results	No additional parameters measured

Table 4: advantages and disadvantages of quantification techniques

2.3.3 Morphological techniques

After these techniques to evaluate and quantify the different compounds present in the sample, other analysis is usually performed to study the appearance of the VLPs. Two main techniques are dynamic light scattering (DLS) and electron microscopy.

DLS is a fast technique to study the homogeneity of the sample and the dimension of the analyzed particles (figure 17 [68]). VLP samples are exposed to a monochromatic wave of light and the result of the interaction is captured by a specific detector. When light encounters the sample, it scatters in a way that is dependent of the size and the shape of the particle [69]. Indeed, small particles can move easily in solution, which results in a very variable evolution of the intensity of scattering through time. Big particles, on the opposite, move slower, which means that the function of scattering through time will have less fluctuations. All these signals are analyzed to obtain the distribution of the dimension of the particles, which shows the average dimension and the homogeneity of that population of compounds.

The result is shown in a graph that correlates the size of the particles with a different possible property of the particle. For example, in VLPs study the most significant parameters are volume distribution and intensity distribution. In volume distribution the graph shows, for each size on the abscissa, the percentage of total sample volume occupied with particles of that size. In the same way, in intensity distribution the weighted parameter is the scattering intensity of particles with the different sizes [69].

Different types of peaks can be found, indicating how many populations of compounds were present (so ideally, with only one type of particles only one peak should be found). The width of the peak shows the size distribution, with narrow distributions corresponding to more homogeneous particles. The parameter to evaluate this aspect is the polydispersity index, which is a dimensionless number ranging from 0 to 1.

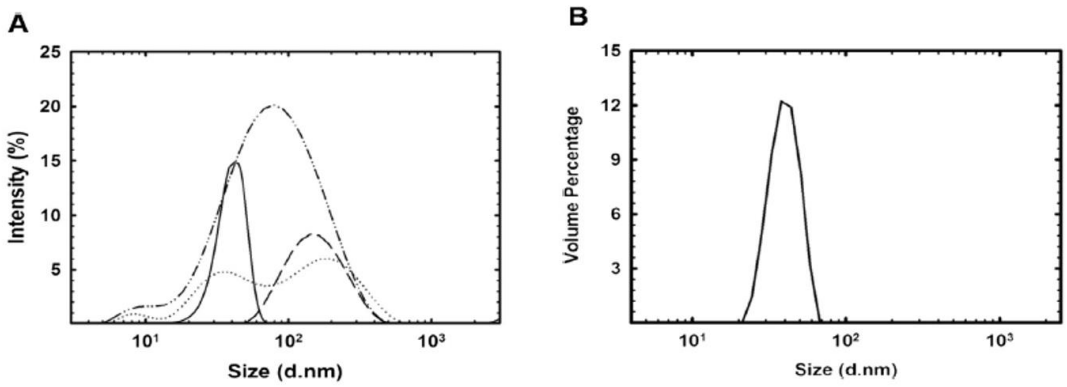

Figure 17: Example of DLS results on Norovirus VLPs. A) results expressed as intensity percentage. The solid line expresses the results of the purified sample while the other lines express the results during different steps of the purification process. B) Results of the purified particles expressed as volume percentage. Obtained from ref. [68]

A different approach to directly study the structure of VLPs is using electron microscopy, which is usually present in VLPs characterization because it gives an overall visual representation of the sample. It can be

used to calculate the dimension of the particles, the presence of undesired agglomerates and to compare the VLPs to the original virus particles (figure 18 [70]).

In transmission electron microscopy (TEM) an electron beam passes through a specimen, transmitting electrons which are collected, focused, and projected onto a viewing device. It is indeed trough the interaction of the electrons with the sample that the image of the sample can be built [71]; however, to allow the transmission of the electrons it is only possible to work with thin samples. To allow the right passage of the electron beam it is also essential to create vacuum in the TEM column linking the source of the beam to the specimen [72].

The preparation of the sample includes a drying process, essential to work in vacuum conditions, and a staining step with a contrast agent, usually a heavy metal salt [72], [73].

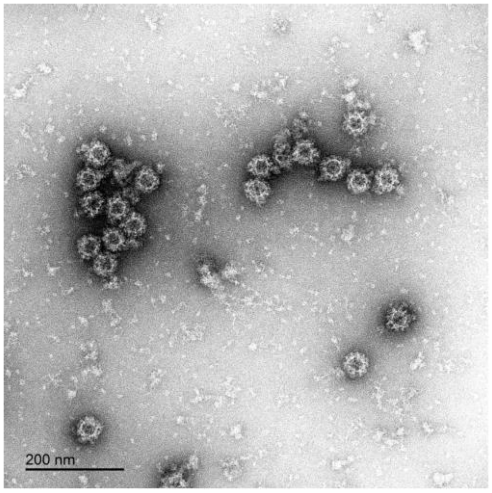

Figure18: example of TEM image of Norovirus VLPs. Obtained from ref. [70]

2.4 *In vivo* and *ex-vivo* characterization

2.4.1 Immune response

Resembling original viruses in both shape and antigen formulations, VLPs are able to stimulate humoral immunity through similar pathways as the original pathogens do. When they reach lymph nodes, they indeed activate strong B cells responses [74], [75].

The pattern of distribution of VLPs allows access and interaction of particles with different cell types in the lymph nodes, which contributes to the immune response generated against those particles [76]. This

response is able to activate both specific IgG antibodies for envelope proteins of the particles and core proteins [75].

VLPs also stimulate cellular immunity activating the innate immune system: they can be recognized by recognition receptors (PRRs) such as the Toll-like receptors (TLRs) of host cells and captured by dendritic cells (DCs) [74]. They are antigen-presenting cells that can recognize and process the particles, leading them to the lymph nodes with an indirect way and activating T cells [75].
The repetitive surface of VLPs also facilitates their interaction with IgM antibodies, which bind the surface of VLPs via low affinity/high avidity interactions. This binding activates C1q molecules resulting in the initiation of the classical complement cascade to activate the humoral response [14], [15].

Thanks to the uptake by the antigen-presenting cells, VLPs interact with major histocompatibility complex (MHC) molecules present on the membrane of both immune system cells (MHC class II) and not immune system cells (MHC class I) [76], [77]. This activates T helper cells that, via release of cytokines, allow the generation of protective IgG antibodies [76].

In figure 19 [76] we see the different paths that VLPs can follow to reach the lymph nodes. As a first way, VLPs can be directly drained into them, in a cell free manner, reaching T cells and B cells sites and activating the humoral response. Alternatively, if VLPs are captured by antigen-presenting cells, they will activate the innate immune system, enter the lymph nodes and preferentially reach T cells.

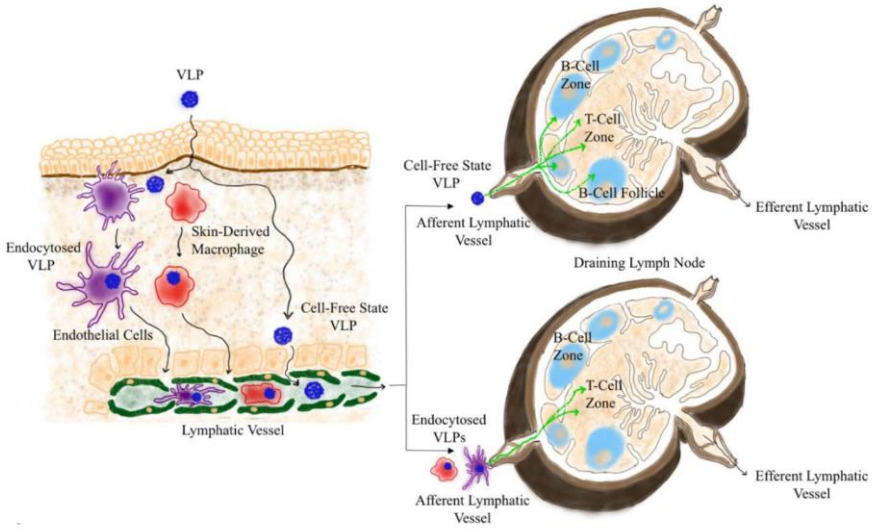

Figure 19: VLPs reaching lymph nodes activate both innate and adaptive immune systems. Obtained from ref. [76]

To display an enhanced immunogenic activity it is also possible to produce chimeric VLPs, obtained with a genetic modification of the plasmid vector to express foreign epitopes on their surface, such as foreign B and T cells epitopes. These new insertions have been proven not to modify the VLP assembly process, rendering VLPs suitable as an antigen presentation tool [74].

The ability to incorporate both self and foreign antigens leads to the possible use of VLPs in immunotherapy to treat patients with chronic diseases associated with viral infections. Therapeutic vaccination involves active clearance of infectious agents, infected cells and tumor cells through breaking immune tolerance or bypassing the mechanisms by which the disease has evaded the immune system [74]. For example, it is possible to obtain VLPs expressing tumor associated antigens on their envelope; in this way we can stimulate antigen specific Cytotoxic T lymphocytes (CTLs) that are capable of inducing the death of tumor cells as well as other dysfunctional somatic cells [75].

2.4.2 Immunogenicity assays

To study the immune response caused by the VLPs, experiments on animals can be performed. Usually, researchers measure the quantity of specific antibodies produced against VLPs with three main assays also used during clinical trials: enzyme-linked immunosorbent assay (ELISA), competitive Luminex immunoassay (cLIA) and neutralization assays [78].

ELISA has already been mentioned in the in vitro characterization since it is used to detect viral proteins after formulation. In this case, it is applied on serum samples from treated animals to quantify the antibodies produced against VLPs epitopes. For example, Young et alia [49] used it to quantify the production of anti-HA IgG in mice after injection of influenza VLPs. First, a solution containing purified HA was prepared, then it was incubated with the serum sample containing anti-HA antibodies and then washed. The sample was eventually incubated with an anti-mouse secondary antibody, linked to the enzyme peroxidase necessary to induce the substrate reaction. The resulting concentration was shown as antibody titer and compared with a control of preimmunization serum.

cLIA is used to test the specificity of produced antibodies against viral epitopes of the same virus but of different types. For example, Roberts and alia [79] applied it to study the different antibodies produced from 9 different types of Human Papilloma virus (HPV) VLPs. It uses a competitive format where the strength of serum antibodies is tested through the capability to bind specific epitopes over unspecific antibodies. This technique was also used in the process of approval of one of the HPV commercial vaccines, Gardasil [79].

Neutralization assays are performed to study the ability of antibodies to stop viral replication. Usually they are coupled with plaque assays, where samples containing an infecting virus are serially diluted and added to cell cultures plates [80]. The virus contains a gene whose activity can be easily measured and that can be used as marker of infection. In this way, all the neutralizing thus protecting antibodies are measured, regardless of immunoglobulin class [78]. An example is given by Pastrana et alia [81], where the activity of immunized human sera is evaluated against Human Papilloma Virus type 16. They constructed an HPV16 pseudovirus encoding secreted alkaline phosphatase (SEAP) that can be detected using a highly sensitive chemiluminescent reporter system. This pseudovirus was serially diluted and added to 293 TT cells culture plates. A serum sample was also added, which was obtained from human individuals vaccinated with HPV-16 VLPs. The antibody titers were obtained from the SEAP signal, which was decreasing with the increasing activity of the antibodies. The endpoint titer was defined as 50% inhibition of the amount of SEAP compared with the virus added without antibody.

2.4.3 Biodistribution

Some types of VLPs for drug delivery or imaging purposes have already been tested in animals to obtain biodistribution profiles. Escherichia Virus MS2 VLPs tested in mice at 24 hours, labeled with ^{64}Cu, accumulated primarily in the liver and in the spleen [82], [83].

Escherichia Virus Qβ VLPs labeled with gadoteric acid were also injected in mice and their profile was studied after 4-5 hours. They accumulated again in the liver, but less in the spleen [82], [84].

Cowpea Mosaic Virus (CPMV) VLPs and Cowpea chlorotic mottle virus (CCMV) were also studied in vivo to monitor their biodistribution profile. They both showed an accumulation in liver, spleen, kidney and gastrointestinal tract [82].

Biodistribution studies have also been performed to mice presenting tumor xenografts. MS2 and CPMV VLPs were studied after 24 hours of injection and found partially in the tumor site, probably due to the EPR effect (enhanced permeability and retention) [82]. Further characterization has to be performed to enhance this distribution with targeting ligands.

2.4.4 Clearance

As for biodistribution, clearance studies still need a much further characterization for VLPs. Prasuhn et alia characterized the plasma clearance of Qβ VLPs in treated mice, obtaining a clearance curve at different times (from 0 to 24 hours) [84]. VLPs were modified on the surface with gadoteric acid and its effect on clearance was studied varying the number of complexes attached to the surface.

Simon-Santamaria and alia [85] studied BK and JC polyomavirus VLPs in mice, in particular the role of liver sinusoidal endothelial cells in the clearance of the particles from the circulation. For both types of VLPs they obtained a clearance curve (from 0 to 60 minutes) showing the decrease of VLP concentration with time.

2.5 VLPs' path through vaccine's market

To approve and commercialize a vaccine a long process of study is needed to evaluate both the safety and the effectiveness of the product. In the European Union, the European Medicines Agency (EMA) carries out the supervision of vaccines, and only at the end the European Commission can issue a marketing authorization [86].

The study of a possible vaccine candidate begins with pre-clinical trials: first the vaccine's quality is tested, meaning that researchers evaluate the vaccine's purity, what are all the components and the manufacturing process of the product [87]. Then, the vaccine's effects are studied, both in vitro and in animals.

The following process is a clinical testing program in humans, which can take up to ten years from initial stages to final authorization [87].

The clinical trials for all type of drugs are generally divided in four main steps, with larger number of involved people in each of them (figure 20).

In phase 1 the number of involved volunteers is low, up to 100 people that are in healthy conditions. The main effects are studied, together with the most common side effects [87].

In phase 2 the number of tested volunteers increases up to several hundreds. The aim is to evaluate the short-term effects, the optimal dose and the immune response to the vaccine [87].

In phase 3 the participants are several thousands. In this phase, researchers try to find out more about the effects and side effects of the product, and also to compare effects on vaccinated and not vaccinated people [88].

The end of the process can only result in an approval if all the evaluations prove that the vaccine's benefits are greater than its risks. Regulatory authorities also organize inspections to ensure all the information from the vaccine developer is trustworthy [87].

After the vaccine is approved and licensed a phase 4 can occur, where the vaccine is further monitored in patients [89].

At the end, the different countries inside EU can decide which vaccines should be part of their national vaccination programs and funded by their national health systems [90].

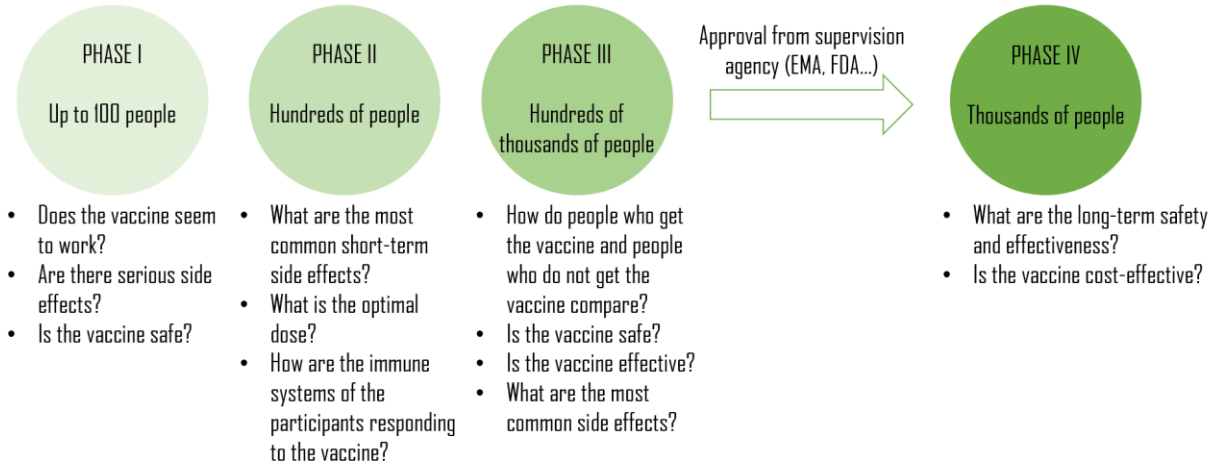

Figure 20: traditional phases of clinical trials

2.5.1 Approved vaccines

Up to date, the two available types of VLP-based vaccines are against Human Papilloma Virus (HPV) and Hepatitis B (HBV), and both are present on the market with different commercial formulations.

HPV are nonenveloped viruses belonging to *Papillomaviridae* family (figure 21 [91]). They contain two viral proteins, L1 and L2, with the first being the most abundant in the formation of the icosahedral capsid, which contains packed dsDNA. More than 100 types of HPV were discovered to infect humans, with approximately 15 that can cause cervical cancer [59].

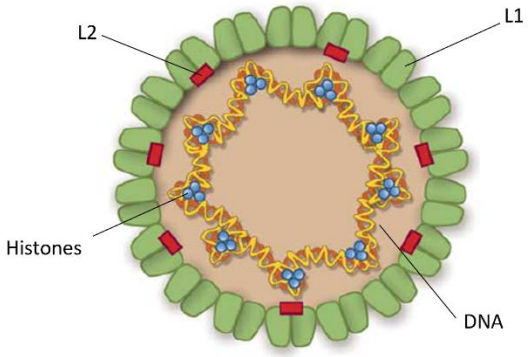

Figure 21: structure of HPV. Obtained from ref. [91]

The first licensed VLP-based vaccine against HPV was Gardasil, approved by both Food and Drug Administration (FDA) and EMA in 2006 [59], [92]. It consists of L1 VLPs comprising 4 different HPV types: HPV-16, -18, -6 and -11 [52].

The production company, Merck and Co., chose *Saccharomyces cerevisiae*, a yeast strain, as expression system. After a harvesting and cell lysis step, VLPs undergo a purification step performed through chromatographic techniques. After that, VLPs are adsorbed onto ad adjuvant of choice, which enhances the immunogenicity of the product, and are finally formulated [59].

The other licensed vaccine for HPV is Cervarix and it has been approved by EMA in 2007 and by FDA in 2009 [59], [93]. This is a bivalent vaccine (contains HPV type 16 and 18) and it is distributed by GlaxoSmithKline (GSK). An insect expression system is in this case used, derived from insect *Trichoplusia ni*.

The production process goes though harvesting, filtration and chromatographic steps. At the end of purification process, L1 proteins assemble into VLP and are then adsorbed to aluminum hydroxide to form the bulk of the particle. An adjuvant owned by GSK is also present in the final formulation [54], [59].

Hepatitis B is an enveloped DNA virus belonging to the *Hepadnaviridae* family (figure 22 [94]). It consists of an outer envelope made of lipids and proteins and a nucleocapsid core. The envelope antigens (surface Ag) are known as small (S), middle (M) and large (L) and self-assemble into the subviral HBsAg particles [59].

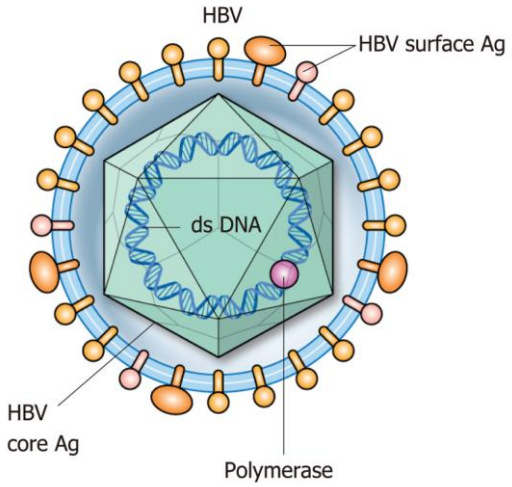

Figure 22: structure of HBV. Obtained from ref. [94]

The infection of HBV is still considered a major global health problem. It can lead to a chronic infection leading to cirrhosis and liver cancer. The WHO estimates that in 2015 HBV resulted in 887 000 deaths, while 257 million people were estimated to live with a chronic Hepatitis B infection [95].

The first HBV vaccine based on VLP technique, Recombivax HB, was approved by FDA in 1986 and distributed by Merck and Co. It consists of HBsAg S protein VLPs obtained by a yeast system (*S. cerevisiae*). Several types of vaccines were then approved and are available worldwide. To avoid yeast expression systems, CHO cells are also a valid alternative used in other approved vaccines, such as GenHevac B by Sanofi Pasteur and Sci-B-Vac by Scigen [59].

Most of the available HBV vaccines are VLPs obtained by the S protein of HBsAg, but it is also possible to introduce other antigens, M or L, to enhance the immunogenicity of the particles [59].

2.5.2 Vaccines undergoing clinical trials

Many other types of VLPs are currently studied to become vaccines. At the date of April 2020 American national library of medicine (clinicaltrials.gov) registers 123 clinical trials about VLPs as vaccines conducted worldwide. In figure 23 we can see the subdivision in the different phases.

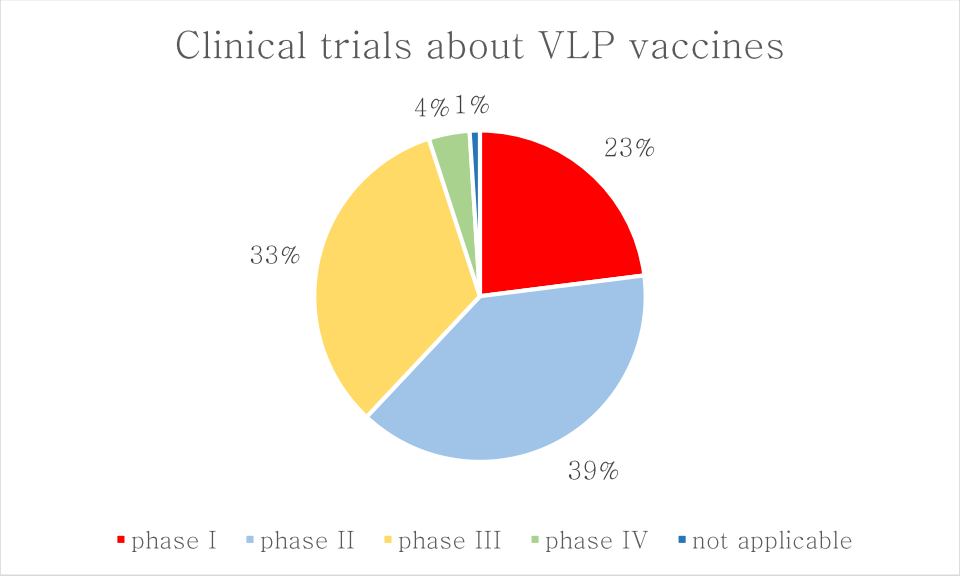

Figure 23: clinical trials about VLPs divided by trial's phase

These numbers include all the studies about new types of VLPs used as vaccine and also further applications HPV vaccines. The 5 studies currently at phase 4 are indeed all regarding HPV vaccines [96].

Between the possible vaccines, influenza VLPs are being studied to prevent both seasonal and pandemic infections. A great variety of possible vaccines is considered, both from the point of view of the antigenic formulation (use of HA, NA, M1 and M2) and from the point of view of expression system (mammalian cells, insect cells, plants) [97]. Several studies already include tests on animals to see the effect on immunogenicity

[96], [97]. In table 5 the 25 clinical trials about influenza VLPs are shown. The status results completed in all 25 cases [37].

Study	Title
1	Quadrivalent Influenza VLP vaccine dose ranging study in young adults
2	Evaluate the safety and immunogenicity of a seasonal Influenza VLP vaccine (recombinant) in healthy adults
3	Safety and immunogenicity of an A (H1N1) 2009 Influenza Virus-like particle (VLP) vaccine
4	Evaluate te safety and immunogenicity of a seasonal Influenza Virus-like particle (VLP) vaccine in older adults
5	Trial to evaluate safety and immunogenicity of trivalent seasonal Influenza Virus-like particles (VLP) vaccie (recombinant)
6	Safety, tolerability and immunogenicity of a plant-made H1 VLP Influenza vaccine in adults
7	Safety, reactogenicity and immunogenicity of an H5N1 VLP
8	H5-VLP + GLA-AF vaccine trial in healthy adult volunteers
9	A/H5N1 Virus-like particle antigen dose ranging study with adjuvant 2
10	A (H7N9) VLP antigen dose ranging study with adjuvant 1
11	A/H5N1 Virus-like particle antigen dose ranging study with adjuvant 1
12	A (H7N9) VLP antigen dose-ranging study with matrix-M1™ adjuvant
13	A study to evaluate the immune response and safety of a seasonal Virus-like particles Influenza vaccine in healthy young adults
14	Efficacy, safety and immunogenicity of a plant-derived quadrivalent Virus-like particles Influenza vaccine in adults
15	Immunogenicity of a quadrivalent Virus-like particles (VLP) Influenza vaccine in healthy adults
16	Safety, tolerability and immunogenicity of a plant-made seasonal quadrivalent VLP Influenza vaccine in adults
17	Immunogenicity, safety, tolerability of a plant-made H5 Virus-like particle (VLP) Influenza vaccine
18	Safety, tolerability and immunogenicity of a plant-made H7 Virus-like particle (VLP) Influenza vaccine in adults
19	Immunogenicity, safety and tolerability of a plant-derived quadrivalent VLP Influenza vaccine in elderly adults
20	Immunogenicity, safety and tolerability of a plant-derived seasonal VLP quadrivalent Influenza vaccine in the elderly population
21	Lot-to-lot consistency of a plant-derived quadrivalent Virus_like particles Influenza vaccine in healthy adults
22	Immunogenicity, safety and tolerability of a plant-derived seasonal Virus-like particle quadrivalent Influenza vaccine in adults

23	Immunogenicity, safety, tolerability of a plant-made H5 VLP Influenza vaccine
24	Safety study of a plant-based H5 Virus-like particles (VLP) vaccine in healthy adults
25	Efficacy of a plant-derived quadrivalent VLP vaccine in the elderly

Table 5: Influenza VLPs studies registered in clinicaltrials.gov

In table 6 a summary of all the types of VLPs found on the American National Library of Medicine register is shown.

Type of VLP	Condition
Influenza VLP	Seasonal/Pandemic Influenza infection
HPV VLP	Cervical/vulvar/vaginal/anal cancer and genital warts
Norovirus VLP	Gastroenteritis from norovirus infection
Melan A vaccine	Malignant melanoma
Venezuelan equine encephalitis virus VLP	Infectious encephalitis
Chikungunya virus VLP	Chikungunya virus infection
HIV VLP	Hiv infection
Pfs25 VLP	Malaria
VLPM01	Malaria
EV71 VLP	Hand, foot and mouth disease

Table 6: types of VLPs registered in clinicaltrials.gov

The study of VLP vaccines has become more and more relevant, given the great properties of VLPs. It is indeed true that the great variability generating from the production process and also linked to the different possible applications needs a long-term study to optimize the safety and the controllability of the final product.
It is therefore important to further study all these steps to better understand how these particles are produced, how can we better characterize and modify them and what are their effects on the human organism.

2.6 VLPs as drug delivery vectors: advantages and main challenges

In cancer therapy, most traditional treatments require invasive techniques and many possible side effects to the whole organism. Targeted delivery offers some major advantages, such as a more specific action (drugs preferentially reach areas of interest), a higher concentration of drug in the targeted area and an improved efficiency in carrying the drug to its site [82]. In addition to cancer therapies, gene therapy is also a big field of study in nanomedicine to treat genetic disorders.
To treat both genetic and cancer diseases, VLPs are a promising tool to build new drug nanocarriers, since their ability to incorporate external agents such as small molecule drugs, peptides, genetic sequences and other types of ligands.
VLPs show several advantages in comparison with other types of nanoparticles studied as drug carriers:

- they naturally result biocompatible because, as native viruses, undergo proteolytical degradation in the cells and thus are naturally digested [28];
-as viruses, they reach the cell and they are encapsulated by endocytosis; only at this point they release their cargo, unlike polymer nanoparticles, which slowly degrade and release cargo over time [82];
-they also show a great uniformity, because they naturally arrange in a self-assembly process that significantly decreases the lot-to-lot variability [28];
- thanks to their virus-like properties, they avoid a rapid lysosomal degradation, which is one of the main problems in the traditional study of other nanoparticles because does not allow a proper release of the cargo to the cytoplasm. This advantage thus results in a more efficacious delivery effect [28];
-They are expressed biologically and evolved to encapsulate their genetic material, thus naturally suited to incorporate a cargo [82];
-their cage naturally includes proteins, which are suitable to perform different types of conjugations making easier the functionalization process [98].

Some VLPs also show some natural tropism to certain tissues, derived from the parental virus. It is the case, for example, of Hepatitis B VLPs, which are mainly directed to the liver, thus resulting as possible vectors targeting hepatocytes. In the same way, rotaviruses display a tropism for the gut, so rotavirus VLPs could become specific gut-delivery vectors [28]. More frequently, though, an external modification is performed, in order to have a personalized design of the particle.

To chemically conjugate VLPs with ligands we can use cysteine and lysine residues found on the surface of the VLPs. Cysteine allows the formation of disulfide bonds with different agents, for example cell penetrating peptides, fluorescent probes and other proteins. To stabilize the chemical bond, instead of using only -SH

groups from cysteine and the attaching agent, compounds based on malemide reaction can be used (figure 24 A), to obtain a stabilization of the linkage at physiologic pH [82].
Lysine residues form amide bonds and have been used to attach PEG chains, peptides, fluorescent probes and also transferrin, which could make possible the crossing of the blood brain barrier [34], [82]. The reaction involves the amine group in lysine residues and reactive NHS ester groups present on the modifying agent (figure 24 B) Alternatively, it is possible to use non-natural ligands to attach molecules, such as azidohomoalanine (AHA) and p-amino-phenylalanine (pAF), used to bind antibody fragments, folic acid and RGD peptides as targeting agents for cancer cells.

Using the same type of chemicals, VLPs can also encapsulate cargos in the inside of the particle, for example fluorescent probes, chemotherapeutics such as taxol and doxorubicin, peptides and other small molecules. Genetic fusions also lead to covalent bonds between the agents of interest, and are used to functionalize both the interior and the exterior of the particle [82].

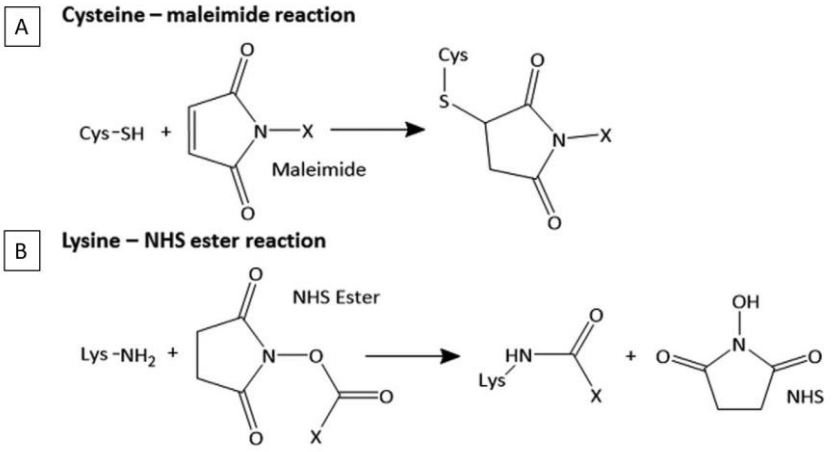

Figure 24: chemical modification using cysteine (A) and lysine (B). Obtained from ref. [82]

To obtain a non-covalent attachment streptavidin can be used as a linker between VLPs and biotinylated antigens [34]. Also, electrostatic interaction could be used to entrap negatively charged species in VLPs capsids that show positive charges [98], as in the case of RNA and DNA sequences for gene therapy uses. These unstable interactions could imply a major drawback if the cargo molecule is too small, because of the natural presence of pores on the VLP structure [82]. On the other hand, they imply an advantage compared to covalent attachment because the cargo can be preserved without requiring a chemical modification.

Ashley et alia [99] used these approaches to obtain a cell specific delivery of VLPs from bacteriophage MS2. They operated a chemical surface modification of the particle to have peptide SP94, which shows an affinity

to Human hepatocellular carcinoma (HCC). Also, they chemically encapsulated in the inside of the particles two types of agents to study their different effect on cultured carcinoma cells. The agents encapsulated were a chemotherapeutic drug (doxorubicin) and ricin toxin A-chains. A third cargo was included, a cocktail of siRNA, that was physically encapsulated without a chemical modification.

They showed how their SP94-targeted VLPs could efficiently reach HCC (figure 25 [99]). They observed the cytotoxicity effect of doxorubicin, an apoptosis effect of the siRNA cocktail, given by a silencing effect on various cyclins, and the inhibition of protein synthesis coming from toxins, which again leads to a cytotoxicity effect.

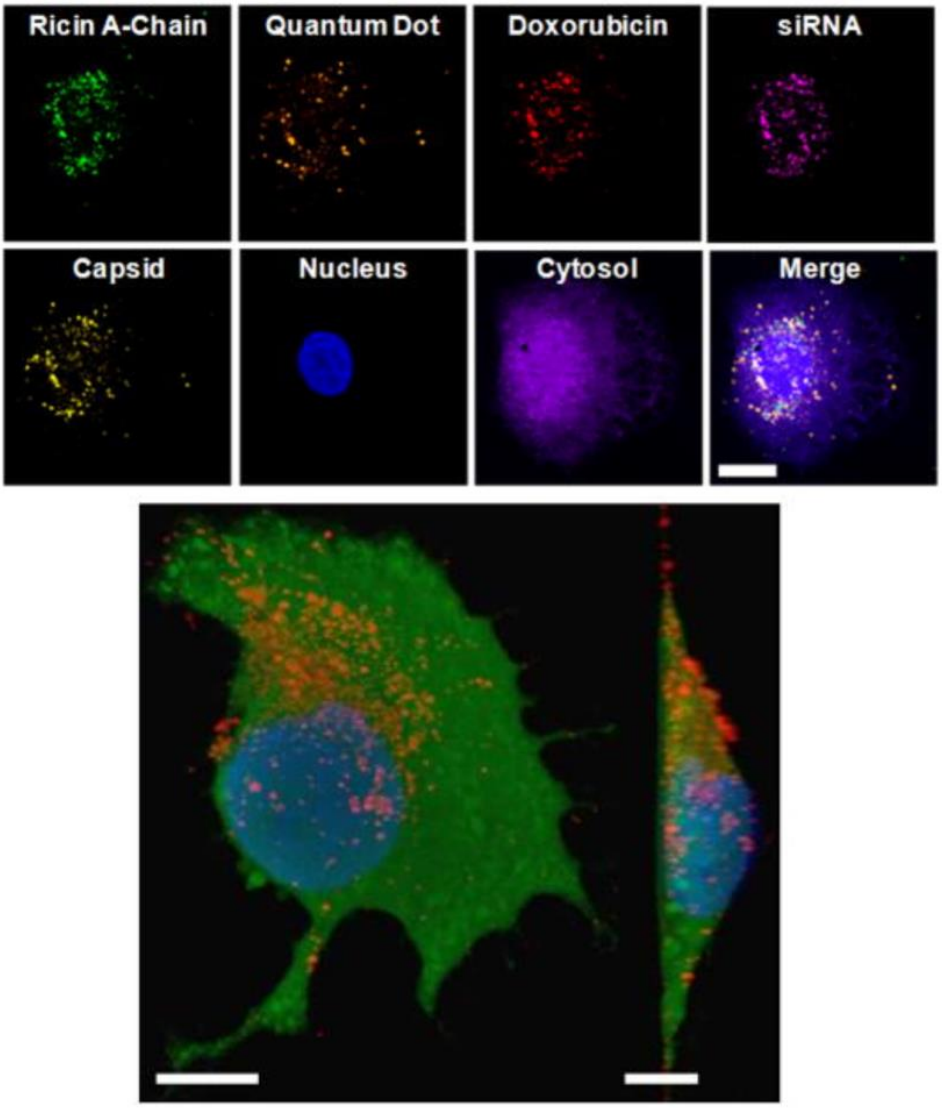

Figure 25: Confocal fluorescence image of HCC cell. It is shown the encapsulation of all three cargos: Ricin-A chains, doxorubicin and siRNA. Functionalized quantum dots were used as marker agents. Scale bars: 20 µm. Obtained from ref. [99]

There are still challenges regarding the use of VLPs in drug delivery. As other NPs, it is needed to slow down the process of clearance by the macrophages, even in presence of PEG chains providing an anti-fouling effect.

It is also important to ensure VLP stability, for example though disulfide bonds, to ensure the targeting to the right site in intact conditions; once the VLPs reach the cytoplasm of the cell it is however important that the cargo is released, so the stabilization of disulfide bonds has to be balanced. A major issue regards the extravasation from blood vessels, which allows VLPs to reach the site of action. One possible idea to enhance this mechanism would be the adding of functional ligands to the VLPs surface, so that they can interact with endothelial cells, cross them and extravasate [82]. Another possible drawback, when VLP is used as drug carrier, would be the high immune response itself, which is one of the characteristic feature of VLPs, because the production of antibodies in large scale could hinder the effect of the cargo [28].

To study VLPs as possible drug carriers it is important to evaluate different parameters after the formulation process, such as their toxicity, drug dose, organ biodistribution, clearance and blood half-life. Only a few types of VLPs have been tested in some of these fields, including Cowpea Mosaic Virus (CPMV) VLPs and Cowpea chlorotic mottle virus (CCMV) VLPs [98]. Although the first results show an overall safety of VLPs and strong immunogenicity, further characterization needs to be performed in vivo and with other types of VLPs [98]. Up to date, there are no clinical trials involving VLPs as drug carriers, while all the advanced studies regard VLPs used as vaccines [96].

3. Materials and methods

3.1 Plasmid expansion

Escherichia Coli cultures were amplified to obtain five different types of plasmids expressing five different proteins: GFP, mGFP, HA, NA and M (figure 26[100]–[102]). Bacterial cultures used were already transformed to contain the plasmids of interest: GFP plasmid comes from Clontech Laboratories[103], mGFP plasmid was designed by Matsuda and Cepko [46]. The plasmids for influenza proteins HA, NA and M (M1 and M2) all come from vector pHW2000 [104]. The influenza strain used was A/Puerto Rico/8/1934(H1N1) [105].

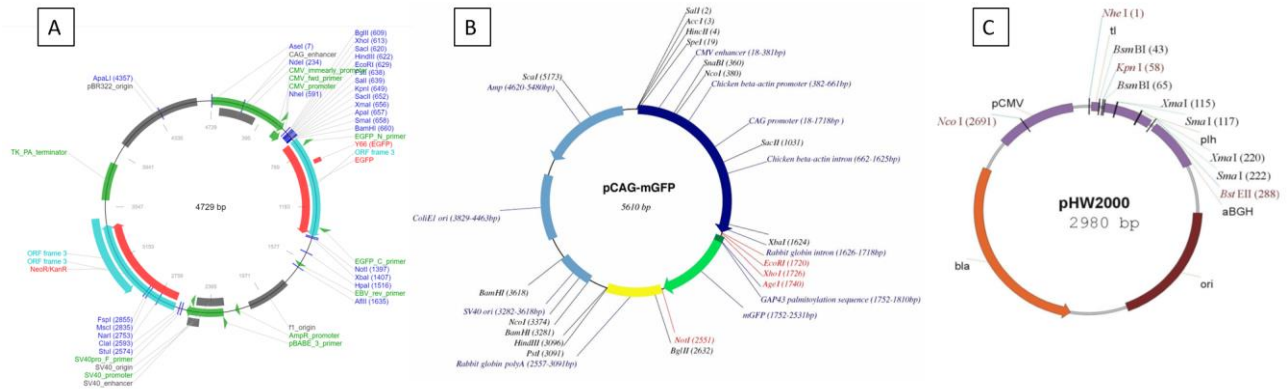

Figure 26: plasmids coding for A) GFP, B) mGFP, C) influenza proteins. Obtained from ref. [100]–[102]

Agarose solution was prepared containing antibiotic in 1:1000 dilution and poured in Petri dishes. The antibiotic added was chosen basing on the resistance given by each of the different plasmid. Ampicillin (MB02101 NZYTech) was used with influenza and mGFP plasmids and kanamycin (MB02001 NZYTech) for GFP plasmid.

The streaking technique was used to grow bacteria in the Petri dishes, which implies a zigzag distribution of bacteria in each plate to obtain single bacteria colonies. Every Petri dish contained a different bacteria culture expressing one of the different plasmids.

After an overnight incubation at 37 °C a single colony of bacteria was selected from each Petri dish and put in an Erlenmeyer containing 10 mL of LB solution (Sigma) and antibiotic in 1:1000 dilution. The Erlenmeyers were left to grow 37°C/shaking (200 rpm) for 8 hours.

New Erlenmeyers were used to transfer the bacterial cultures obtained. A 1:2000 dilution of each bacterial solution in 150 mL of LB solution was made, and antibiotic was added in a 1:1000 dilution. All the Erlenmeyers were put to grow 37°C/shaking (200 rpm) overnight, then the spectrophotometer (UV-VIS

Spectrophotometer UVmini -1240 – Shimadzu) was used to measure the absorbance at 600 nm, to have an approximate indication on bacterial density in the solution.

With the obtained bacterial solutions the Midiprep procedure was followed (GeneJET plasmid Midiprep kit from Thermofisher (K0481) [106]) to extract and purify plasmids of each type. In the end NanoDrop (Nanodrop ND-1000 Spectrophotometer) was used to calculate the DNA concentration of the five different samples. The plasmids were aliquoted and kept at -20°C.

3.2 Cell culture

The expression system used was COS7, a mammalian cell line obtained from monkey kidney tissue (ACTT CRL-1651).

Frozen cells were kept at -80° C in a solution of full DMEM (Dulbecco's modified Eagle's medium, Sigma Aldrich) and 5% of DMSO (dimethyl sulfoxide, Sigma Aldrich). To defreeze them, the vial containing cells was located in a 37°C bath and gently swirled until there was almost no ice left. Then 1 mL of full DMEM at 37°C was added in the vial, mixed, and then the whole volume was added in a tube containing 9 mL of full DMEM (37°C). The sample was centrifuged at 300 g for 7 minutes.

The supernatant was removed from the tube and 4 mL of new full DMEM at 37°C were added. 4 mL of full DMEM (37°C) were put in an 8 mL flask and finally the cell solution was added. The flask was kept in a cell incubator (37°C, 5% CO2). Cells were kept like that 7-10 days before using them.

Cell pass was performed every 4-5 days to maintain a confluency of approximately 80-90%. First cells were checked under the optical microscope to evaluate health and confluency. Full DMEM was removed and the flask was washed with 5 mL of PBS at 37°C, then 1 mL of trypsin was added (37°C) and left in the flask for 2-3 minutes to permit the disattachment of the cells from the bottom. At this point 7 mL of full DMEM (37°C) were added to block trypsin action. In a new flask full DMEM (37°C) and a fraction of the cell solution were added, to arrive at a final volume of 8 mL. The dilution made was decided each time depending on the confluency of the cells, but it was approximately 1:10.

The remaining cell solution was discarded and the new flask was kept in the incubator.

3.3 Transfection with GFP and mGFP plasmids

COS7 cells were seeded in 8 well glass bottom labteks and left there overnight. The medium used was full DMEM at 37°C. The following day transfection was performed using Lipofectamine 2000 reagent (Thermofisher) (figure 27 [107]). The samples were divided in three groups: transfection with GFP plasmids, transfection with mGFP plasmids and control (no transfection) (figure 28).

First, DNA solutions and lipofectamine solutions were prepared in serum free DMEM at 37°C, mixed together in accordance with the protocol of the company (serum free DMEM was used instead of Opti-MEM medium) [107] . Labteks containing cells were washed with PBS at 37°C and the DNA/lipofectamine solution was added to each well. In the control wells there was only serum free DMEM. After 4 hours serum free DMEM was removed from the wells, the labteks washed with PBS at 37°C and the cells incubated with new full DMEM at 37° C.

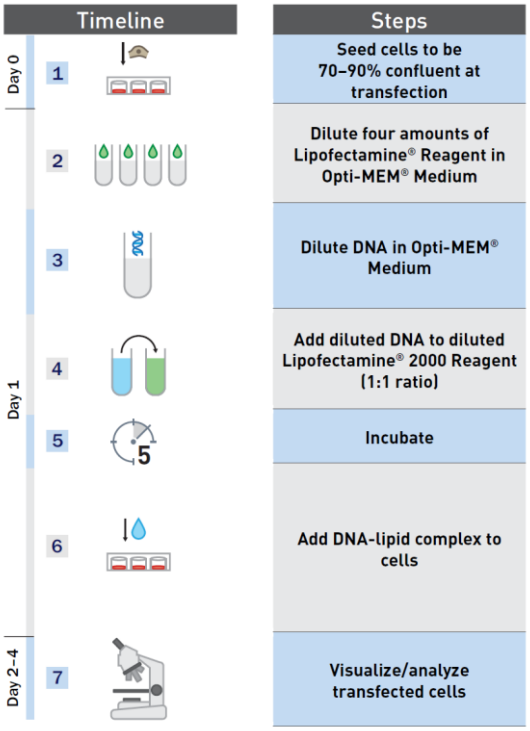

Figure 27: transfection protocol. Obtained from ref. [107]

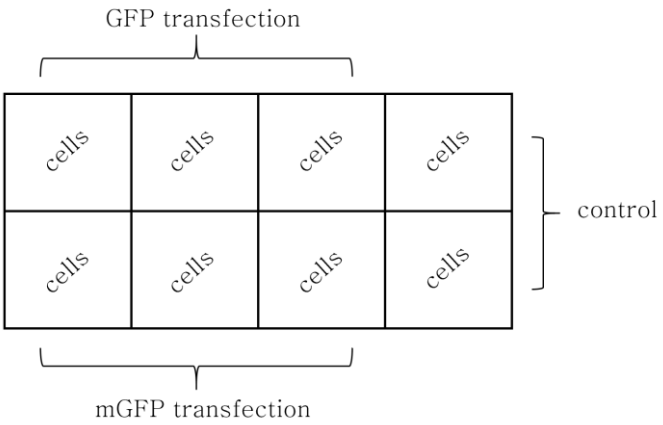

Figure 28: scheme of a labtek used for transfection. The cells are divided in three groups basing on the type of plasmid they will be transfected with.

After the incubation time, cells were washed with PBS at room temperature and fixed with 4% paraformaldehyde (PFA) for 15 minutes. The samples were stored at 4°C with PBS 1x.

Different trials of transfection were performed with both GFP and mGFP varying three parameters: DNA amount per well was tested between 0,1 µg and 2 µg, lipofectamine amount per well was tested between 0,1 µL and 0,8 µL and incubation times checked were 24, 48 and 72 hours (table 7).

Type of wells	8 well labteks
Plated cells per well	2-4 x 10^4 cells
Amount of DNA per well	0,1 to 2 µg
Amount of lipofectamine per well	0,1 to 0,8 µL
Final volume per well	200 µL
Incubation time	24-48-72 hours

Table 7: settings for transfection with GFP and mGFP plasmids

Fluorescence microscopy

To check the results of the transfection, fluorescence microscopy (Nikon Eclipse Ti2) was used. Microscopy parameters were set as follows: objective was 40x in oil immersion and exposure time was 100 ms. For the GFP channel, excitation wavelength was 490 nm with a LED power of 30%, while for bright field images the white light was regulated according to the sample, so as the contrast range of the image.

To evaluate the transfection two parameters were considered, the transfection ratio (transfected cells/total cells) and the average intensity of fluorescence in transfected cells. In both cases the analysis has been performed with software Fiji.

3.3.1 Transfection ratio

To count the total number of cells bright field images of the samples were used, considering for each tested parameter between 120 and 150 cells. Cells were manually counted using the cell counter plug-in of ImageJ.

Starting from that selected group of total cells the number of transfected cells were counted in the GFP channel images. Two different ways were used to calculate the number of transfected cells, a manual and an automated method.

Manual method

The manual method was based on the same cell counter plug-in used to count cells in the bright field. An appropriate contrast range of the image was selected by eye and all the fluorescent cells were counted manually. With the same set of total cells, the count of fluorescent cells for each parameter was performed in triplicate.

Automated method

The automated count was again performed in Fiji starting from Christine Labno method [108] and was used to evaluate the transfection trials with the same amount of lipofectamine and the varying amounts of DNA plasmids, both for GFP and mGFP transfections. Stating from the initial grayscale image (figure 29A), a threshold level was selected to obtain a binary image using IsoData algorithm; two ranges were in this way created, the first was a lower range, from 0 to the selected threshold level, and it represented the black background, while the second was the upper range, from the selected threshold level to the maximum grayscale value, 65 535, and it represented the white areas to count (figure 29B). Then the Watershed filter was used (figure 29C) to separate attaching cells. In the “Analyze Particles” window, an area threshold of 500 μm^2 was selected, to only include in the count particles of that size or bigger. In the end, the processed image was obtained, showing the outlines of all the resulting areas automatically counted (figure 29D).

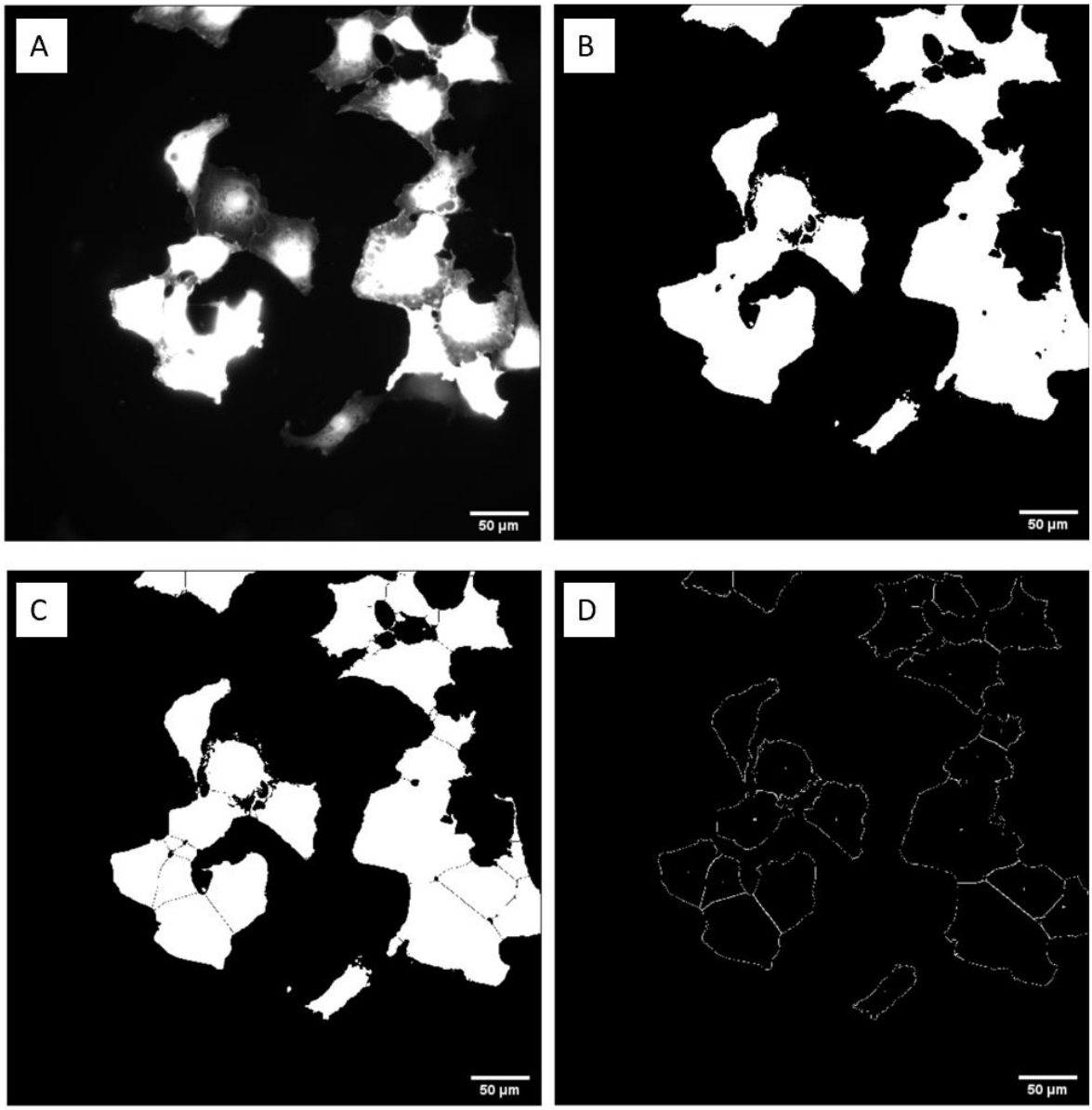

Figure 29: automated count. A) Initial gray scale image B) binary image C) application of the Watershed filter to separate cells D) outlines of the resulting areas automatically counted

Two different approaches to analyze the images were considered: the first way was to set the same exact parameters to all the images, obtaining an automated count. The parameters were the following: the threshold level was 12 000 (black range: 0 to 12 000, white range: 12 000 to 65 535), the threshold algorithm was IsoData, then it was applied the Watershed filter and the area threshold was 500 µm².

The second way was to choose and evaluate the parameters image by image, so it was a semi-automated method. In this way, the appearance of each image was taken into consideration and the parameters were selected accordingly, to try to have a more specific result. The parameters that remained the same were the application of IsoData algorithm and the Watershed filter, and the threshold area that was still 500 µm². The

threshold level set at the beginning could vary, depending on the overall brightness of the image (figure 30). In some images, where there were a lot of cells of different brightness, two threshold levels were applied to try to include the less bright cells in one range and the more bright ones in another range (figure 31); the specific values of the ranges were selected case by case. Another parameter considered in this alternative approach was the circularity of the selected area, found in the "Analyze Particles" window and used to discard noise coming from long and irregular shapes.

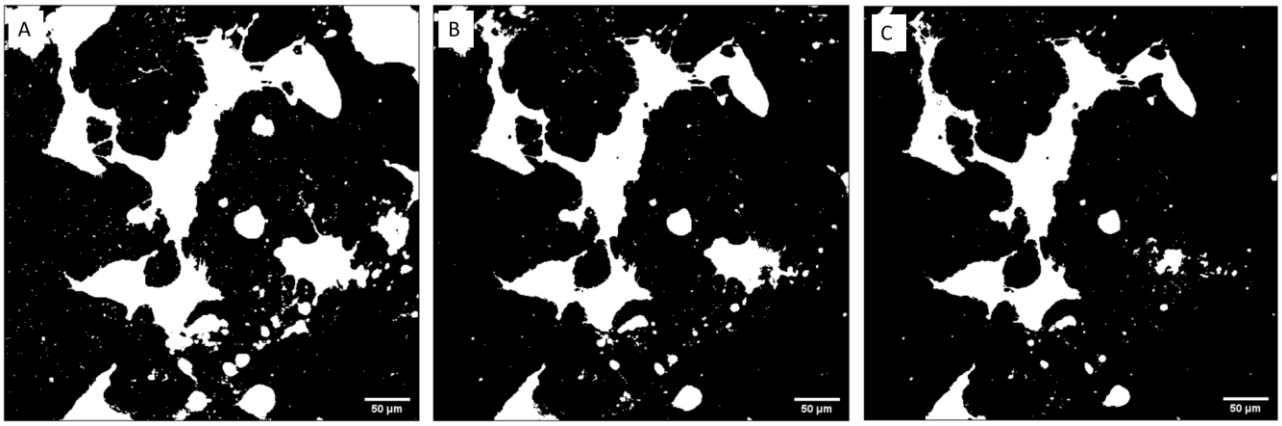

Figure 30: the binary image changes varying the threshold level. In this example, the threshold level is A) 6000, B) 12 000 and C) 18 000

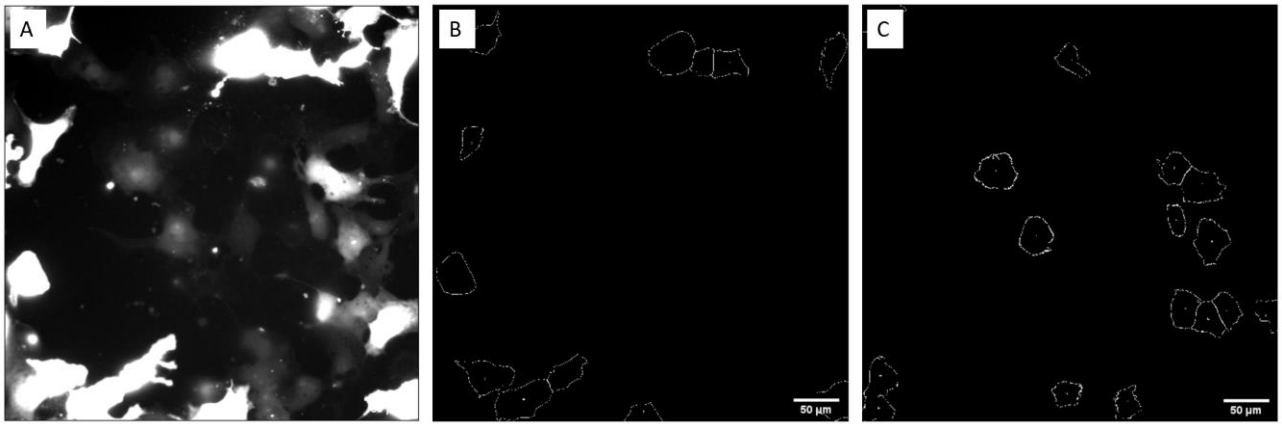

Figure 31: application of two ranges. A) initial grey scale image B) outlines of the brighter cells. The white range in this case was from 30 000 to 65 535 C) outlines of cells with lower brightness. The white range was in this case from 6 000 to 25 000

3.3.2 Average intensity of fluorescence

To measure the average intensity of transfected cells, between 20 and 25 fluorescent ROIs in the GFP channel were considered for each tested parameter; each ROI consisted of 1 to 3 cells. When it was not possible to arrive at 20 ROIs because the transfected cells were too few, all the fluorescent cells present were

considered. To take into account possible background signals, the average intensity of a blank area was subtracted to each ROI intensity.

The intensity of each ROI was calculated as the average of the grayscale value of all the pixels present in that ROI. Having 16 bit images, the grayscale ranged between 0 and 65 535. The procedure was performed for both GFP and mGFP transfection, in the different trials with the changing parameters.

3.4 Transfection with GFP, mGFP and Influenza plasmids

Two groups of transfection were first considered, one with only influenza plasmids (HA + NA + M) and one with influenza plasmids and GFP plasmid. The parameters for the first group of transfection were set as 2 µg of DNA per well (0,67 µg each type of plasmid) and 0,8 µL of lipofectamine per well. For the second group, the amounts of influenza plasmids were kept the same and 0,5 µg of GFP plasmid was added. In this group the lipofectamine amount per well was tested between 0,8 µL and 1,6 µL (table 8).

Once the amount of lipofectamine used for the second group was decided, it was also used for a third group of transfection, with influenza plasmids and mGFP plasmid.

The main transfection protocol was the same followed before. The incubation time was set at 48 hours.

Type of wells	8 well labteks
Plated cells per well	2-4 x 10^4 cells
Amount of DNA per well	2 µg (first group) 2,5 µg (second group) 2,5 µg (third group)
Amount of lipofectamine per well	0,8 µL (first group) 0,8 to 1,6 µL (second group) Optimized amount from second group (third group)
Final volume per well	200 µL
Incubation time	48 hours

Table 8: settings for transfection with GFP, mGFP and influenza plasmids

After fixing with PFA, an immunostaining step was performed to allow the visualization of influenza proteins with fluorescence microscopy. First cells were incubated with bovine serum albumin (BSA, Sigma Aldrich) 1%

w/v and glycine (Sigma Aldrich) 0,3 M in PBS for 30 minutes at room temperature (blocking step). Then the primary antibody was added in a concentration of 3 µg/mL in 1% BSA and left soft shaking for 1 hour at room temperature. The primary antibodies used were mouse anti-HA, mouse anti-M2 and rabbit anti-NA (Vitro; Abcam). Since both HA and M2 were linked to mouse antibodies, only one of the two proteins could be stained in the same well.

The samples were washed three times with PBS at room temperature, then secondary antibodies were added in a concentration of 8 µg/mL in BSA. Rabbit anti-mouse secondary antibody was linked to dye Alexa-647 and used to show either HA or M2, while goat anti-rabbit secondary antibody was linked to dye Alexa-488 and used to show NA. The sample was left soft shaking for 1 hour at room temperature, then washed with PBS three times and stored at 4°C. Since excitation wavelength of Alexa-488 is almost the same as GFP, it could only be visualized where GFP or mGFP were not used, so in the transfection group with only influenza plasmids.

In the end, a two colors visualization was possible on the same sample: GFP or mGFP with either HA or M2, and NA with either HA or M2. In this last case the incubation of secondary antibodies had to be performed sequentially because of the two antibodies that can produce crosslinking (rabbit antibodies and anti-rabbit antibodies). So first the goat anti-rabbit was added, and after 1 hour soft shaking and a washing step with PBS, the sample was also incubated with rabbit anti-mouse.

Microscopy images of the second group of transfection (influenza proteins + GFP) were analyzed to optimize the amount of lipofectamine per well. To evaluate the transfection, the transfection ratio and the average fluorescence intensity of GFP transfected cells were again considered. This time, for the cell count it was only used the manual method, while the quantification of fluorescence intensity was performed in the same way as before.

To evaluate the expression of influenza proteins, 490 nm was set as excitation wavelength for Alexa-488 and 660 nm for Alexa-647, while the other parameters were kept as previous analysis. To compare the transfection of Influenza plasmids with and without GFP or mGFP, 20 ROIs for each case were considered and the average intensity of fluorescence was calculated. The results were compared with average intensity of two types of control, a control with no transfection and no immunostaining and a control without transfection with immunostaining.

A preliminary colocalization test was eventually performed to check if transfected cells were expressing Influenza proteins together with GFP or mGFP. This step was performed in the case of HA and M2 staining, because of the impossibility to stain NA with GFP and mGFP. 30 cells were considered for each parameter (HA with GFP, HA with mGFP, M2 with GFP and M2 with mGFP), and a manual count was used to check how many transfected cells combined the expression of the two proteins.

3.5 VLPs production and purification

To produce VLPs the same transfection protocol was used with the same groups of transfection (only influenza, influenza + GFP and influenza + mGFP), but in this case 24 well plates instead of labteks were used to obtain more VLPs (table 9). In the wells with only influenza plasmids the amount of DNA was 4 µg per well (1,33 µg each type of plasmid) and the lipofectamine was 2 µL per well. In the other two groups, the amount of influenza plasmids was the same, the amount of GFP and mGFP was 1 µg per well and the amount of lipofectamine was 2,8 µL per well. Each group of transfection was tested in triplicate. Three control-wells without transfection were also included.

Type of wells	24 well plate
Plated cells per well	6 x 10^4 cells
Amount of DNA per well	4 µg (first group) 5 µg (second group) 5 µg (third group)
Amount of lipofectamine per well	2 µL (first group) 2,8 µL (second group) 2,8 µL (third group)
Final volume per well	400 µL
Incubation time	48 hours

Table 9: settings for transfection to obtain VLPs

Cells were transfected as previously mentioned in a 24 well plate and after 48 hours of incubation time, the supernatant was collected from the three groups and the control. Supernatant was passed through a 0,45 µm pore size filter and centrifuged at 2500 g for 30 minutes.

A sucrose solution 60% w/v in PBS was prepared and left mixing in a stirring plate for 10 minutes. From this stock 11 serial dilutions were then obtained, with a total of 12 solutions with decreasing concentrations of sucrose in PBS, from 60% to 20% sucrose (figure 32). For each sample and for the control an ultracentrifugation tube was filled with the 12 layers of sucrose solutions (1 mL each layer), from the more to the least concentrated. On the top the sample and the control solutions were also added. The tubes were ultracentrifuged at 35 000 rpm at 4ºC for 2 hours.

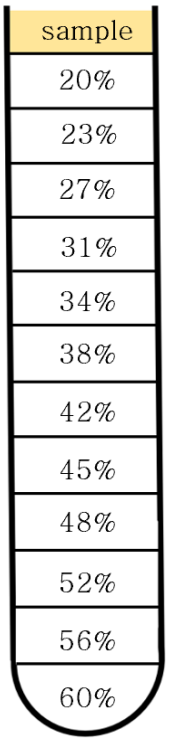

Figure 32: sucrose layers from 60% w/v (bottom) to 20% w/v (top)

The obtained solutions from each tube were collected and transferred to 6 Eppendorfs; each Eppendorf contained 2 mL of sucrose solution, which was 2 layers. From previous DLS measures, it was known that Eppendorf 4 was the one containing VLPs, so its content was considered and divided in three new Eppendorfs (0,6 mL each). To each Eppendorf 0,8 mL PBS were also added to dilute the sample.12 Eppendorfs were in total obtained (9 for the sample + 3 for the control) and ultracentrifuged at 40 000 rpm for 1 hour at 4°C.

From each of the 12 Eppendorfs the supernatant was discarded, and then the samples from the same type were recombined in one Eppendorf with 50 µL of PBS, obtaining at the end 3 VLPs Eppendorfs for the three different samples and 1 control Eppendorf. The VLPs were stored at 4°C in the dark.

3.6 VLPs characterization

The characterization of VLPs has been performed by Maria Arista, PhD student, due to the impossibility for me to access the laboratory during the COVID-19 pandemic.

It has been done through DLS (dynamic light scattering, Zetasizer Nano-ZS ZEN 3600 (Malvern Instruments, Germany)) and TIRF (total internal reflection fluorescence) microscopy. In DLS the sample was analyzed in a

dilution of 1:10 in PBS at 4°C. The measures were obtained for the three groups of VLPs (only influenza proteins, influenza proteins + GFP and influenza proteins + mGFP).

TIRF images were obtained for the VLPs containing either GFP or mGFP and were compared with the images of the control (no transfection). The parameters set at the microscope were the following: the excitation wavelength was 488 nm with a power of 4%, and the exposure time was 100 ms.

4. Results and discussion

4.1 Transfection with GFP and mGFP plasmids

The final goal of the thesis was to obtain VLPs with GFP and mGFP incorporated in them. Before the cell transfection with influenza proteins, an initial step of GFP/mGFP transfection optimization was performed. This optimization was performed to obtain the parameters for the best transfection efficiency; the parameters to optimize were three: the amount of DNA plasmids per well, the amount of lipofectamine per well and the incubation time. Having both GFP and mGFP plasmids, for each of them different trials of transfection have been performed changing DNA amount per well, lipofectamine amount per well and incubation time, and all of them are discussed in the next paragraphs.

In the end, to test the efficiency of each trial, two aspects were considered: the transfection ratio (fluorescent cells/total cells) and the average intensity of fluorescence.
In the first optimization process (optimization of DNA amount), three different methods were considered to obtain the transfection ratio, a manual and two automated methods, which have been subsequently compared.

4.1.1 Optimization of DNA amount

The transfection ratios (with manual count) and the average fluorescence changing the amount of DNA plasmids are shown in figure 33. The tested amounts of DNA vary between 0,1 µg per well to 2 µg per well, while other parameters are kept constant: the lipofectamine is 0,8 µL per well and the incubation time is 48 hours. The results are shown for both GFP and mGFP. For the statistical analysis of the data, a one-way ANOVA was applied, with Tukey test for the multiple comparisons (data not shown).

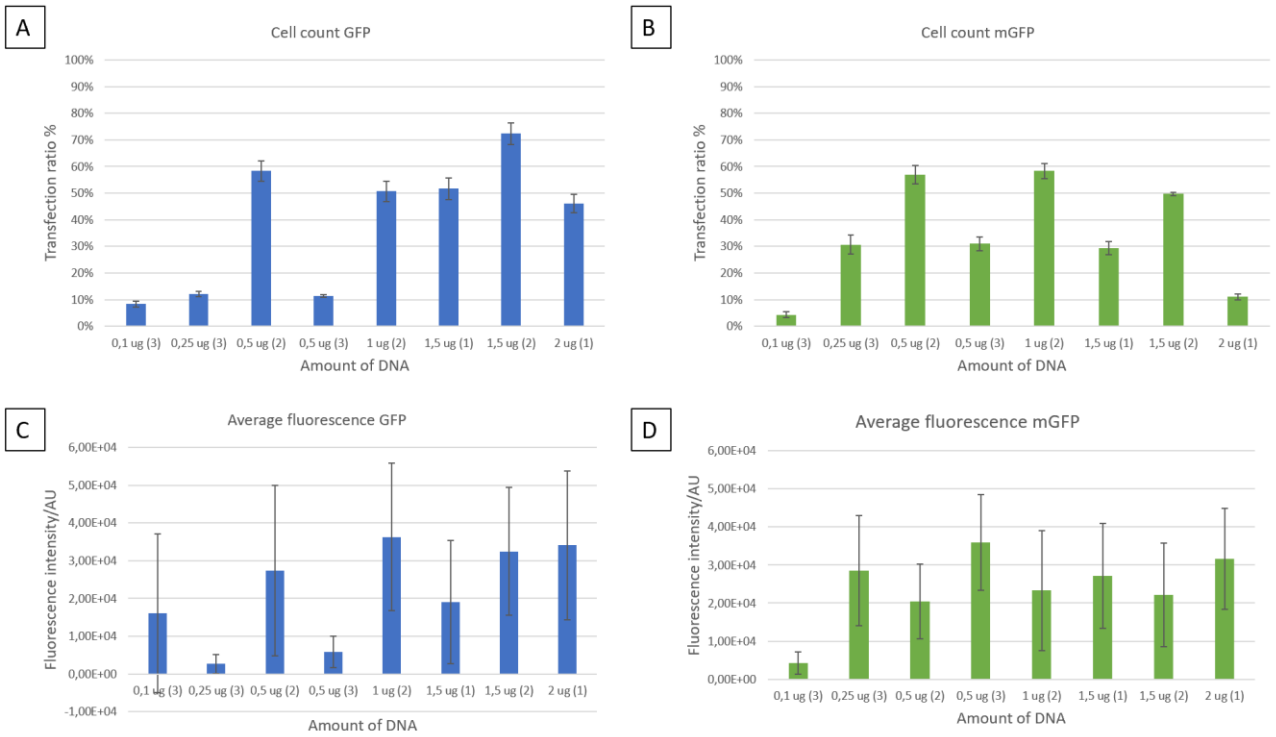

Figure 33: Evaluation of transfection varying DNA amount per well. A) Transfection ratio for GFP B) Transfection ratio for mGFP C) Intensity of fluorescence for GFP D) Intensity of fluorescence for mGFP. In parenthesis it is indicated the experiment where I used those parameters (trials 1, 2, 3). In all trials, lipofectamine amount is kept constant at 0,8 µL per well and the incubation time is 48 hours.

As it is possible to see from the resulting standard deviations, the cells' fluorescence was very variable, which is also visible from figure 34, where the same GFP data with a box plot (figure 34A) and a vertical scatter plot are plotted (figure 34B). In this part of the process the focus was taken to the transfection ratio rather than considering the variability of fluorescence intensity, because the final aim was to have GFP and mGFP inside the VLPs, so as long as a fluorescent signal was observed the result was considered positive. More importantly, the fluorescent cells all showed fluorescence intensities in an order of magnitude of 10^3 or 10^4, which was sufficient to allow an easy recognition under the fluorescence microscope.

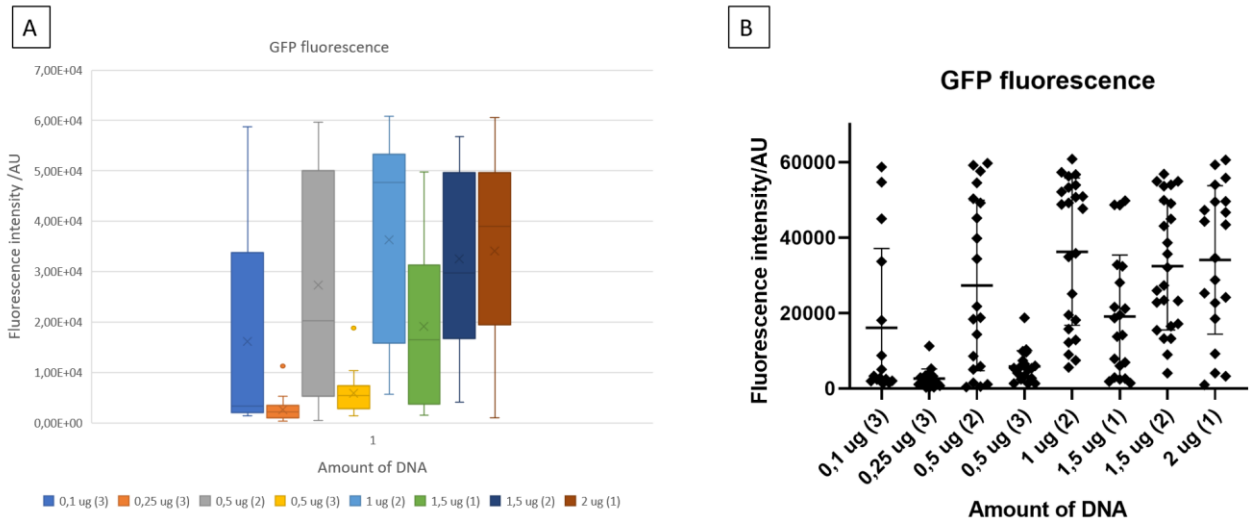

Figure 34: GFP fluorescence varying the amount of DNA per well showed in a box plot (A) and a vertical scatter plot (B). In all trials, lipofectamine amount is kept constant at 0,8 µL per well and the incubation time is 48 hours.

In general, the transfection process resulted very heterogeneous between the trials both from the point of view of the transfection ratio and the average intensity of fluorescence. Different parameters could influence the result, such as the general health of the cell line (number of passages, medium, confluency) and possible manual errors during the transfection process. An important factor influencing the final result for trial 3 (0,1, 0,25 and 0,5 µg of DNA) is that the live-cell imaging was performed, instead of fixed cells (trials 1 and 2). Thus, in this case, samples were kept outside the incubator for the whole time of the microscopy analysis, resulting in a major cell detachment and death. The effect of this was directly visible on the sample post-imaging, from the bright field images obtained at the microscope.

The average intensity of fluorescence was quite variable within the samples, especially in the cited samples (trial 3), but still reached 10^3 and 10^4 as orders of magnitude, which allowed a good visualization under the microscope.

The final choice of DNA amount per well for both GFP and mGFP transfection was 0,5 µg, which resulted in a good transfection ratio (about 60% for both GFP and mGFP) and good levels of fluorescence. Moreover, this choice was made over higher amounts of DNA to avoid the waste of DNA plasmids and to stay closer to the optimized amount of DNA used for the influenza plasmids transfection (already set at 0,67 µg each, previously optimized in the laboratory).

4.1.2 Comparison between manual count method and the two automated methods

The comparison between these different methods has been performed to evaluate new possible ways to count transfected cells, possibly faster than the traditional manual way. An automatized method could also avoid a subjective selection, thus resulting in a more reliable analysis.

The automated count was obtained applying the same exact parameters to each image where the count is performed (threshold range, filtering, threshold area), while in the semi-automated method the appearance of each image was taken into consideration, and the parameters were set accordingly, for example changing the threshold levels and applying more than one threshold when there were many cells with different levels of brightness.

For both GFP and mGFP transfection, it is shown the transfection ratio calculated with the manual method, the automated method and the semi-automated method. The results are shown in figure 35 and 36.

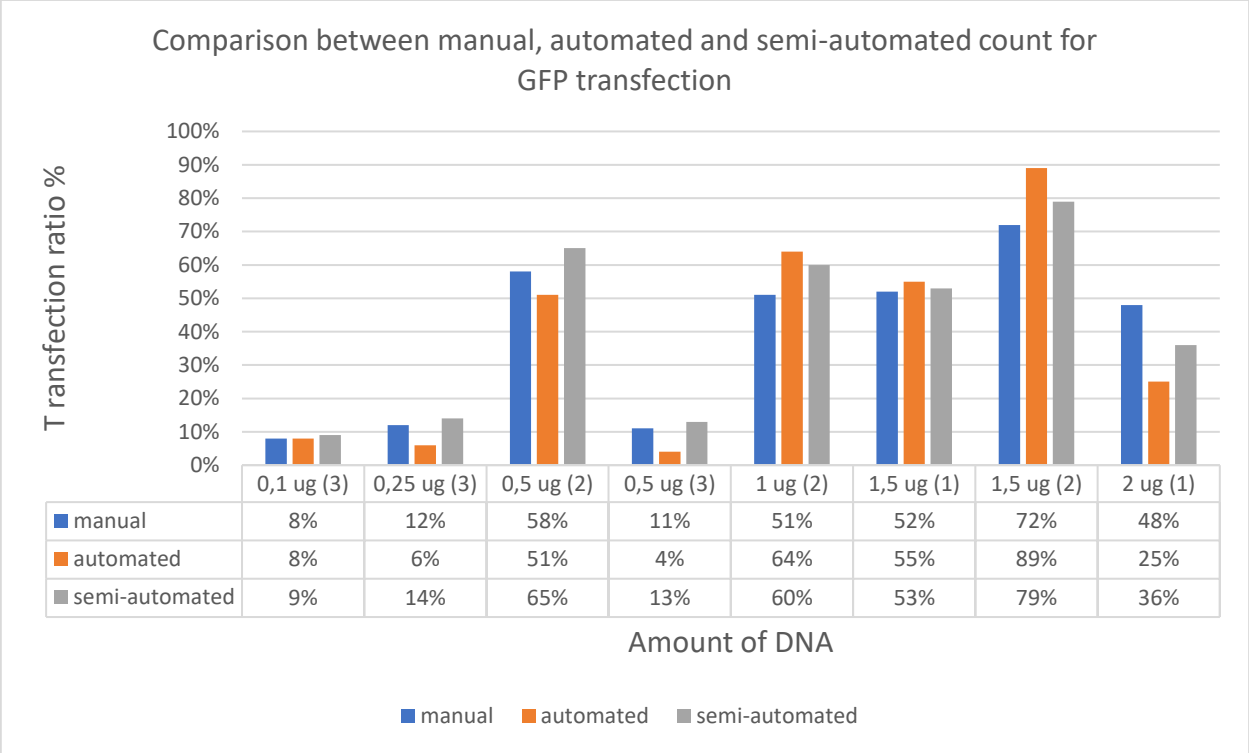

	0,1 ug (3)	0,25 ug (3)	0,5 ug (2)	0,5 ug (3)	1 ug (2)	1,5 ug (1)	1,5 ug (2)	2 ug (1)
manual	8%	12%	58%	11%	51%	52%	72%	48%
automated	8%	6%	51%	4%	64%	55%	89%	25%
semi-automated	9%	14%	65%	13%	60%	53%	79%	36%

Figure 35: counting methods in GFP transfection. For the manual method, it is reported the average value of three repetitions, while in the automated count it is reported the exact result automatically obtained.

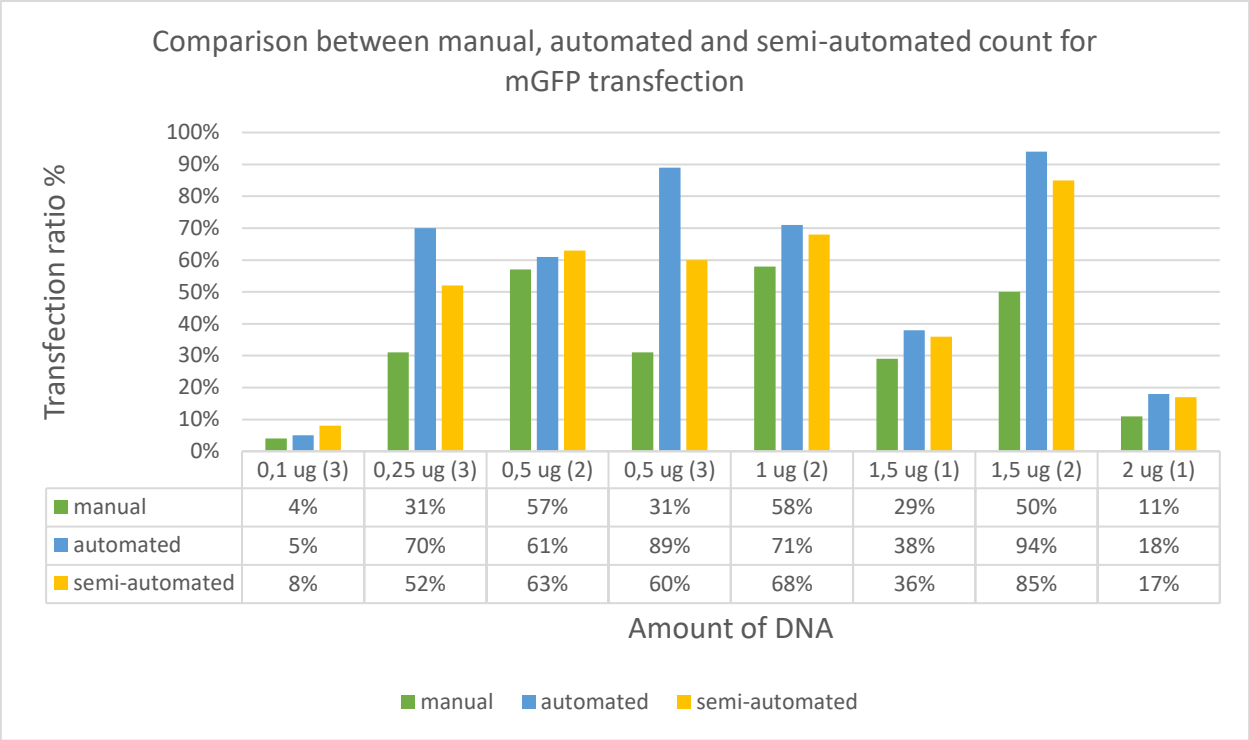

	0,1 ug (3)	0,25 ug (3)	0,5 ug (2)	0,5 ug (3)	1 ug (2)	1,5 ug (1)	1,5 ug (2)	2 ug (1)
manual	4%	31%	57%	31%	58%	29%	50%	11%
automated	5%	70%	61%	89%	71%	38%	94%	18%
semi-automated	8%	52%	63%	60%	68%	36%	85%	17%

Figure 36: counting methods in mGFP transfection. For the manual method, it is reported the average value of three repetitions, while in the automated count it is reported the exact result automatically obtained.

The semi-automated method resulted in cell counts generally more similar to the manual method, used as a reference, even though the percentages of the full-automated method still resulted decent in most of the cases.

The main drawback of this technique was its dependence on the appearance of the image itself: when the cells had a good contrast, they were not overlapping and not forming aggregates, and when in general the image did not present noise (detaching and dead cells, detaching parts of cells such as membranes), both the semi-automated and the automated method seemed to work properly (figure 37). On the other hand, if the image was too crowded or presented too many bright spots, the results started to differ from the reference values, and this aspect did not change going from the automated to the semi-automated method, because it was an intrinsic error of the image (figure 38).

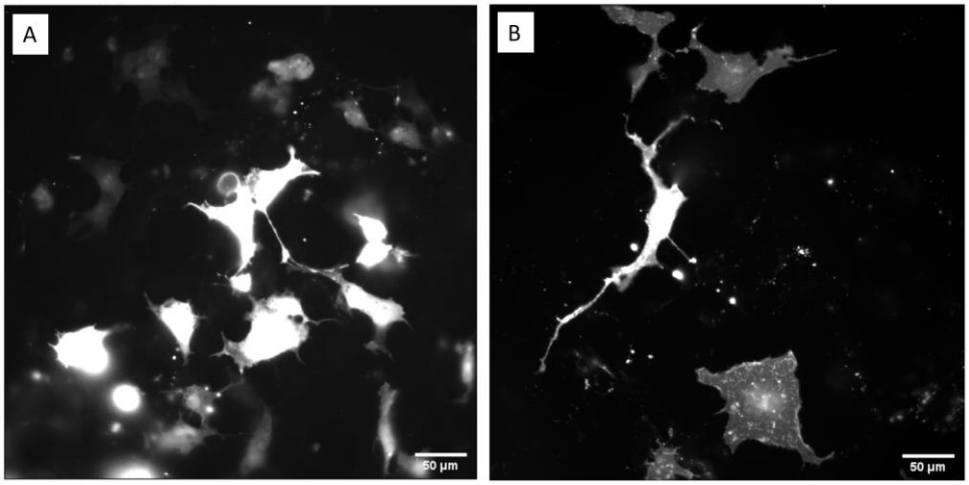

Figure 37: examples of images where the automated methods worked properly. The images are not overcrowded and there's a good contrast between fluorescent cells and the background. A) example of GFP transfection. The manual cell count was 24 and the automated was 22. B) example of mGFP transfection. The manual cell count was 5 and the automated was 6

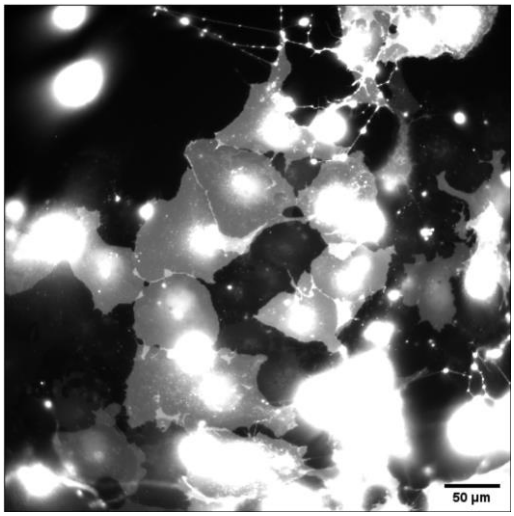

Figure 38: example of mGFP transfection. The acquisition was performed in live-cell conditions, which resulted in several cell detachment and death. For this reason the image appears very crowded and noisy, and both the semi-automated and the automated methods overcounted the total number of cells. The manual count was in this case 13, the semi-automated 26 and the automated 38

Another main issue was given by possible errors in the Watershed segmentation, which did not always result in a correct recognition of cells and possibly led to an overcounting effect (figure 39).

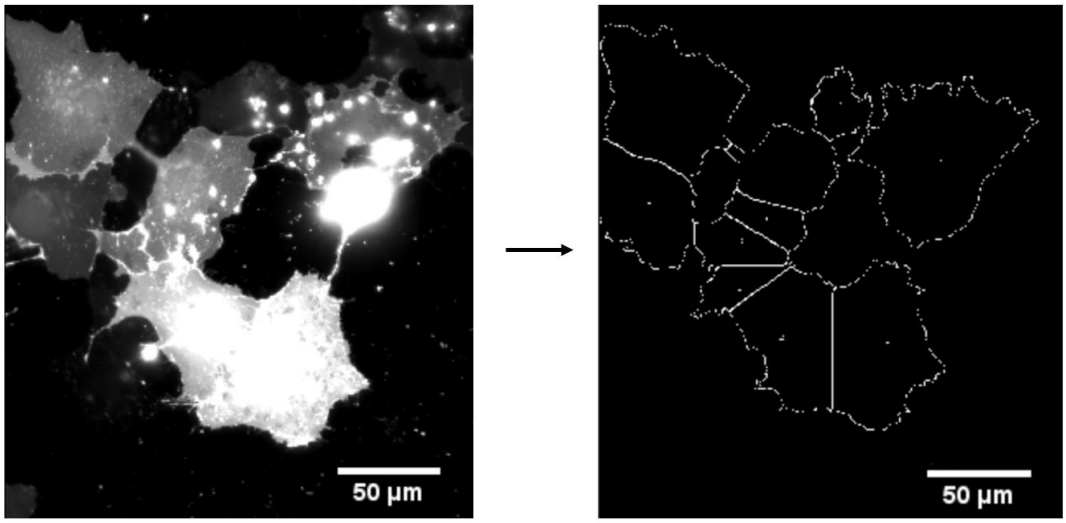

Figure 39: example of bad segmentation resulting in an overcounting

Moreover, it is interesting to note that in the automated method a “compensation” effect could occur: in figure 40A we see the initial gray scale image with red points indicating the manual count thus serving as reference to differentiate actual fluorescent cells from noise spots. In this case there were many cells with different levels of brightness, so in the semi-automated method two ranges were used to include in one of them the less bright spots and in the other one the brighter ones. The semi-automated count indicated 23 cells, differing by only one cell to the reference value (22). In the automated count (figure 40B) the result was 24, which is still very close. Anyway, comparing the two images, it is possible to see that the automated count missed some cells (the less bright were excluded from the white range), while it counts some areas that should not be considered (because they were noise spots or the result of bad segmentation), and this turned out in a compensation effect of the final result.

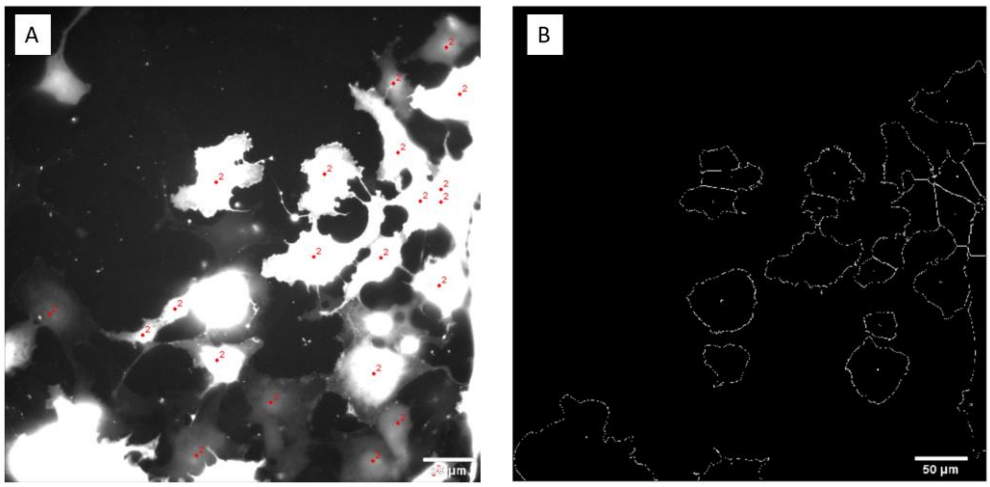

Figure 40: comparison between manual and automated count with a "compensation" effect. The manual count (A) results in 22 cells, and the automated count (B) is 24.

Another aspect to consider is the time needed to process these images: the manual method required a careful analysis of the image and a constant comparison with the bright field image to differentiate between fluorescent cells and other types of bright spots. Each image required between 3 and 4 minutes to be analyzed; moreover, being a manual count, it required the test to be performed in triplicate, to have a more accurate result. The semi-automated method was faster but still challenging because the parameters, for each image, could be changed different times before finding the most convincing ones for that specific image. The time needed could vary from 2 to more than 3 minutes, when different parameters were changed to find the most suitable one. In this case, the test was not performed in triplicate, because once you have set the parameters, the results will be all the same. The automated method was surely the fastest alternative: it required an initial optimization to find the parameters to set, but then the same parameters would be applied to all the images without any change. Each image required 20-30 seconds to be analyzed, and also in this case there was no need to perform the test in triplicate.

I still find the manual method as the most reliable alternative, because the different appearances of the images and the choice of parameters in the two automated methods could significantly influence the final results. Also, as mentioned before, there were some intrinsic errors in the automated count that could not be excluded and again depend on the specific appearance of the image.

4.1.3 Optimization of lipofectamine amount

Both GFP and mGFP transfection were evaluated with different amounts of lipofectamine per well, from 0,1 µL per well to 0,8 µL per well (figure 41). Amount of DNA and incubation time were kept constant (0,5 µg per well and 48 hours). For the statistical analysis of the data, a one-way ANOVA was applied, with Tukey test for the multiple comparisons (data not shown).

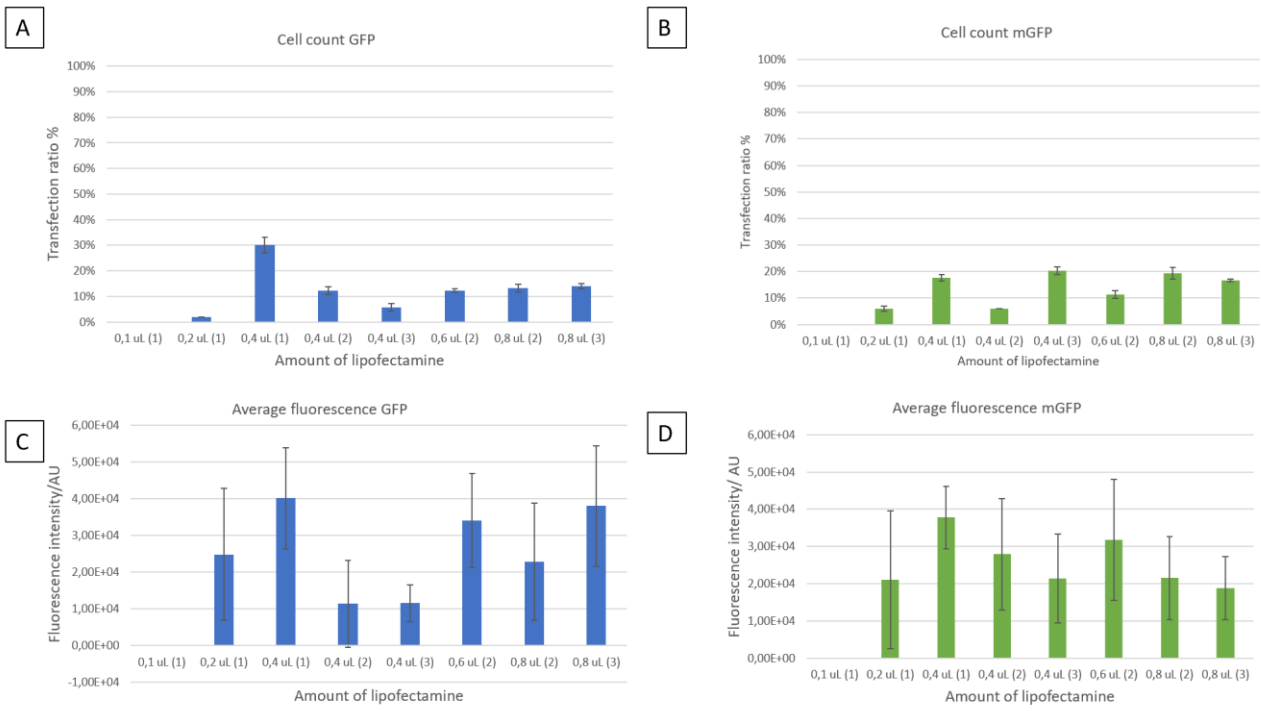

Figure 41: evaluation of transfection varying lipofectamine amount per well. A) Transfection ratio for GFP B) Transfection ratio for mGFP C) Intensity of fluorescence for GFP D) Intensity of fluorescence for mGFP. In parenthesis it is indicated the experiment where I used those parameters (trials 1, 2, 3). In all trials, DNA amount is kept constant at 0,5 µg per well and the incubation time is 48 hours.

As for the optimization of DNA amount, the results were quite heterogeneous and, from the point of view of transfection ratio, very inconsistent. The reasons could again include several aspects regarding the cell viability, confluency and possible manual errors in the transfection protocol. With the lack of a consistent result for this parameter it was decided to move on to a new optimization process of lipofectamine amount in the transfection with GFP/mGFP and influenza plasmids.

4.1.4 Optimization of incubation time

Both GFP and mGFP transfections were tested in three consequent days to evaluate three different incubation times: 24, 48 and 72 hours. The analysis was performed in live-cell conditions, so, after the transfection, the cells were kept in the incubator for 24 hours, then analyzed for the first time, then kept again in the incubator for 24 hours, analyzed a second time, kept for the last 24 hours in the incubator and analyzed for the last time.

The test was performed keeping constant the amount of lipofectamine (0,8 µL per well) and varying the amount of DNA (0,1, 0,25 and 0,5 µg per well) (figure 42). For the statistical analysis of the data, a one-way ANOVA was again applied, with Tukey test for the multiple comparisons (data not shown).

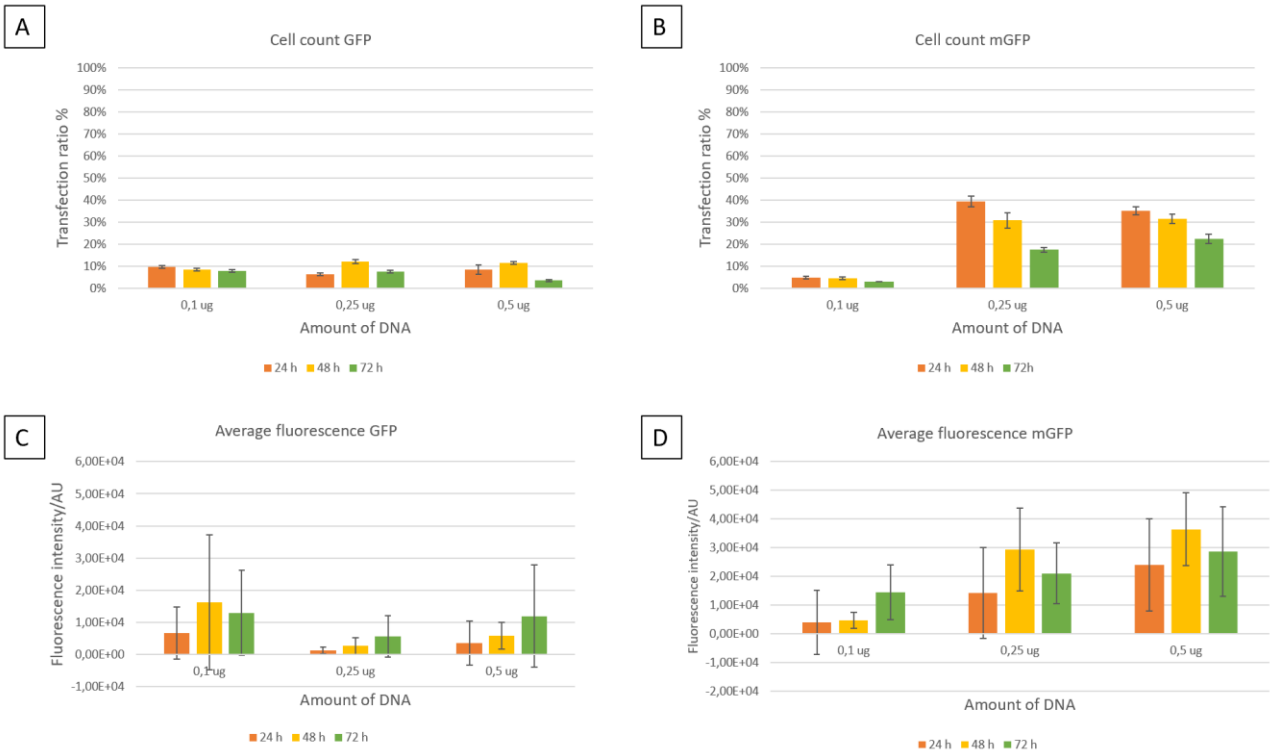

Figure 42: evaluation of transfection at different incubation times varying DNA amount per well. A) Transfection ratio for GFP B) Transfection ratio for mGFP C) Intensity of fluorescence for GFP D) Intensity of fluorescence for mGFP. In all trials, lipofectamine amount is kept constant at 0,8 µL per well.

This process was the most affected by the fact that analysis was performed in live-cell conditions. Indeed, after 24 hours of incubation, cells were brought to the microscope to be analyzed, then brought back to the incubator and analyzed again after 48 hours of incubation. The fixation with PFA was done only at the end, after 72 hours of incubation. Despite the microscopy environment was controlled (37°C, 5% CO_2, 60% humidity) the cells suffered the moving from one place to the other, resulting in cell detachment and death.

In the end, 48 hours was selected as preferred incubation time because it generally showed the best results both from the point of view of transfection ratio and average intensity of fluorescence.

In mGFP expression, 24 hours of incubation time also was a possible alternative because it resulted in better transfection ratios. In the successive VLPs production an idea to increase protein expression was indeed to use 24 hours as incubation time for mGFP and 48 hours for influenza proteins, but it was not possible to further investigate this aspect due to the impossibility to access the laboratory in the final stages of my internship.

4.2 Transfection with GFP, mGFP and Influenza plasmids

After the initial optimization of the expression of GFP and mGFP in mammalian cells by transfection, the optimization of the co-expression of the previous proteins with influenza proteins was performed. This way it was possible to study if Influenza proteins could be co-expressed with GFP and mGFP to subsequently obtain VLPs with those fluorescence proteins.

For this purpose, another type of transfection was evaluated. In this case, together with GFP and mGFP, the influenza plasmids were used, so the expression of all these proteins on transfected cells was checked.

Three groups of transfection were considered, one group with only influenza plasmids, one with influenza and GFP plasmids and one with influenza and mGFP plasmids. The first group of transfection was already previously optimized in the laboratory in terms of DNA amount and lipofectamine amount per well, while the second and the third group were optimized in terms of DNA amount and incubation time, but not in terms of lipofectamine amount per well, because the previous lipofectamine optimization didn't bring any consistent result.

The first step, then, was the optimization of the lipofectamine amount in the group of transfection with influenza and GFP plasmids. Different trials have been considered changing the amount of lipofectamine and then the transfection ratio and the average intensity of fluorescence have been calculated. The optimized parameters were then used for the third group as well, where there were influenza and mGFP plasmids.

The second step consisted in the evaluation of the expression of influenza proteins in these three groups of transfection and the comparison between them. The evaluation has been performed through the analysis of the intensity of fluorescence in the different cases.

The two steps have been summarized in table 10:

Group of transfection	**Step 1: optimization of lipofectamine amount**	**Step 2: evaluation of influenza proteins' expression**
1 - Only influenza plasmids	NO (parameters were already set)	YES
2 - Influenza + GFP plasmids	YES	YES
3 - Influenza + mGFP plasmids	NO (optimized parameters from group 2 have been used)	YES

Table 10: study of transfection groups with influenza plasmids

4.2.1 Optimization of lipofectamine amount in transfection with GFP and Influenza plasmids

Transfection with influenza plasmids and GFP was performed in different trials to optimize the amount of lipofectamine per well (figure 43). The amounts of DNA plasmids were 0,67 µg per well for influenza plasmids and 0,5 µg per well for GFP plasmid, while the incubation time was 48 hours.

The evaluation was done based on the results of transfection ratio (manual method) and average fluorescence of GFP. One-way ANOVA with Tukey test for the multiple comparisons were applied (data not shown).

A

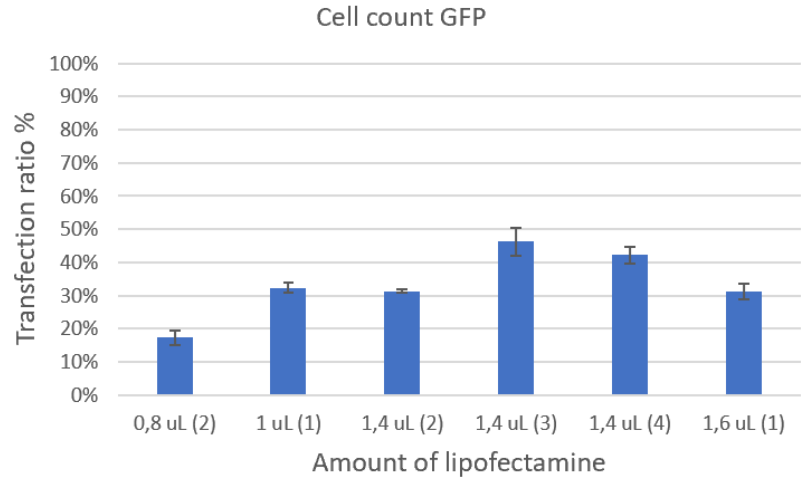

B

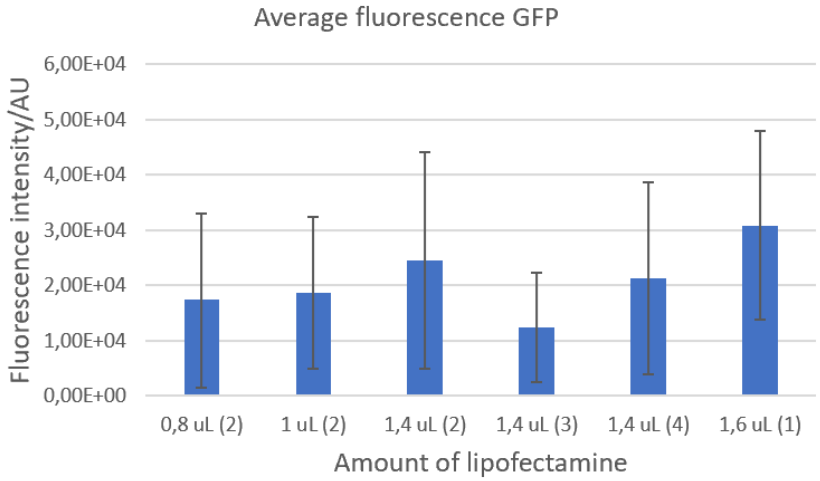

Figure 43: evaluation of transfection with influenza plasmids and GFP plasmids varying the amount of lipofectamine per well. A) Transfection ratio B) Average intensity of fluorescence. In parenthesis it is indicated the experiment where I used those parameters (trials 1, 2, 3)

From the different lipofectamine amounts in the transfection process with influenza and GFP plasmids, the final amount of lipofectamine per well was chosen to be 1,4 μL per well. Despite the transfection ratio changes in the different trials with same DNA amounts, the average intensity of fluorescence in all cases was maintained at the same order of magnitude.

The final choice for the lipofectamine amount was also used in subsequent transfection with influenza plasmids and mGFP.

4.2.2 Evaluation of Influenza proteins' expression

The transfection of influenza plasmids was evaluated in the three groups of transfection (influenza plasmids alone, influenza plasmids + GFP plasmids and influenza plasmids + mGFP plasmids). The amounts of DNA plasmids were 0,67 μg per well for influenza plasmids and 0,5 μg per well for GFP/mGFP plasmids while the incubation time was 48 hours. The lipofectamine amount per well was 0,8 μL in the first group (only influenza plasmids) and 1,4 μL per well in the second and third group (influenza plasmids + GFP and influenza plasmids + mGFP).

The immunostaining process included the incubation with primary antibodies against the expressed influenza protein (HA, NA and M2) and an incubation with a secondary antibody labeled with a fluorescent dye, used in fluorescence microscopy to detect the proteins.

The intensity of fluorescence was compared with two controls, one with no transfection and immunostaining and one with no transfection and no immunostaining (figure 44).

NA was labeled with dye Alexa-488, which has almost the same excitation wavelength as GFP and mGFP, so its transfection could be only evaluated in the group with only influenza plasmids.

In this case the results are shown in a vertical scatter plot: this transfection process indeed results in an intensity which in visibly inferior compared with GFP/mGFP transfections. So, it was more convenient to analyze a little more in detail the distribution of results.

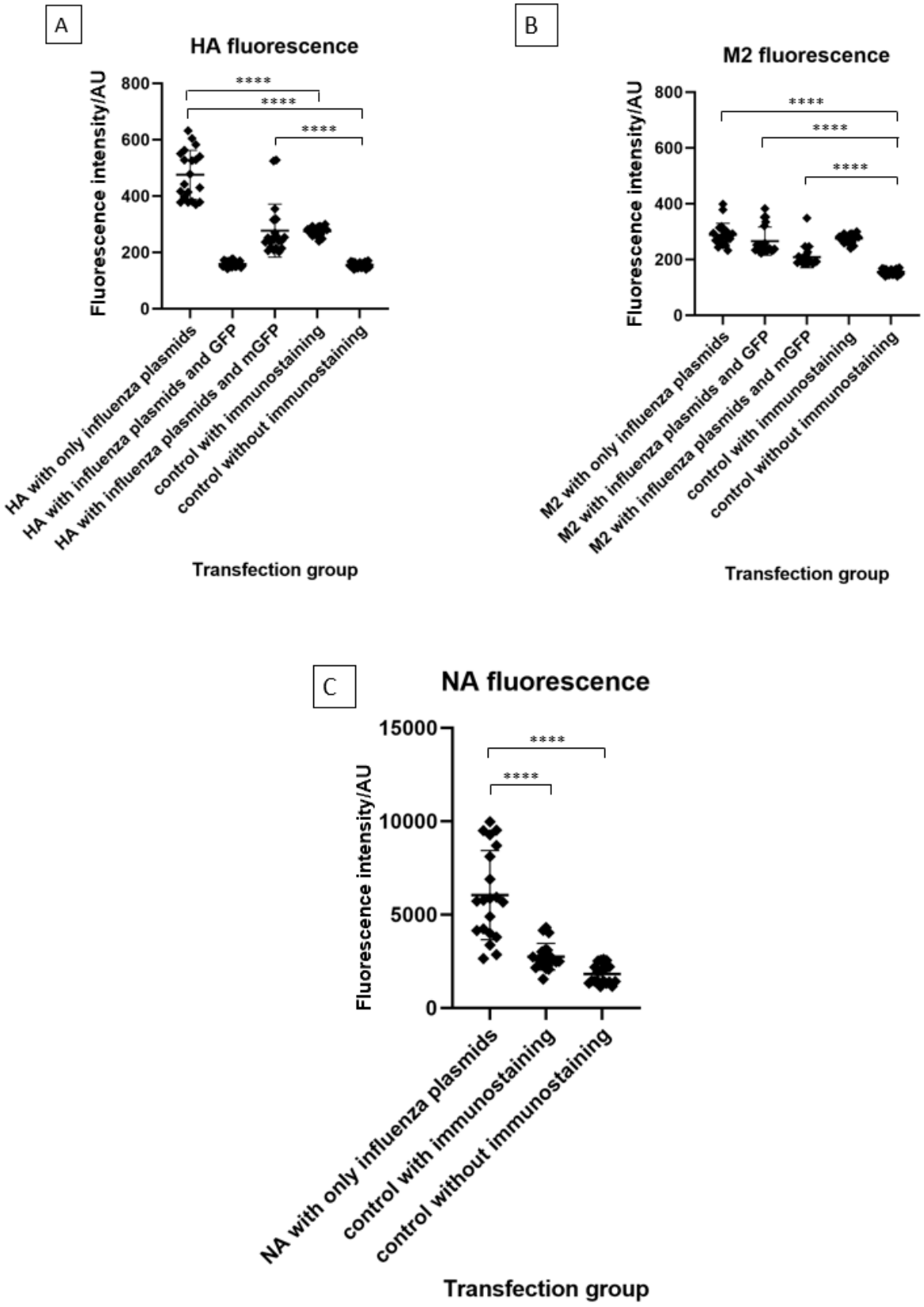

*Figure 44: intensity of fluorescence in the different groups of transfection. A) HA fluorescence B) M2 fluorescence C) NA fluorescence. ****p<0,0001.*

In figure 45 it is shown the Influenza proteins' expression in the three groups of transfection. Given the different levels of transfection in HA case, to allow a visualization in all three groups it was needed to apply different contrast ranges to the images, so the comparison between the three cases is just qualitative. In the case of M2 the contrast ranges are the same in all three groups.

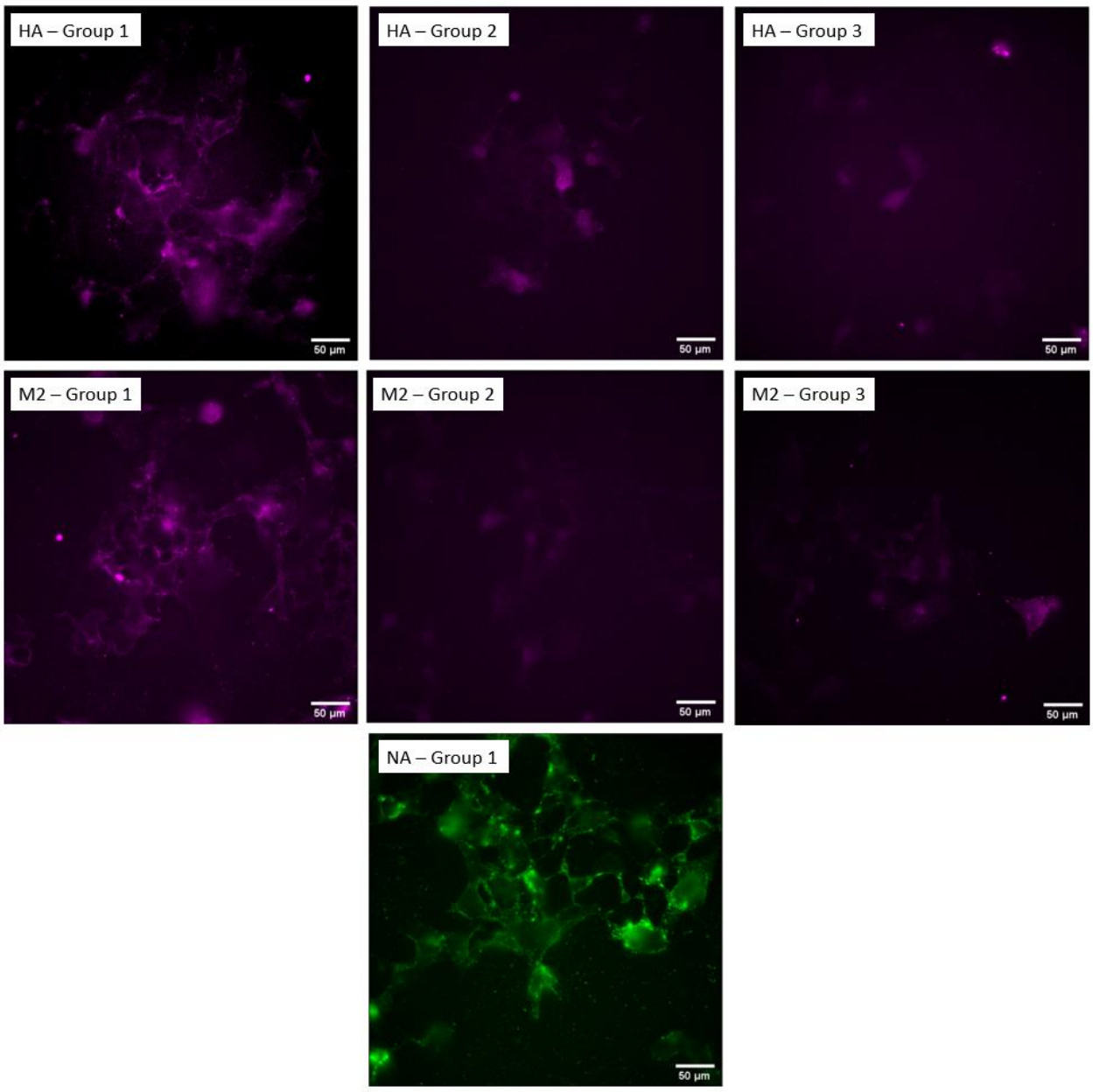

Figure 45: Cell expression of Influenza proteins in the three groups of transfection. Group 1: transfection with only influenza plasmids, Group 2: transfection with GFP and Influenza plasmids, Group 3: transfection with mGFP and Influenza plasmids.

The intensity of HA and M2 fluorescent signals were much lower compared to NA signal. This could be due to the fact that it was not possible from the microscopy setting to select an appropriate excitation wavelength

for dye Alexa-647 (the closest one was 660 nm, the one used), while the match between dye Alexa-488 and its excitation wavelength (490 nm) was definitely more appropriate.

NA expression showed a significant difference compared with the two controls, and also in the HA case, in the group where the transfection only included influenza plasmids, the results were significant compared with the two controls. In M2 case, the difference between the three samples and the control with immunostaining were not visible, indicating a poor transfection efficacy possibly given by the fact that M2 is the less abundant in Influenza proteins' expression. Another possible reason of M2 result would be a manual error in the immunostaining protocol, since the volumes involved were small and thus very delicate. Again, it was not possible to replicate the experiment, given the impossibility to access the laboratory during to the COVID-19 pandemic.

The important aspect, visible in HA case, is the decrease of transfection efficacy when influenza plasmids were coupled with either GFP or mGFP. The strength of the promotors used in the different plasmids could influence this aspect, creating a sort of competitive format leading to the decreased expression of influenza proteins. Also, both influenza and GFP plasmids used the same promotor, CMV, which again could interfere with the protein expression.

Colocalization count

A preliminary colocalization test was performed on transfected cells to check if it was possible to achieve, on the same cells, the co-expression of either GFP or mGFP and influenza proteins. Images from group 2 and 3 of transfection (transfection with influenza plasmids and either GFP or mGFP plasmids) were studied, considering both HA and M2 staining. In each case, 30 cells were selected in the bright field channel and manually analyzed. The results are shown in table 11.

GFP + HA	**mGFP + HA**
Total cells: 30	Total cells: 30
GFP transfected cells: 15	mGFP transfected cells: 14
HA transfected cells: 12	HA transfected cells: 6
Co-transfected cells: 7	Co-transfected cells: 4
GFP + M2	**mGFP + M2**
Total cells: 30	Total cells: 30
GFP transfected cells: 10	mGFP transfected cells: 8
M2 transfected cells: 2	M2 transfected cells: 0
Co-transfected cells: 2	Co-transfected cells: 0

Table 11: evaluation of colocalization in transfected cells

The colocalization was influenced by the low transfection ratio of influenza proteins, especially in the case of M2. In accordance with the results of figure 44, M2 transfection was difficult to study, because the brightness of the cells was very similar to the one of the control, meaning that the signal could be a result of autofluorescence or noise coming from the immunostaining process, and not a result of the expression of the protein.

4.3 VLPs characterization

After the characterization of transfection on cells, a final transfection process was performed with the previous transfection groups (only influenza plasmids, influenza + GFP plasmids, influenza + mGFP plasmids). In this case, the goal was not to study the response of the cell, but to use the previous optimized parameters to produce VLPs and have a characterization, which was performed through DLS and TIRF analysis.

The VLPs were previously obtained from transfected cell samples and isolated through subsequent steps of filtration, centrifugation, ultracentrifugation in sucrose gradient, and then collected with a final ultracentrifugation step.

In figure 46 the results of DLS measurements are shown as intensity distribution. Four groups have been considered: VLPs alone, GFP-VLPs, mGFP-VLPs and a control without VLPs (obtained from the sample where the transfection was not performed). For each sample, the test has been repeated in triplicate, and from the three repetitions the average size of the particle and the polydispersity index have been obtained (table 12).

In figure 47 TIRF images are shown. The three groups considered were GFP-VLPs, mGFP-VLPs and a control where the transfection was not performed, thus it was a control without VLPs. The images all show the same contrast.

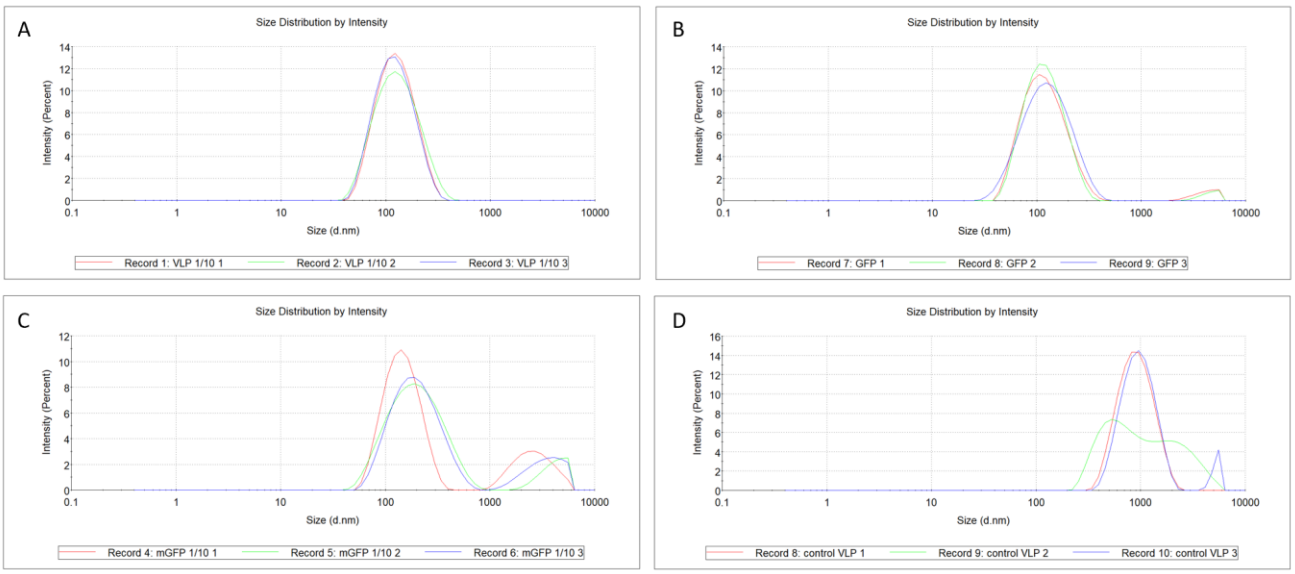

Figure 46: DLS measures as intensity percentage. A) bare VLPs. B) GFP-VLPs . C) mGFP-VLPs. D) control

Sample	Average size	Polydispersity index
A - Bare VLPs	108,0 nm	0,222
B - GFP-VLPs	105,0 nm	0,267
C - mGFP-VLPs	156,5 nm	0,660
D - control	870,3 nm	0,302

Table 12: average sizes and PdI of the DLS samples

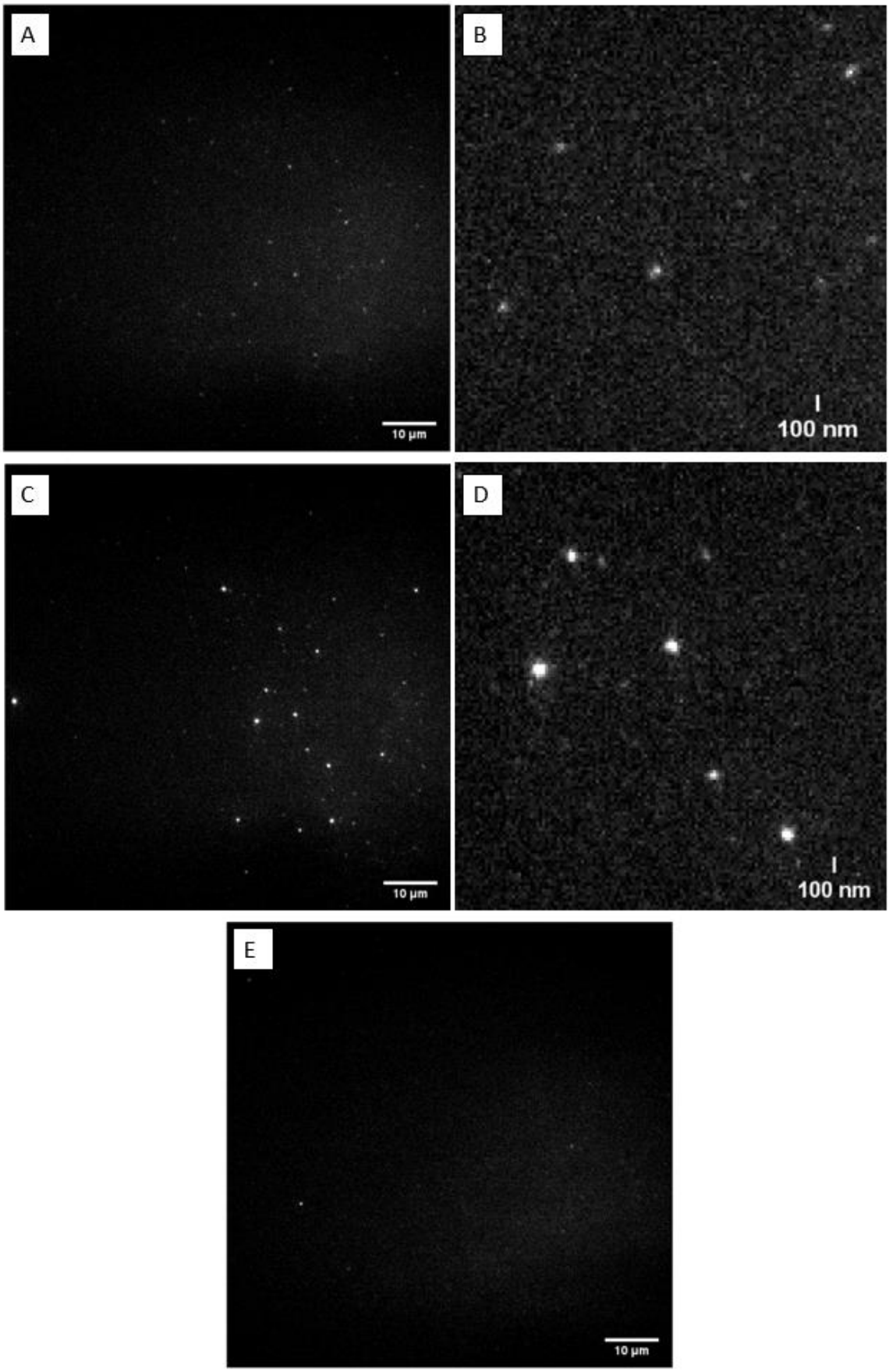

Figure 47: TIRF images. A) GFP VLPs. B) zoom of GFP VLPs. C) mGFP-VLPs. D) zoom of mGFP-VLPs. E) control

DLS showed a well visible peak at 100 nm for bare VLPs and GFP-VLPs, indicating the presence of VLPs, while in the case of mGFP-VLPs two main peaks were found. The first one is found at about 200 nm an the second one, broader, between 5000 and 6000 nm. This last peak could represent different types of agglomerates resulted from the purification step, for example some cell residues or other type of vesicles expelled by the cells.

Despite the unclear results from cell transfection with influenza plasmids, then, it seems that we were able to obtain VLPs within the expected size range. It is possible that the poor transfection efficiency obtained from cells was still enough to lead to a budding process and the production of VLPs.

TIRF images also confirmed the presence of fluorescent spots in both GFP and mGFP samples. It is very clear that in this last case the particles appear much brighter, which means that mGFP was better encapsulated in the VLPs. This is a result that we could have expected, because mGFP is localized on lipid raft domains, where HA and NA are found, and so it was easier for mGFP to be included in the budding process. On the contrary, GFP was dispersed in the cytoplasm of the cell, so it was more complicated to be encapsulated.

5. Conclusions and further outlook

The aim of this thesis was to produce and characterize Influenza Virus-like particles modified with GFP and mGFP, and an optimization process of transfection was followed to obtain the most suitable way to do it.

The first optimization process regarded the DNA amount to use to obtain the expression of GFP and mGFP on cells. Increasing amounts of DNA have been tested and evaluated through the transfection ratio (transfected cells/total cells) and the intensity of fluorescence of transfected cells. In the end, 0,5 μg of DNA plasmids per well was chosen over higher amounts, because it still led to a good transfection efficiency.

The optimization of lipofectamine amount per well in the transfection with GFP and mGFP plasmids was subsequently studied, but it did not show consistent results neither for GFP nor for mGFP transfections. Both transfection ratios and fluorescence intensity did not allow to choose an ideal parameter, which made necessary a further study on lipofectamine optimization during the transfection with GFP and influenza plasmids.

The optimization of incubation time in GFP and mGFP transfection was a delicate step because it involved a live-cell imaging, which led to a loss of cell vitality and attachment to the bottom of the wells and eventually caused decreased levels of transfection ratios. 48 hours was chosen as the best incubation time, but for the study of mGFP transfection 24 hours could have been another possible alternative.

Overall, the optimization of GFP and mGFP transfection was a challenging process because of the large variability of cell behavior and the impossibility to control every parameter influencing the process. The transfection efficiency indeed was influenced by different factors as cell viability, number of passages, degree of confluency, type of serum used, choice of cell line and it could also be operator-dependent, indeed varying from trial to trial.

After the optimization of GFP and mGFP transfection, the co-transfection of GFP and mGFP plasmids together with influenza plasmids was studied. First, the optimization of lipofectamine per well was studied, since it did not give good results in the previous optimization step. To choose the best parameter to use, increasing amounts of lipofectamine have been considered and evaluated through the transfection ratio and the intensity of fluorescence of GFP transfected cells. The final amount to use in the co-transfection with either GFP or mGFP and the influenza plasmids was 1,4 μL per well.

The subsequent study in co-transfected cells regarded the fluorescence intensity of influenza proteins in the different groups of transfection considered (influenza proteins alone, with GFP and with mGFP). The results showed how it was possible to obtain the expression of HA and NA in the group without GFP and mGFP, but they also showed, in HA case, how the expression decreased when the co-transfection also included GFP and mGFP. In the study of M2 expression, it was not possible to verify the actual expression of the protein,

because the fluorescence levels of transfected cells were not significantly different from the non-transfected stained cells.

The co-transfection of 4 different types of plasmids at the same time is a complicated process itself, because it involves different types of plasmids having different effects on cell behavior, so, again, the controllability of the process was reduced. The response of the cell to the transfection depends on its general health and also on the properties of the plasmids, such as their strength and purity.

In the end, the production and the characterization of VLPs showed that it was possible to obtain the fluorescent VLPs despite the variability of the previous optimization steps. More studies should have been performed to verify the presence of all the influenza proteins on the particles, thus studying its final homogeneity.

The project was highly influenced by the impossibility to access the laboratory during the last three months of my internship. The further studies and characterization steps would have included different aspects:

-The characterization of co-transfected cells needed to be studied much more in detail, to verify the expression on influenza proteins, and to better understand what the effects of GFP and mGFP were in the expression of influenza proteins. My general idea was that the co-presence of all 4 plasmids together significantly reduced the expression of influenza proteins, which maybe could imply a limited production of VLPs or a reduced homogeneity of transfected cells. One possible solution to improve the co-transfection process and homogeneity of the particles would be to modify the structure of the plasmid itself, inserting all the types of sequences for the proteins of interest and, for example, creating a plasmid coding for both an influenza protein and GFP. In the context of this project this could not be considered for both technical issues, since it involves delicate and complex genetic modifications and time constraints.

-The study of incubation time for transfected cells would have been another interesting field of study, to try to optimize the competitive format resulting from the same-time transfection, thus improving the expression of influenza proteins. In this context, the transfection would have been first performed with influenza plasmids, and after 24 hours with GFP or mGFP plasmids. An incubation time of further 24 hours would have followed, to obtain a final incubation time of 48 hours for influenza plasmids' transfection and of 24 hours for GFP/mGFP transfection.

-It was also not possible to further characterize the obtained VLPs, for example to have a morphological visualization in electron microscopy.

-The characterization process of VLPs was intended to use super-resolution microscopy (STORM and DNA-PAINT), which would have served as qualitative as well as quantitative technique. Super-resolution microscopy indeed allows a single-particle characterization, so it would have been used to check the presence

of the different proteins and estimate a quantification of the proteins at a single particle level. The overall homogeneity of the particles would have been in this way tested, together with its size.

Indeed, one of the problems with traditional fluorescence microscopy is that if we are working with structures in the nanoscale, the spatial resolution we can obtain is limited, around 250 nm. This means that if we have two points 250 nm away or less we are not able to distinguish one from the other; when we have different fluorophores concentrated in one area in this dimension-range, we will only see a blurred region, and it will not be possible to recognize the single molecules or their actual position. This is what happened with the TIRF images shown in the result section: we could only see some bright spots at a low resolution, so we could not properly estimate the localization and the size of the particle.

Super-resolution microscopy would have played a central role in the development of my project, because it would have made possible a more specific characterization of VLPs. In this context, GFP and mGFP would have been used as reference markers to check the presence of VLPs, while super-resolution techniques would have been used to detect Influenza proteins in their surroundings. A single-particle analysis would have been possible, in contrast with traditional ensemble techniques such as Western Blot and ELISA.

In the end of my project we were at least able to prove the production of fluorescent VLPs and also to verify how mGFP was a better alternative for this application. The possibility to obtain a modification of the bare nanoparticles confirms the possible use of GFP and mGFP as markers for fluorescence microscopy characterization and therefore the suitability of VLPs for further modification to obtain drug delivery systems.

Acknowledgements

First of all I would like to thank my supervisors from Politecnico di Torino, Professors Gianni Ciofani and Danilo Demarchi, for coordinating, supporting and following my work during these months. Thank you to Professor Ciofani also for giving me the possibility to contact Professor Albertazzi and his group at IBEC.

Thank you to Professor Lorenzo Albertazzi who allowed me entering Nanoscopy for Nanomedicine Group to have this special experience.

Thank you to Professor Sílvia Pujals, who supervised my project through all its delicate moments: thank you for your constant guidance, your advices and for putting so much care and passion in your work supporting me.

Thank you to Maria Arista-Romero for sharing her experience guiding me in the daily life at the lab. Thank you for being my teacher and my friend, thank you for your practical help, your suggestions and your patience.

Many thanks to all of you for believing in my project and supporting it, giving me the opportunity to finish it despite the unimaginable developments of the past few months.

Thank you to the whole Nanoscopy for Nanomedicine group for making me feel part of the team and for creating such a warm and motivating environment in the lab.

Finally, the biggest thank you goes to my family, who always believed in me and made all this possible.

Bibliography

[1] World Health Organization, “Influenza (Seasonal),” *Influenza (Seasonal)*, Nov. 06, 2018. https://www.who.int/en/news-room/fact-sheets/detail/influenza-(seasonal).

[2] World Health Organization, “Global influenza strategy 2019 20130.” .

[3] Centers for disease control and prevention, “How the Flu Virus Can Change: ‘Drift’ and ‘Shift,’” Oct. 15, 2019. https://www.cdc.gov/flu/about/viruses/change.htm.

[4] S. Vijayakrishnan, C. Loney, D. Jackson, W. Suphamungmee, F. J. Rixon, and D. Bhella, “Cryotomography of Budding Influenza A Virus Reveals Filaments with Diverse Morphologies that Mostly Do Not Bear a Genome at Their Distal End,” *PLoS Pathog.*, vol. 9, no. 6, p. e1003413, Jun. 2013, doi: 10.1371/journal.ppat.1003413.

[5] J. S. Rossman and R. A. Lamb, “Influenza virus assembly and budding,” *Virology*, vol. 411, no. 2, pp. 229–236, Mar. 2011, doi: 10.1016/j.virol.2010.12.003.

[6] Vincent Racaniello, David Tuller, and Gertrud U. Rey, “Structure of influenza virus,” Apr. 30, 2009. https://www.virology.ws/2009/04/30/structure-of-influenza-virus/.

[7] D. P. Nayak, R. A. Balogun, H. Yamada, Z. H. Zhou, and S. Barman, “Influenza virus morphogenesis and budding,” *Virus Res.*, vol. 143, no. 2, pp. 147–161, Aug. 2009, doi: 10.1016/j.virusres.2009.05.010.

[8] R. M. Pielak and J. J. Chou, “Influenza M2 proton channels,” *Biochim. Biophys. Acta BBA - Biomembr.*, vol. 1808, no. 2, pp. 522–529, Feb. 2011, doi: 10.1016/j.bbamem.2010.04.015.

[9] Centers for disease control and prevention, “Influenza Type A Viruses,” Apr. 19, 2017. https://www.cdc.gov/flu/avianflu/influenza-a-virus-subtypes.htm.

[10] Centers for disease control and prevention, “Types of Influenza Viruses,” Nov. 18, 2019. https://www.cdc.gov/flu/about/viruses/types.htm.

[11] KY Yuen and SSY Wong, “Human Infection by avian Influenza A H5N1,” *Honk Kong Medical Journal*, vol. 11, no. 3, pp. 189–199, Jun. 2005.

[12] B. S. Kamps, C. Hoffmann, and W. Preiser, *Influenza report 2006*. Paris, France: Flying Publisher, 2006.

[13] Jie Zhang, Andrew Pekosz, Robert A. Lamb, “Influenza Virus Assembly and Lipid Raft Microdomains: a Role for the Cytoplasmic Tails of the Spike Glycoproteins,” *Journal of Virology*, vol. 74, pp. 4634–4644, May 2000.

[14] D. S. Goodsell, “Hemagglutinin,” *RCSB Protein Data Bank*, Apr. 2006, doi: 10.2210/rcsb_pdb/mom_2006_4.

[15] D. S. Goodsell, “Influenza Neuraminidase,” *RCSB Protein Data Bank*, May 2009, doi: 10.2210/rcsb_pdb/mom_2009_5.

[16] Safo, M.K., Musayev, F.N., Mosier, P.D., Xie, H., and Desai, U.R., “Crystal Structure of Influenza A Virus Matrix Protein M1,” Oct. 22, 2014. http://www.rcsb.org/structure/4PUS.

[17] Cho, K.J. *et al.*, “Three-dimensional structure of the extracellular domain of Matrix protein 2 of influenza A virus,” Oct. 22, 2014. http://www.rcsb.org/structure/4N8C.

[18] S. Buffin *et al.*, “Influenza A and B virus-like particles produced in mammalian cells are highly immunogenic and induce functional antibodies,” *Vaccine*, vol. 37, no. 46, pp. 6857–6867, Oct. 2019, doi: 10.1016/j.vaccine.2019.09.057.

[19] N. W. Schmidt, A. Mishra, J. Wang, W. F. DeGrado, and G. C. L. Wong, “Influenza Virus A M2 Protein Generates Negative Gaussian Membrane Curvature Necessary for Budding and Scission,” *J. Am. Chem. Soc.*, vol. 135, no. 37, pp. 13710–13719, Sep. 2013, doi: 10.1021/ja400146z.

[20] National Cancer Institute, “Trivalent influenza vaccine.” https://www.cancer.gov/publications/dictionaries/cancer-drug/def/trivalent-influenza-vaccine.

[21] C. S. Ambrose and M. J. Levin, “The rationale for quadrivalent influenza vaccines,” *Hum. Vaccines Immunother.*, vol. 8, no. 1, pp. 81–88, Jan. 2012, doi: 10.4161/hv.8.1.17623.

[22] S.-S. Wong and R. J. Webby, “Traditional and New Influenza Vaccines,” *Clin. Microbiol. Rev.*, vol. 26, no. 3, pp. 476–492, Jul. 2013, doi: 10.1128/CMR.00097-12.

[23] World Health Organization, “Vaccines against influenza WHO position paper – November 2012,” vol. 87, pp. 461–476, Nov. 2012.

[24] A. Zeltins, “Construction and Characterization of Virus-Like Particles: A Review,” *Mol. Biotechnol.*, vol. 53, no. 1, pp. 92–107, Jan. 2013, doi: 10.1007/s12033-012-9598-4.
[25] J. Fuenmayor, F. Gòdia, and L. Cervera, “Production of virus-like particles for vaccines,” *New Biotechnol.*, vol. 39, pp. 174–180, Oct. 2017, doi: 10.1016/j.nbt.2017.07.010.
[26] Y. A. S. N. V. Bovin and L.V. Mochalova, “Influenza Virus Neuraminidase: Structure and function,” vol. 2, 2009, [Online]. Available: http://actanaturae.ru/2075-8251.
[27] Promega, “An Introduction to Transfection.” https://www.promega.com/resources/guides/cell-biology/transfection/.
[28] M. Zdanowicz and J. Chroboczek, “Virus-like particles as drug delivery vectors,” *Acta Biochim. Pol.*, vol. 63, no. 3, Jul. 2016, doi: 10.18388/abp.2016_1275.
[29] S.-M. Kang, J.-M. Song, F.-S. Quan, and R. W. Compans, “Influenza vaccines based on virus-like particles,” *Virus Res.*, vol. 143, no. 2, pp. 140–146, Aug. 2009, doi: 10.1016/j.virusres.2009.04.005.
[30] S.-M. Kang, M.-C. Kim, and R. W. Compans, “Virus-like particles as universal influenza vaccines,” *Expert Rev. Vaccines*, vol. 11, no. 8, pp. 995–1007, Aug. 2012, doi: 10.1586/erv.12.70.
[31] T. Douglas and M. Young, “Host–guest encapsulation of materials by assembled virus protein cages,” *Nature*, vol. 393, no. 6681, pp. 152–155, May 1998, doi: 10.1038/30211.
[32] D. Wojta-Stremayr and W. Pickl, “Fluorosomes: Fluorescent Virus-Like Nanoparticles that Represent a Convenient Tool to Visualize Receptor-Ligand Interactions,” *Sensors*, vol. 13, no. 7, pp. 8722–8749, Jul. 2013, doi: 10.3390/s130708722.
[33] A. Rynda-Apple, D. P. Patterson, and T. Douglas, “Virus-like particles as antigenic nanomaterials for inducing protective immune responses in the lung,” *Nanomed.*, vol. 9, no. 12, pp. 1857–1868, Aug. 2014, doi: 10.2217/nnm.14.107.
[34] Z. Shirbaghaee and A. Bolhassani, “Different applications of virus-like particles in biology and medicine: Vaccination and delivery systems: Different Applications of Virus-Like Particles,” *Biopolymers*, vol. 105, no. 3, pp. 113–132, Mar. 2016, doi: 10.1002/bip.22759.
[35] A. Venereo-Sánchez *et al.*, “Characterization of influenza H1N1 Gag virus-like particles and extracellular vesicles co-produced in HEK-293SF,” *Vaccine*, vol. 37, no. 47, pp. 7100–7107, Nov. 2019, doi: 10.1016/j.vaccine.2019.07.057.
[36] National library of medicine, “Influenza VLP.” https://pubmed.ncbi.nlm.nih.gov/?term=influenza+vlp.
[37] U.S. national library of medicine, “VLP | influenza.” https://clinicaltrials.gov/ct2/results?cond=influenza&term=VLP&cntry=&state=&city=&dist=.
[38] P. Pushko *et al.*, “Mono- and quadri-subtype virus-like particles (VLPs) containing H10 subtype elicit protective immunity to H10 influenza in a ferret challenge model,” *Vaccine*, vol. 34, no. 44, pp. 5235–5242, Oct. 2016, doi: 10.1016/j.vaccine.2016.09.012.
[39] O. Shimomura, F. H. Johnson, and Y. Saiga, “Extraction, Purification and Properties of Aequorin, a Bioluminescent Protein from the Luminous Hydromedusan,Aequorea,” *J. Cell. Comp. Physiol.*, vol. 59, no. 3, pp. 223–239, Jun. 1962, doi: 10.1002/jcp.1030590302.
[40] M. Chalfie, Y. Tu, G. Euskirchen, W. Ward, and D. Prasher, “Green fluorescent protein as a marker for gene expression,” *Science*, vol. 263, no. 5148, pp. 802–805, Feb. 1994, doi: 10.1126/science.8303295.
[41] Roger Y. Tsien, “The green fluorescent protein,” *Annu. Rev.*, no. 67, pp. 509–544, 1998.
[42] Mats Ormo, Andrew B. Cubitt, Karen Kallio, Larry A. Gross, Roger Y. Tsien, and S. James Remingtont, “Crystal Structure of the Aequorea victoria Green Fluorescent Protein,” *Science*, vol. 273, Sep. 1996, [Online]. Available: https://www.sciencemag.org/.
[43] Richard N. Day and Michael W. Davidson, “Education in Microscopy and Digital Imaging.” http://zeiss-campus.magnet.fsu.edu/articles/probes/jellyfishfps.html.
[44] Uniprot, “UniProtKB - P42212 (GFP_AEQVI).” https://www.uniprot.org/uniprot/P42212.
[45] N. C. Shaner, P. A. Steinbach, and R. Y. Tsien, “A guide to choosing fluorescent proteins,” *Nat. Methods*, vol. 2, no. 12, pp. 905–909, Dec. 2005, doi: 10.1038/nmeth819.
[46] T. Matsuda and C. L. Cepko, “Controlled expression of transgenes introduced by *in vivo* electroporation,” *Proc. Natl. Acad. Sci.*, vol. 104, no. 3, pp. 1027–1032, Jan. 2007, doi: 10.1073/pnas.0610155104.

[47] A. Charpilienne *et al.*, "Individual Rotavirus-like Particles Containing 120 Molecules of Fluorescent Protein Are Visible in Living Cells," *J. Biol. Chem.*, vol. 276, no. 31, pp. 29361–29367, Aug. 2001, doi: 10.1074/jbc.M101935200.
[48] Peter A. Kratz, Bettina Bottcher, and Michael Nassal, "Native display of complete foreign protein domains on the surface of hepatitis B virus capsids," *Proc. Natl. Acad. Sci.*, vol. 96, pp. 1915–1920, Mar. 1999.
[49] Katie R. Young *et al.*, "Generation and characterization of a trackable plant-made influenza H5 virus-like particle (VLP) containing enhanced green fluorescent protein (eGFP)," *FASEB J.*, vol. 29, pp. 3817–3827, 2015.
[50] E. Kim, J. Yang, M.-H. Sung, and H. Poo, "Oral Administration of Poly-Gamma-Glutamic Acid Significantly Enhances the Antitumor Effect of HPV16 E7-Expressing Lactobacillus casei in a TC-1 Mouse Model," *J. Microbiol. Biotechnol.*, vol. 29, no. 9, pp. 1444–1452, Sep. 2019, doi: 10.4014/jmb.1906.06021.
[51] A. H. Mohseni, S. Taghinezhad-S, and H. Keyvani, "The First Clinical Use of a Recombinant *Lactococcus lactis* Expressing Human Papillomavirus Type 16 E7 Oncogene Oral Vaccine: A Phase I Safety and Immunogenicity Trial in Healthy Women Volunteers," *Mol. Cancer Ther.*, vol. 19, no. 2, pp. 717–727, Feb. 2020, doi: 10.1158/1535-7163.MCT-19-0375.
[52] European Medicines Agency, "Gardasil EPAR document." Sep. 25, 2009.
[53] T. Vicente, A. Roldão, C. Peixoto, M. J. T. Carrondo, and P. M. Alves, "Large-scale production and purification of VLP-based vaccines," *J. Invertebr. Pathol.*, vol. 107, pp. S42–S48, Jul. 2011, doi: 10.1016/j.jip.2011.05.004.
[54] European Medicines Agency, "Cervarix EPAR document." .
[55] U.S. national library of medicine, "Safety Study of a Plant-based H5 Virus-Like Particles (VLP) Vaccine in Healthy Adults." https://clinicaltrials.gov/ct2/show/NCT00984945?term=plant+based+vlp&draw=2&rank=1.
[56] U.S. national library of medicine, "Safety, Tolerability and Immunogenicity of a Plant-made H7 Virus-like Particle (VLP) Influenza Vaccine in Adults." https://clinicaltrials.gov/ct2/show/NCT02022163?term=plant+based+vlp&draw=2&rank=2.
[57] Z. Huang *et al.*, "Virus-like particle expression and assembly in plants: hepatitis B and Norwalk viruses," *Vaccine*, vol. 23, no. 15, pp. 1851–1858, Mar. 2005, doi: 10.1016/j.vaccine.2004.11.017.
[58] Q. Chen and H. Lai, "Plant-derived virus-like particles as vaccines," *Hum. Vaccines Immunother.*, vol. 9, no. 1, pp. 26–49, Jan. 2013, doi: 10.4161/hv.22218.
[59] A. Roldão, M. C. M. Mellado, L. R. Castilho, M. J. Carrondo, and P. M. Alves, "Virus-like particles in vaccine development," *Expert Rev. Vaccines*, vol. 9, no. 10, pp. 1149–1176, Oct. 2010, doi: 10.1586/erv.10.115.
[60] C. Peixoto, M. F. Q. Sousa, A. C. Silva, M. J. T. Carrondo, and P. M. Alves, "Downstream processing of triple layered rotavirus like particles," *J. Biotechnol.*, vol. 127, no. 3, pp. 452–461, Jan. 2007, doi: 10.1016/j.jbiotec.2006.08.002.
[61] Adam Blatter, "Choosing the Right Method for Nucleic Acid Quantitation," Mar. 2018. https://www.promega.es/resources/pubhub/choosing-the-right-method-for-nucleic-acid-quantitation/.
[62] P. Steppert, D. Burgstaller, M. Klausberger, A. Tover, E. Berger, and A. Jungbauer, "Quantification and characterization of virus-like particles by size-exclusion chromatography and nanoparticle tracking analysis," *J. Chromatogr. A*, vol. 1487, pp. 89–99, Mar. 2017, doi: 10.1016/j.chroma.2016.12.085.
[63] ThermoFisher Scientific, "Overview of Protein Assays Methods." https://www.thermofisher.com/es/es/home/life-science/protein-biology/protein-biology-learning-center/protein-biology-resource-library/pierce-protein-methods/overview-protein-assays.html.
[64] ThermoFisher Scientific, "BCA Assay and Lowry Assays." https://www.thermofisher.com/es/es/home/life-science/protein-biology/protein-assays-analysis/protein-assays/bca-protein-assays.html.

[65] I. González-Domínguez, E. Puente-Massaguer, L. Cervera, and F. Gòdia, “Quality Assessment of Virus-Like Particles at Single Particle Level: A Comparative Study,” *Viruses*, vol. 12, no. 2, p. 223, Feb. 2020, doi: 10.3390/v12020223.
[66] S. Heider and C. Metzner, “Quantitative real-time single particle analysis of virions,” *Virology*, vol. 462–463, pp. 199–206, Aug. 2014, doi: 10.1016/j.virol.2014.06.005.
[67] P. P. Aguilar, I. González-Domínguez, T. A. Schneider, F. Gòdia, L. Cervera, and A. Jungbauer, “At-line multi-angle light scattering detector for faster process development in enveloped virus-like particle purification,” *J. Sep. Sci.*, p. jssc.201900441, Jun. 2019, doi: 10.1002/jssc.201900441.
[68] J. Tomé-Amat, L. Fleischer, S. A. Parker, C. L. Bardliving, and C. A. Batt, “Secreted production of assembled Norovirus virus-like particles from Pichia pastoris,” *Microb. Cell Factories*, vol. 13, no. 1, p. 134, Dec. 2014, doi: 10.1186/s12934-014-0134-z.
[69] J. Stetefeld, S. A. McKenna, and T. R. Patel, “Dynamic light scattering: a practical guide and applications in biomedical sciences,” *Biophys. Rev.*, vol. 8, no. 4, pp. 409–427, Dec. 2016, doi: 10.1007/s12551-016-0218-6.
[70] The Native Antigen Company, “TEM images of our virus-like particles,” Sep. 18, 2019. https://thenativeantigencompany.com/tem-images-of-our-virus-like-particles/.
[71] ThermoFisher Scientific, “An Introduction to Electron Microscopy.” https://www.fei.com/introduction-to-electron-microscopy/tem/.
[72] Ł. Mielańczyk, N. Matysiak, O. Klymenko, and R. Wojnicz, “Transmission Electron Microscopy of Biological Samples,” in *The Transmission Electron Microscope - Theory and Applications*, K. Maaz, Ed. InTech, 2015.
[73] D. F. Barreto-Vieira and O. M. Barth, “Negative and Positive Staining in Transmission Electron Microscopy for Virus Diagnosis,” in *Microbiology in Agriculture and Human Health*, M. M. Shah, Ed. InTech, 2015.
[74] D. Yan, Y.-Q. Wei, H.-C. Guo, and S.-Q. Sun, “The application of virus-like particles as vaccines and biological vehicles,” *Appl. Microbiol. Biotechnol.*, vol. 99, no. 24, pp. 10415–10432, Dec. 2015, doi: 10.1007/s00253-015-7000-8.
[75] R. Cubas *et al.*, “Virus-like Particle (VLP) Lymphatic Trafficking and Immune Response Generation After Immunization by Different Routes:,” *J. Immunother.*, vol. 32, no. 2, pp. 118–128, Feb. 2009, doi: 10.1097/CJI.0b013e31818f13c4.
[76] M. Mohsen, A. Gomes, M. Vogel, and M. Bachmann, “Interaction of Viral Capsid-Derived Virus-Like Particles (VLPs) with the Innate Immune System,” *Vaccines*, vol. 6, no. 3, p. 37, Jul. 2018, doi: 10.3390/vaccines6030037.
[77] Encyclopaedia Britannica, “Major histocompatibility complex,” Jul. 20, 1998. https://www.britannica.com/science/major-histocompatibility-complex.
[78] J. T. Schiller and D. R. Lowy, “Immunogenicity Testing in Human Papillomavirus Virus-Like-Particle Vaccine Trials,” *J. Infect. Dis.*, vol. 200, no. 2, pp. 166–171, Jul. 2009, doi: 10.1086/599988.
[79] C. Roberts *et al.*, “Development of a human papillomavirus competitive luminex immunoassay for 9 HPV types,” *Hum. Vaccines Immunother.*, vol. 10, no. 8, pp. 2174–103, Aug. 2014, doi: 10.4161/hv.29205.
[80] S. Payne, “Methods to Study Viruses,” in *Viruses*, Elsevier, 2017, pp. 37–52.
[81] D. V. Pastrana *et al.*, “Reactivity of human sera in a sensitive, high-throughput pseudovirus-based papillomavirus neutralization assay for HPV16 and HPV18,” *Virology*, vol. 321, no. 2, pp. 205–216, Apr. 2004, doi: 10.1016/j.virol.2003.12.027.
[82] M. J. Rohovie, M. Nagasawa, and J. R. Swartz, “Virus-like particles: Next-generation nanoparticles for targeted therapeutic delivery: ROHOVIE et al.,” *Bioeng. Transl. Med.*, vol. 2, no. 1, pp. 43–57, Mar. 2017, doi: 10.1002/btm2.10049.
[83] M. E. Farkas *et al.*, “PET Imaging and Biodistribution of Chemically Modified Bacteriophage MS2,” *Mol. Pharm.*, vol. 10, no. 1, pp. 69–76, Jan. 2013, doi: 10.1021/mp3003754.
[84] D. E. Prasuhn, P. Singh, E. Strable, S. Brown, M. Manchester, and M. G. Finn, “Plasma Clearance of Bacteriophage Qβ Particles as a Function of Surface Charge,” *J. Am. Chem. Soc.*, vol. 130, no. 4, pp. 1328–1334, Jan. 2008, doi: 10.1021/ja075937f.

[85] J. Simon-Santamaria *et al.*, “Efficient Uptake of Blood-Borne BK and JC Polyomavirus-Like Particles in Endothelial Cells of Liver Sinusoids and Renal Vasa Recta,” *PLoS ONE*, vol. 9, no. 11, p. e111762, Nov. 2014, doi: 10.1371/journal.pone.0111762.
[86] Health and Food safety Commission department, “Vaccination.” https://ec.europa.eu/health/vaccination/overview_en.
[87] European vaccination information program, “Approval of vaccines in the European Union,” Mar. 13, 2020. https://vaccination-info.eu/en.
[88] Centers for disease control and prevention, “The Journey of Your Child’s Vaccine,” Jan. 26, 2018. https://www.cdc.gov/vaccines/parents/infographics/journey-of-child-vaccine.html?CDC_AA_refVal=https%3A%2F%2Fwww.cdc.gov%2Fvaccines%2Fparents%2Finfographics%2Fjourney-of-child-vaccine-text.html.
[89] Centers for disease control and prevention, “Vaccine Testing and the Approval Process,” May 01, 2014. https://www.cdc.gov/vaccines/basics/test-approve.html.
[90] European vaccination information program, “Decisions on vaccines in use in different European countries,” Mar. 13, 2020. https://vaccination-info.eu/en/vaccine-facts/decisions-vaccines-use-different-european-countries.
[91] S. Mohammed, N. Bakshi, N. Chaudri, J. Akhter, and M. Akhtar, “Cancer Vaccines: Past, Present, and Future,” *Adv. Anat. Pathol.*, vol. 23, no. 3, pp. 180–191, May 2016, doi: 10.1097/PAP.0000000000000116.
[92] European Medicines Agency, “Gardasil,” Mar. 23, 2020. https://www.ema.europa.eu/en/medicines/human/EPAR/gardasil.
[93] European Medicines Agency, “EMA to further clarify safety profile of human papillomavirus (HPV) vaccines,” Jul. 13, 2015. https://www.ema.europa.eu/en/news/ema-further-clarify-safety-profile-human-papillomavirus-hpv-vaccines.
[94] C. Gilman, T. Heller, and C. Koh, “Chronic hepatitis delta: A state-of-the-art review and new therapies,” *World J. Gastroenterol.*, vol. 25, no. 32, pp. 4580–4597, Aug. 2019, doi: 10.3748/wjg.v25.i32.4580.
[95] World Health Organization, “Hepatitis B,” Jul. 18, 2019. https://www.who.int/news-room/fact-sheets/detail/hepatitis-b.
[96] U.S. national library of medicine, “ClinicalTrials.gov is a database of privately and publicly funded clinical studies conducted around the world.” https://clinicaltrials.gov/.
[97] F.-S. Quan, S. Basak, K.-B. Chu, S. S. Kim, and S.-M. Kang, “Progress in the development of virus-like particle vaccines against respiratory viruses,” *Expert Rev. Vaccines*, vol. 19, no. 1, pp. 11–24, Jan. 2020, doi: 10.1080/14760584.2020.1711053.
[98] Y. Ma, R. J. M. Nolte, and J. J. L. M. Cornelissen, “Virus-based nanocarriers for drug delivery,” *Adv. Drug Deliv. Rev.*, vol. 64, no. 9, pp. 811–825, Jun. 2012, doi: 10.1016/j.addr.2012.01.005.
[99] C. E. Ashley *et al.*, “Cell-Specific Delivery of Diverse Cargos by Bacteriophage MS2 Virus-like Particles,” *ACS Nano*, vol. 5, no. 7, pp. 5729–5745, Jul. 2011, doi: 10.1021/nn201397z.
[100] Addgene, “Vector database/pEGFP-N3.” https://www.addgene.org/vector-database/2493/.
[101] Addgene, “pCAG-mGFP.” http://www.addgene.org/14757/.
[102] T. A. F. Bouback and N. A. Redwan, “Approaches toward the development of DNA vaccine for influenza virus,” *African Journal of Biotechnology*, vol. 10(26), pp. 5209–5218, Jun. 2011, doi: 10.5897/AJB10.2715.
[103] BD Biosciences Clontech, “pEGFP-N3 vector information.” Oct. 03, 2002, [Online]. Available: http://www.synthesisgene.com/vector/pEGFP-N3.pdf.
[104] E. Hoffmann, G. Neumann, Y. Kawaoka, G. Hobom, and R. G. Webster, “A DNA transfection system for generation of influenza A virus from eight plasmids,” *Proc. Natl. Acad. Sci.*, vol. 97, no. 11, pp. 6108–6113, May 2000, doi: 10.1073/pnas.100133697.
[105] Influenza research database, “Influenza Strain Details for A/Puerto Rico/8/1934(H1N1),” May 03, 2020. .
[106] ThermoFisher Scientific, “Thermo Scientific GeneJET Plasmid Midiprep Kit #K0481, #K0482.” [Online]. Available: www.thermoscientific.com/onebio.

[107] Invitrogen, “Lipofectamine® 2000 DNA Transfection Reagent Protocol.” .
[108] Christine Labno, “Two Ways to Count Cells with ImageJ.” .